

University of Windsor

## Scholarship at UWindor

---

Electronic Theses and Dissertations

Theses, Dissertations, and Major Papers

---

7-11-2015

# Tribological Behaviours Influenced by Surface Coatings and Morphology

Guang Wang  
*University of Windsor*

Follow this and additional works at: <https://scholar.uwindsor.ca/etd>

---

### Recommended Citation

Wang, Guang, "Tribological Behaviours Influenced by Surface Coatings and Morphology" (2015).  
*Electronic Theses and Dissertations*. 5305.  
<https://scholar.uwindsor.ca/etd/5305>

This online database contains the full-text of PhD dissertations and Masters' theses of University of Windsor students from 1954 forward. These documents are made available for personal study and research purposes only, in accordance with the Canadian Copyright Act and the Creative Commons license—CC BY-NC-ND (Attribution, Non-Commercial, No Derivative Works). Under this license, works must always be attributed to the copyright holder (original author), cannot be used for any commercial purposes, and may not be altered. Any other use would require the permission of the copyright holder. Students may inquire about withdrawing their dissertation and/or thesis from this database. For additional inquiries, please contact the repository administrator via email ([scholarship@uwindsor.ca](mailto:scholarship@uwindsor.ca)) or by telephone at 519-253-3000ext. 3208.

**Tribological Behaviours Influenced by Surface Coatings and  
Morphology**

By

**Guang Wang**

A thesis

Submitted to the Faculty of Graduate Studies  
through the Department of Mechanical, Automotive & Materials Engineering  
in Partial Fulfillment of the Requirements for  
the Degree of Master of Applied Science  
at the University of Windsor

Windsor, Ontario, Canada

2015

©2015 Guang Wang

Tribological Behaviours Influenced by  
Surface Coatings and Morphology

By

**Guang Wang**

APPROVED BY:

---

Dr. B. Zhou

Department of Mechanical Automotive and Materials Engineering

---

Dr. V. Stoilov

Department of Mechanical, Automotive and Materials Engineering

---

Dr. X. Nie

Advisor

Department of Mechanical, Automotive and Materials Engineering

---

Dr. H. Hu

Chair of Defense

Department of Mechanical, Automotive and Materials Engineering

1 May 2015

## DECLARATION OF CO-AUTHORSHIP/PREVIOUS PUBLICATION

### I. CO- AUTHORSHIP DECLARATION

I hereby declare that this thesis does not incorporate material that is result of joint research. In all cases, the key ideas, primary contributions, experimental designs, data analysis and interpretation, were performed by the author and Dr. X. Nie as advisor. Dr. Jimi Tjong is co-author of papers published in chapters 5, 6, and 7 of my thesis.

I am aware of the University of Windsor Senate Policy on Authorship and I certify that I have properly acknowledged the contribution of other researchers to my thesis, and have obtained written permission from each of co-author(s) to include the above materials in my thesis.

I certify that, with the above qualification, this dissertation, and the research to which it refers, is the product of my own work.

### II. DECLARATION OF PREVIOUS PUBLICATION

This thesis includes 4 original papers that have been previously published / submitted for publication in peer reviewed journals/conference proceedings, as follows:

Thesis Chapter	Publication title/full citation	Publication status
Chapter4	Wang, G. and Nie, X., "Effect of Surface Roughness and Sliding Velocity on Tribological Properties of an Oxide-Coated Aluminum Alloy," SAE Technical Paper 2014-01-0957, 2014, doi:10.4271/2014-01-	Published
Chapter 5	Wang, G. Nie, X., and Tjong, J., "Surface Effect of a PEO Coating on Friction at Different Sliding Velocities," SAE Technical Paper 2015-01-0687, 2015.	Published
Chapter 6	Wang, G. Nie, X., and Tjong, J., "Friction influenced by surface roughness and sliding speeds at oil lubricating conditions," ICMCTF 2015,1926-E3-1-11	Submitted

Chapter 7	Wang, G. Nie, X., and Tjong, J., "High speed tribotests on a PEO coated aluminum liner after flex honing"	Proceed
-----------	---	---------

I hereby certify that I have obtained a written permission from the copyright owner(s) to include the above published material(s) in my thesis. I certify that the above material describes work completed during my registration as graduate student at the University of Windsor.

I declare that, to the best of my knowledge, my thesis does not infringe upon anyone's copyright nor violate any proprietary rights and that any ideas, techniques, quotations, or any other material from the work of other people included in my dissertation, published or otherwise, are fully acknowledged in accordance with the standard referencing practices. Furthermore, to the extent that I have included copyrighted material that surpasses the bounds of fair dealing within the meaning of the Canada Copyright Act, I certify that I have obtained a written permission from the copyright owner(s) to include such material(s) in my dissertation.

I declare that this is a true copy of my thesis, including any final revisions, as approved by my thesis committee and the Graduate Studies office, and that this thesis has not been submitted for a higher degree to any other University or Institution.

## **ABSTRACT**

Plasma electrolytic oxidizing (PEO) is an advanced technique that has been widely used in automotive industry to produce ceramic coatings on light metal components due to their high hardness, wear resistance, corrosion resistance and low friction coefficient. In this work, PEO process was used to produce a relatively thick (~20  $\mu\text{m}$ ) coating on A356 Al alloy for improving the wear resistance and tribological properties of the Al alloy. Effects of surface roughness and sliding velocity on the coefficient of friction (COF) of PEO coatings were particularly investigated in different tribological tests including low speed pin-on-disc tests, high speed pin-on-disc tests, and high speed piston ring on liner tests. Cast iron was used as reference material for comparison with PEO coatings. The research results indicated that the PEO coatings could have excellent tribological properties potential for linerless aluminium engine applications.

## **DEDICATION**

I would like to dedicate this dissertation to my parents for their unconditional love, support and encouragement.

I also would like to thank Dr. Xueyuan Nie for his unwavering support and encouragement over the years.

## **ACKNOWLEDGEMENTS**

This study could not have been done forward without the financial support from the Natural Sciences and Engineering Research Council of Canada (NSERC).

I would like to thank my thesis advisor, Dr. Xueyuan Nie, for his valuable suggestions and excellent supervision of this research work during my study.

Many thanks to my committee members (Dr. Henry Hu, Dr. Vesselin Stoilov, Dr. Biao Zhou) for their helpful comments and careful review of this work.

I would like to thank Mr. Andy Jenner from University of Windsor for his assistance with the experiments.

Finally, I am thankful to the faculty, staff and graduate students at the Department of Mechanical, Automotive and Materials Engineering of the University of Windsor, particularly my colleagues at the Plasma Surface Engineering and Nanotechnology Lab, for their support and encouragement.



# TABLE OF CONTENTS

<b>DECLARATION OF CO-AUTHORSHIP/PREVIOUS PUBLICATION .....</b>	<b>III</b>
<b>ABSTRACT .....</b>	<b>V</b>
<b>DEDICATION.....</b>	<b>VI</b>
<b>ACKNOWLEDGEMENTS.....</b>	<b>VII</b>
<b>LIST OF TABLES .....</b>	<b>XI</b>
<b>LIST OF FIGURES .....</b>	<b>XII</b>
<b>CHAPTER 1 .....</b>	<b>1</b>
<b>INTRODUCTION.....</b>	<b>1</b>
OBJECTIVE AND CONTENTS OF THIS STUDY .....	6
ORGANIZATION OF THE THESIS .....	6
REFERENCES:.....	8
<b>CHAPTER 2 .....</b>	<b>10</b>
<b>LITERATURE REVIEW .....</b>	<b>10</b>
1. BACKGROUND OF APPLICATION OF ALUMINUM IN AUTOMOTIVE INDUSTRY .....	10
2. THE CHARACTERISTICS OF ALUMINUM.....	11
3. FUNCTIONAL REQUIREMENTS FOR MATERIAL OF THE ENGINE BLOCK .....	12
4. ALUMINUM ENGINE BLOCK WITH CAST IRON LINERS.....	14
5. THERMAL SPRAY COATING TREATMENT.....	14
6. PLASMA ELECTROLYTE OXIDATION COATING TREATMENT .....	16
7. SUMMARY OF LITERATURE REVIEW .....	18
REFERENCES:.....	19
<b>CHAPTER 3 .....</b>	<b>22</b>
<b>EXPERIMENTAL PROCEDURES .....</b>	<b>22</b>
1. LOW SPEED PIN-ON-DISC TESTS .....	22
2. HIGH SPEED PIN-ON-DISC TESTS .....	23
3. HIGH SPEED PISTON RING ON LINER TESTS.....	24

<b>CHAPTER 4.....</b>	<b>26</b>
<b>EFFECT OF SURFACE ROUGHNESS AND SLIDING VELOCITY ON TRIBOLOGICAL PROPERTIES OF AN OXIDE-COATED ALUMINUM ALLOY .....</b>	<b>26</b>
1. INTRODUCTION.....	26
2. EXPERIMENT DETAILS .....	27
3. RESULTS AND DISCUSSION .....	30
3.1 The effect of roughness .....	30
3.2 The effect of velocity .....	36
3.3 The effect of oil thickness .....	37
3.4 Other influences on COF .....	37
4. CONCLUSION .....	38
REFERENCES.....	39
<b>CHAPTER 5.....</b>	<b>41</b>
<b>SURFACE EFFECT OF A PEO COATING ON FRICTION AT DIFFERENT SLIDING VELOCITIES.....</b>	<b>41</b>
1. INTRODUCTION.....	41
2. EXPERIMENT DETAILS .....	44
3. RESULTS AND DISCUSSION .....	47
3.1 Roughness effect on the COF of PEO coating .....	47
3.2 Sliding velocity effect on the COF of PEO coating .....	52
3.3 Steel ball wear against the PEO coatings .....	54
4. CONCLUSIONS.....	55
ACKNOWLEDGEMENT .....	56
REFERENCES.....	57
<b>CHAPTER 6.....</b>	<b>59</b>
<b>FRICTION INFLUENCED BY SURFACE ROUGHNESS AND SLIDING SPEEDS AT OIL LUBRICATING CONDITIONS .....</b>	<b>59</b>
1. INTRODUCTION.....	59
2. EXPERIMENT DETAILS .....	63
3. RESULTS AND DISCUSSION .....	66
3.1 THE EFFECT OF ROUGHNESS .....	66
3.2 THE EFFECT OF SLIDING VELOCITY .....	77

<b>4. CONCLUSIONS .....</b>	<b>79</b>
ACKNOWLEDGEMENTS .....	79
REFERENCES.....	80
<b>CHAPTER 7.....</b>	<b>82</b>
<b>HIGH SPEED TRIBOTESTS ON A PEO COATED ALUMINUM LINER AFTER FLEXIBLE HONING.....</b>	<b>82</b>
1. INTRODUCTION.....	82
2. EXPERIMENTAL DETAILS .....	85
3. RESULTS AND DISCUSSION.....	91
3.1 Effects of roughness on COF.....	91
3.2 Effect of oil flow rate on COF.....	95
4. CONCLUSIONS.....	97
ACKNOWLEDGEMENTS.....	97
REFERENCES.....	98
<b>CHAPTER 8.....</b>	<b>100</b>
<b>SUMMARY AND FUTURE WORK.....</b>	<b>100</b>
1. SUMMARY.....	100
I. Effect of surface roughness and sliding velocity on tribological properties of an oxide-coated aluminum alloy. ....	100
III. Friction influenced by surface roughness and sliding speeds at oil lubricating conditions. ....	101
IV. High speed tribotests on a PEO coated aluminum liner after flex honing. ....	102
2. FUTURE WORK .....	102
<b>APPENDIX.....</b>	<b>105</b>
<b>VITA AUCTORIS .....</b>	<b>107</b>

## LIST OF TABLES

Table 4.1 Process parameters, thickness and roughness of coatings.....	29
Table 4.2 Roughness and thickness of all samples after polish.....	30
Table 4.3 Skewness and kurtosis of all samples after polish.....	32
Table 4.4 COF of each sample with different roughness.....	32
Table 4.5 Ball wears of each sample with different roughness-displayed in diameter ( $\mu\text{m}$ ).....	32
Table 4.6 The COF of each sample tested at different velocity ( $R_a=0.6\mu\text{m}$ ).....	36
Table 5.1 The original roughness and thickness of two PEO coatings.....	46
Table 5.2 Changes of roughness and thickness after polish.....	47
Table 5.3 DIN factors and volumes of holes on PEO coating.....	51
Table 5.4 Ball wears vs different coating roughness - showed in diameter.....	54
Table 6.1 The original PEO coating thickness and surface roughness of samples.....	64
Table 6.2 $R_{sk}$ and $R_{ku}$ data of PEO coating S3 and S12 after polished to different surface roughness.....	67
Table 6.3 DIN surface parameters and oil retentions of PEO coatings and cast iron.....	73
Table 7.1 Record of thickness and diameter changes in the honing process.....	87
Table 7.2 DIN surface parameters and oil retention volume of the polished PEO coated liner.....	93

## LIST OF FIGURES

Figure.2.1 Buick 215 V8 aluminum engine.....	11
Figure.2.2 Aluminum cylinder block in V inline.....	13
Figure.2.3 Aluminum cylinder engine block with inserted cast iron liners.....	14
Figure.2.4 Schematic view of the PTWA spray process.....	15
Figure.2.5 Schematic view of the PEO process.....	16
Figure.3.1 Experimental instruments of low speed pin-on-disc tests, (a) Optical microscope, (b) stylus type surface profilometer, (c) low speed pin-on-disc tribometer.....	23
Figure.3.2 High speed pin-on-disc tribometer.....	24
Figure.3.3 High speed piston ring on liner tribometer, (a) liner holder, (b) piston ring holder, (c) high speed piston ring on liner tribometer.....	25
Figure.4.1 Coated samples before polishing.....	28
Figure.4.2 Surface topography of coated samples.....	29
Figure.4.3 Surface morphology of S3 after polish.....	31
Figure.4.4 COF of A356 samples with different roughness.....	33
Figure.4.5 Ball wears after tested on sample S1.....	34
Figure.4.6 Ball wears after tested on sample S3.....	35
Figure.4.7 Ball wears after tested on sample S7.....	35
Figure.4.8 The relationship between COF and velocity.....	36
Figure.5.1 The ring-shaped aluminum 6061 sample.....	45
Figure.5.2. PEO coated samples S2 and S3.....	45
Figure.5.3. The original profile of two PEO coatings.....	46
Figure.5.4. Surface profile of polished coating S2.....	48
Figure.5.5. Surface profile of polished coating S3.....	48
Figure.5.6. Roughness effect on the COF of PEO coating S2.....	50
Figure.5.7. Roughness effect on the COF of PEO coating S3.....	50
Figure.5.8. Sliding velocity effect on COF of PEO coating S3.....	53
Figure.6.1. A typical Stribeck curve [18].....	62
Figure.6.2. Schematic view of high speed pin-on-disc tribometer.....	62

Figure.6.3. Original surface roughness and profiles of the PEO coatings and cast iron, (a) S3, and (b) S12, and (c) cast iron.....	65
Figure.6.4. The relationship between roughness and thickness of coating S3 and S12.....	66
Figure.6.5. Surface profile of coating S3 after being polished to different roughness, Ra: (a) 0.80 $\mu$ m, (b) 0.70 $\mu$ m, (c) 0.50 $\mu$ m, (d) 0.35 $\mu$ m, and (e) 0.25 $\mu$ m.....	68
Figure.6.6. Surface profile of coating S12 after being polished to different roughness, Ra: (a) 0.80 $\mu$ m, (b) 0.60 $\mu$ m, (c) 0.35 $\mu$ m, (d) 0.25 $\mu$ m, and (e) 0.20 $\mu$ m.....	68
Figure.6.7. Roughness effect on COFs of coating S3, (a) 2D plot, (b) 3D plot.....	69
Figure.6.8. Roughness effect on COFs of coating S12, (a) 2D plot, (b) 3D plot.....	70
Figure.6.9. Roughness effect on COFs of cast iron, (a) 2D plot, (b) 3D plot.....	71
Figure.6.10 Schematic illustration of the topographic changes with different roughness.....	74
Figure.6.11 Wear tracks on the finally polished surfaces ( $\times 200$ ) on, (a) coating S3, (b) coating S12, and (C) cast iron.....	75
Figure.6.12. Sliding velocity effect on COF of PEO coating S3 (Ra = 0.35 $\mu$ m).....	77
Figure.7.1. PEO coated liner and the original coating surface profile: (a) PEO coated liner, (b) original coating profile.....	86
Figure.7.2. Honing brush and the honing process.....	87
Figure.7.3 Diameter measurement using a dial bore gage.....	88
Figure.7.4. PEO coating surface profiles after honing: (a) Ra = 0.80 $\mu$ m, (b) Ra = 0.60 $\mu$ m, (c) Ra = 0.45 $\mu$ m, (d) Ra = 0.35 $\mu$ m.....	89
Figure.7.5. High speed piston ring on liner tribometer: (a) liner holder, (b) piston ring holder, (c) schematic view of the tribometer.....	90
Figure.7.6. Calibration results of the load cell.....	91
Figure.7.7. Roughness and sliding velocity effects on the COF of PEO coated liner at a high oil flow rate (100 ml/min).....	92
Figure.7.8 Roughness and sliding velocity effects on the COF of PEO coated liner at a high oil flow rate (200 ml/min).....	95

# Chapter 1

## INTRODUCTION

Recently, environmental problems caused by fuel emissions and limited fuel supplies have forced the automotive industry to reduce the weight of vehicles and improve the fuel efficiency. The need to improve fuel economy and reduce exhaust emissions has caused new revolutions in components design, including material selection, friction and weight reduction, and high wear resistance for a long serve life [1]. Gray cast iron is the standard material for the casting of the engine block in the past. However, the high weight of the cast iron engine consumes more fuel and emits more emissions. One approach to increase an automobile's fuel economy, by reducing vehicle weight and friction loss simultaneously, is to remove the cast iron engine block and replace it with a lighter and more thermally efficient material. Aluminum (Al) alloys are popular for their unique combination of desirable characteristics, including their high strength-to-weight-ratio, good castability, good thermal conductivity, and high corrosion resistance [2]. Thus, Al alloys are usually used to cast an engine block and replace the heavy cast iron engine block. Replacing cast iron engine blocks with aluminum engine blocks has the potential for a great reduction in block weight, up to 45% for gasoline engines [3]. The disadvantage to using aluminum as the engine block material is that the traditional aluminum alloys do not have the required tribological properties for the engine block material, such as high hardness, wear resistance, and low coefficient of friction (COF) [4]. Besides, the mechanical properties of aluminum alloys, such as Young modulus, tensile strength, and hardness, are not as good as gray cast iron. Therefore, switching to aluminum for engine blocks has brought the need for surface engineering technologies to overcome these tribological characteristic deficiencies.

Historically, the cast iron liners are inserted or cast in the aluminum engine blocks to meet the required surface characteristics. Cast iron liners are low-cost, durable, and easy to manufacture, which are the key considerations for mass production in automotive industries. The graphite cast inside the iron is also good for reducing the friction between piston rings and the liner wall [5]. Besides, crosshatches can be engraved on the surface of cast iron liner, which is good for improving the oil retention. Presently, most of the

passenger cars use this kind of technology. However, the cast iron liners in aluminum engine blocks also have drawbacks in the inherent heavy weight, thermal conductivity, and thermal expansion mismatching problems. The thermal expansion and heat conduction coefficients of cast iron and aluminum alloys are different, and this will cause a heat transfer problem and a deformation of the liner [6]. The deformation of the liner gives rise to an increase of fuel consumption and emissions.

To avoid using the cast iron liners in the aluminum engine block, high-silicon (17%) aluminum alloy is used to cast linerless engine blocks. Germany is the leading manufacturer of the all-aluminum engine blocks (by Porsche, Audi, Daimler-Benz and BMW). Conversely, US automotive manufacturers do not yet produce linerless all-aluminum blocks in production, but the goal of reducing the automobile's weight by 40% forces US automakers to change their research interest to all-aluminum engine block. The high amount of separated silicon can provide good tribological properties. However, the high-silicon aluminum alloy engine block is difficult to machine and potentially suffer a corrosion problem when a biofuel is used [7].

Surface coating can be used to minimize the possibility of severe wear by lowering friction and hardening the surface. Various coatings have been developed to improve wear properties of the alloys. Titanium nitride and diamond-like carbon (DLC) coatings are deposited by vacuum vapour deposition (PVD and CVD) methods which need high vacuum in vacuum chambers [8-9]. Electroplating and electroless plating-Nickel based ceramic composite coatings (NCC) have a function to increase the wear resistance but could be corroded when sulphur-contained fuel is used [10].

One option to improve the wear resistance and tribological properties of the aluminum alloy cylinder bore is applying the thermal spray coatings to protect the soft aluminum bore surface [11]. Thermal spray coatings are widely used in a variety of industrial applications, for example, they can protect products from wear, temperature extremes, and chemicals. Thermal spray coating processes are distinguished by heat source and base materials including combustion flame spraying, high velocity oxy-fuel spraying (HVOF), two-wire electric arc spraying, plasma transferred wire arc (PTWA) spraying, and vacuum plasma spraying process [12].



Now, the PTWA thermal spray coating is already successfully applied on the aluminum alloy engine block to protect the surface of the cylinder bore, for example, Ford Mustang and Nissan GTR. During the PTWA process, a supersonic plasma jet melts a single conductive wire, atomizes it, and propels it onto the substrate to be coated. After atomization, the stream of molten droplets is transported by forced air onto the bore wall. The particles impinge on the surface of the substrate and flatten due to the high kinetic energy. The particles rapidly solidify upon contact and stack to make up a high wear resistant coating [13]. PTWA thermal spray coating is a kind of nanoscale depositing coating, and the thickness of this coating can be varied easily by treating time. Besides, it is also hard enough to bear the wear from the sliding piston rings. Due to the high density of the PTWA coating, the porosity of the coating is low (only 4%), so the oil retention is not good [14]. Thus, cross hatches need to be honed on the surface of PTWA coating to increase the oil retention. Recently, Ford tries to improve the PTWA process and increase the porosity up to 10% to obtain a better oil retention [15].

Plasma electrolytic oxidation (PEO) is a relatively new plasma-assisted electrochemical treatment, which is considered as a cost-effective and environmentally friendly surface engineering technique and can be broadly applied to metal surface cleaning, metal-coating [16], carburizing, nitriding [17], and oxidizing [18-21]. A PEO process in a silicate solution can produce Al-Si-O ceramic coatings with a high adhesion, hardness, and thickness on Al-based materials. Compared to other thermal spray coatings such as PTWA, Alusil, Nikasil, etc., PEO coatings have the advantages such as high bonding adhesion to substrate material, high hardness, high corrosion resistance, high wear resistance, low production cost, low environmental pollution, and especially the excellent tribological performance by the good oil retention ability of their porous structures [22]. Besides, PEO coating surfaces can be varied in roughness and morphology easily by changing the processing parameters such as electrolyte composition, current density and treatment time. This variety provides PEO coatings the ability to optimize the surface in friction reduction [23]. In this regard, a good understanding of the tribological behaviours of PEO coatings is essential.

For internal combustion engines, piston rings and the wall of cylinder bores work under different lubricating regimes, including boundary lubricating regime at the top dead

center (TDC) and the bottom dead center (BDC) of the cylinder, and mixed and hydrodynamic lubricating regimes in the middle of the cylinder. In the TDC and BDC areas, the combustion load is high and the moving speed is low, however, the sliding speed is high in the middle part of the cylinder bore where an oil film can be formed between piston rings and cylinder wall [24]. The tribological properties of PEO coatings in different lubricating regimes are different. To study the tribological performances of PEO coatings, tribological tests have been done under different lubrications using pin-on-disc tests and reciprocating sliding tests, which were conducted at relatively low sliding speeds.

Low speed pin-on-disc tribological testing is used to measure the friction and sliding wear properties of the dry or lubricated surface of various bulk materials or thin films. Usually, small samples are used to do the lubricated tests. Due to the low speed, the lubricating condition in low speed pin-on-disc test is boundary lubrication. The tribological properties of PEO coatings in boundary are necessary to investigate, since the lubricating conditions in TDC and BDC area of the cylinder bore are of boundary lubrications. In the low speed pin-on-disc tribological tests, the contact between the counterface materials is microasperities contact, and hydrodynamic effects of lubricating oil or rheological characteristics of bulk do not significantly influence tribological characteristics in boundary lubricant. A better understanding of the tribological performance of PEO coatings in a boundary lubricating condition would benefit to minimize the COF in boundary lubricating frictions (in TDC and BDC areas).

Most of the time, an engine works at different speeds, and the sliding velocity of the piston ring on the wall of cylinder always changes. In the middle part of the cylinder bore, the sliding speed of piston is very high compared with that in TDC and BDC areas. The Stribeck curve was first used to illustrate a relationship between COF and sliding velocity under different lubrication conditions. When the speed is high enough, an oil pressure is generated, by the combination of surface topography, oil viscosity, and the surface moving speed, to support the load applied through on the counterface pin. The oil pressure increases with the increase of sliding velocity, and when it is high enough, the contact surfaces will be forced to separate. There will be an oil film between the two related contact surfaces, and the mixed and hydrodynamic oil lubricating conditions are

formed as a result [26]. In the mixed and lubricating regime, the frictional force between the counterfaces is a mix of solid contact friction and viscous shear force, and it is only viscous shear force in hydrodynamic lubrication. According to the Stribeck curve, which is an overall view of friction variation in the entire range of lubrication, including the hydrodynamic, mixed, and boundary lubrication regimes, the tribological properties are various in different lubricating regimes. Thus, a high speed pin-on-disc is essential to understand the tribological properties of PEO coatings under different lubricating friction regimes.

Different from the pin-on-disc test, the real contact between the piston rings and the wall of the cylinder is arc surface contact other than point to surface contact. The tribological properties can be affected by a number of factors, for example, the viscosity of the oil, the roughness of the counterface, the load, the sliding velocity, the temperature and the area of the counterface [27]. In this regard, a piston ring on PEO coated liner tribological test is essential to understand the tribological performance of piston ring on PEO coated liner with presence of oil lubricants.

In this work, the objective is to find an optimal PEO coating to improve the wear resistance and tribological properties of the surface of aluminum cylinder in regarding both of reducing engine's weight and friction to improve the fuel efficiency. Different kinds of aluminum alloy samples were treated by PEO process including small round-shaped samples, big ring-shaped samples, and aluminum liners. Different tribometers were used to carry out the tribological tests in different lubricating regimes. A low speed pin-on-disc tribometer was used to study the tribological properties of PEO coatings in the boundary lubricating regime. A high speed pin-on-disc tribometer was applied to study the tribological properties of PEO coatings under three lubrications including boundary, mixed and hydrodynamic lubrications. A high speed piston ring on liner tribometer was used to investigate the tribological properties of piston ring on PEO coated liner again in all above lubricating regimes. Surface roughness and sliding velocity effects on the COF of PEO coatings were particularly studied. Cast iron was used as reference material to compare the tribological properties with the PEO coatings.

## **Objective and contents of this study**

This project is to study the influence of sliding speeds on tribological behaviours of PEO coatings with different coating morphology through altering the process parameters and the degree of polishing.

The goal is to obtain knowledge of correlation between surface characteristics and friction, which can be applied on cylinder liners for friction reduction.

Contents of this study:

1. Develop plasma electrolytic oxidation (PEO) coatings on aluminium alloys for improving their wear resistance and tribological properties at a wide range of sliding velocities.

2. Investigate the surface roughness and sliding velocity effects on the COF of PEO coatings under the boundary lubrication using the low speed pin-on-disc tests.

3. Design a high speed pin-on-disc tribometer to generate different lubricating conditions, study surface roughness and sliding velocity effects on the COF of PEO coatings in all lubricating regimes, compare the tribological properties of PEO coatings with that of cast iron under the same experimental conditions.

4. Design a high speed piston ring on liner tribometer to study the tribological properties of piston ring on PEO coated liner in different lubricating regimes, particularly to study effects of surface roughness, sliding velocity and oil flow rate on the COF of PEO coated liner.

## **Organization of the thesis**

This thesis contains eight chapters. Chapter 1 gives introductory information on the usage of aluminum alloy in automotive applications and the need for improved wear resistance and tribological properties. Following the introduction, the relevant literatures regarding PEO coating technology on Al alloys and previous research on the PEO coating formation and tribological properties are reviewed in Chapter 2. Chapter 3 describes the experimental instruments and procedures. Chapter 4 reports investigation

results of surface roughness and sliding velocity effects on the COF of PEO coatings in the boundary lubricating regime, and wear resistance for different roughness. Chapter 5 presents the results and discussion of the surface roughness and sliding velocity effects on the COF of PEO coated A6061 aluminum alloy in all three lubricating regimes, including boundary, mixed, and hydrodynamic lubricating regimes. In chapter 6, two new PEO coatings were developed on A356 aluminum alloy, and their tribological properties were investigated under the three lubricating conditions with different surface roughness and sliding velocity. Cast iron was used as reference material for comparison. Chapter 7 presents tribological properties of the PEO coated aluminum alloy liner, exhibited during the study of roughness, sliding velocity and oil flow rate effects on the COF of the PEO coated liner. Chapter 8 is to summarize the research results of this thesis and also to provide suggestion of future work.

## References:

- [1] R. D. Naranjo, F. Huang, Her-Ping, M. Gwyn, Castings Drive Fuel Efficiency. *Modern Casting*; Sep 2004; 94, 9; ABI/INFORM Trade & Industry pg. 20.
- [2] A.M. Sherman, in E.A. Starke, Jr., T.H. Sanders, Jr., W.A. Cassada (ed.), *Aluminium alloys: their physical and mechanical properties*, Vol. 331-337, Part 1, Trans tech publications Ltd., 2000, p3-4.
- [3] Grosselle, Fabio, G. Timelli, Bonollo, Franco, et. Al. Correlation between microstructure and mechanical properties of Al-Si diecast engine blocks. *Metallurgical Science and Technology*. Vol 27-2 – Ed 2009.
- [4] Y. Sun, *Materials Letters* 58 (2004) 2635- 2639.
- [5] B.S. Shabel, D.A. Granger, W.G. Truckner, in D. Olson Hardbound (ed.), *ASM Handbook*, Vol. 18, 1992, p785-794.
- [6] A. A. Voevodin, A. L. Yerokhin, V. V Lyubimov, M. S. Donley, J. S. Zabinski, *Surface & Coatings Technology*, 86-87 (1996), 516-521.
- [7] A.E. Ostermann, *Experiences with Nickel-Silicon Carbide Coatings in Cylinder Bores of Small Aluminum Engines*, TP 790843, Society of Automotive Engineers, 1979.
- [8] J. W Cox, in R.F. Bunshah (ed.), *Handbook of Hard Coatings*, William Andrew Publishing, 2001, p420-457.
- [9] Y.C. Wang, S.C. Tung, *Wear*, 225-229 (1999), 1100-1108.
- [10] A.E. Ostermann, *Experiences with Nickel-Silicon Carbide Coatings in Cylinder Bores of Small Aluminum Engines*, TP 790843, Society of Automotive Engineers, 1979.
- [11] R.K. Betts, *Motor Vehicle Applications of Thermally Sprayed Specialty Coatings*, Proceedings of the 1st International Surface Engineering Congress and the 13th, IFHTSE, Congress of the International Federation for Heat Treatment and Surface Engineering, 13, ISEC, International Surface Engineering Congress, 2003, Vol 1, p 716-721.
- [12] D.R. Marantz, K.A. Kowalsky, J.R. Baughman, and D.J. Cook, *Plasma Transferred Wire Arc Thermal Spray Apparatus and Method*, U.S. patent No. 799242, Sept. 15, 1998.
- [13] P. Zhang, X. Nie, L. Han, and H. Hu, *SAE Int. J. Mater. Manuf.* 3, 55 (2010).
- [14] K. Bobzin, et al., *Thermal Spraying of Cylinder Bores with the PTWA Internal Coating System*, Conf. Proc., ASME Internal Combustion Engine, Charleston, SC,

ICEF07-1745, Oct. 14-17, 2007.

[15] Ford Motor press release,

[http://media.ford.com/images/10031/2011\\_GT500\\_Engine.pdf](http://media.ford.com/images/10031/2011_GT500_Engine.pdf), Feb. 2010.

[16] E.I. Meletis, X. Nie, F.L. Wang, J.C. Jiang, *Surface & Coatings Technology*, 150 (2002), 246-256.

[17] X. Nie, C. Tsotsos, A. Wilson, A.L. Yerokhin, A. Leyland, A. Matthews, *Surface & Coatings Technology*, 139 (2001), 135-142.

[18] A. L. Yerokhin, A. A. Voevodin, V. V. Lyubimov, J. Zabinski, M. Donley, *Surface & Coatings Technology*, 110 (1998), 140-146.

[19] X. Nie, E.I. Meletis, J.C. Jiang, A. Leyland, A.L. Yerokhin, A. Mathews, *Surface & Coatings Technology*, 149 (2002), 245-251.

[20] L.Rama Krishna, K.R.C. Somaraju, G. Sundararajan, *Surface & Coatings Technology*, 163-164 (2003), 484-490.

[21] G. Sundararajan, L. Rama Krishna, *Surface & Coatings Technology*, 167 (2003), 269-277.

[22] Su, J.F., X. Nie, H. Hu, and J. Tjong, Friction and counterface wear influenced by surface profiles of plasma electrolytic oxidation coatings on an aluminum A356 alloy, *J. Vac. Sci. Technol. A* 30, 061402 (2012); doi: 10.1116/1.4750474.

[23] G. Sundararajan, L.R. Krishna, Mechanisms underlying the formation of thick alumina coatings through the MAO coating technology, *Surf. Coat. Technol.* 167(2003) 269–277.

[24] C. Friedrich, G. Berg, E. Broszeit, F. Rick, and J. Holland, PVD CrxN coatings for tribological application on piston rings. *Surf. Coat. Technol.* 1997. 97(1-3): p. 661-668.

[25] G. Wang, X. Nie, J. Tjong, Effect of Surface Roughness and Sliding Velocity on Tribological Properties of an Oxide-coated Aluminum Alloy, SAE-2014-01-0957 (2014).

[26] B. Armstrong, C.C. de Wit, *Friction Modeling and Compensation, The Control Handbook*, (CRC Press, Boca Raton, 1995).

[27] B. Andersson, *Tribol. Ser.* 18, 503 (1991).

## Chapter 2

### LITERATURE REVIEW

Research showed that the carbon dioxide (CO<sub>2</sub>) generated by the burning of gasoline and diesel fuel in the automotive engines is contributing to global climate change [1]. A fuel economy program requires an increase of average fuel economy from 25 miles per gallon to 35.5 miles per gallon by 2016 [2]. This program would save 1.8 billion barrels of oil over the lifetime of the vehicles sold in the next five years. The increased miles per gallon should reduce greenhouse emissions by more than 900 million tons [3]. One approach to reduce the fuel consumption and improve fuel efficiency is to reduce the vehicle's weight and frictional loss between components. A modern car with components made of aluminum can reduce 24 percent weight of the one with components made of steel or cast iron, which also reduces the fuel consumption to 2 liters per 100 kilometers [4]. One hundred years ago, aluminum was first started to use in automotive industries. In that period, aluminum was a new and a poorly explored metal material. However, its light weight and corrosion resistance showed its great potential for the application in the automotive industries.

#### 1. Background of application of aluminum in automotive industry

The first sport car body made of aluminum was showed to the general public at the Berlin international motor show in 1899. The first engine assembled with aluminum parts was made two years later by Carl Benz, and this engine performed very nice in the testing [5]. However, a lot negative factors impeded the mass production of this kind of aluminum engine including difficulties in metal working, limited knowledge about aluminum, and the high prices. It was not until the 1940s that some automotive companies restarted research in to the application of aluminum in automotive industries. The first aluminum alloy engine was manufactured by Buick in 1961, and later this kind of engine was launched in mass production. This engine was an eight-cylinder V8 engine, and the weight was only 144 kg [6]. In the beginning, the aluminum engine was used in the race cars, and it demonstrated great performance in races. Later, this light engine was civilianized. The first aluminum engine is shown in Fig.2.1.





Fig.2.1 Buick 215 V8 aluminum engine [7].

In the seventies, the oil crisis broke out. All the car manufacturers began to search for ways to reduce the fuel consumption of the automotive. The best approach was to reduce the weight of the vehicle. The calculations showed that a medium size vehicle would save 700 liters of fuel during its serve lifetime by reducing its weight by 100 kg [8]. Thus, car manufacturers started to replace numerous car units using aluminum, therefore reducing the total weight of vehicles. Today, an average of 110-145 kg of aluminum is used in a passenger car [9]. Another way to reduce the fuel consumption is to reduce the frictional loss between components, including the frictional loss between piston rings and cylinder wall. Thus, a good understanding of the mechanical and tribological properties of aluminum alloy is essential.

## 2. The characteristics of aluminum

Aluminum is a kind of soft, durable, lightweight, ductile and malleable metal with a silvery appearance. Aluminum weighs roughly one-third as much as most of the common metals, but is one and a half times as heavy as magnesium. It is used to reduce the weight of components and structures, particularly in the area of transport, and aerospace. It is easily machined, cast, drawn and extruded [10]. Aluminum has a high strength-to-weight ratio which saves a lot commercially, when dead weight is decreased and payload of transport is increased. Aluminum has good thermal and electrical conductivities, having 59% of the conductivity of thermal and electrical compared with copper, while having

only 30% of copper's density. Aluminum is also capable of being a superconductor [11]. Aluminum has excellent corrosion resistance due to a thin surface layer of aluminium oxide that forms when the metal is exposed to air, effectively preventing further oxidation. However, the corrosion resistance will be decreased when other metals are alloyed to increase the hardness, because the other alloyed metals will have galvanic corrosion with aluminum [12].

Various types of aluminum alloys are continually being developed to improve their wear resistance and hardness. Among these alloys, aluminum-silicon (Al-Si) alloys have been found to have the potential to be beneficial in many industrial applications and can be used as substitutes for cast iron components. The silicon in the aluminum alloys can improve the corrosion resistance, casting, and machining characteristics [13]. Al-Si alloys typically have an elastic modulus of about 70 GPa, which is about one-third of the elastic modulus of most kinds of steel and steel alloys. Therefore, for a given load, a component or unit made of an Al-Si alloy will experience a greater deformation in the elastic regime than a steel part of the identical size and shape [14]. Even though aluminum alloys have a lot of advantages compared with other metals or alloys, they may not be good enough to be used as casting material for a cylinder bore in an engine block due to the mechanical and tribological requirements for the surface of the cylinder wall.

### 3. Functional requirements for material of the engine block

An engine block is the core of an engine which houses almost all of the components required for the engine to work properly. An engine block having more than 6 cylinders is typically arranged in a “V” inline, or 4 horizontally-opposed configuration, and the number of cylinders range from 3 to as many as 16. A typical aluminum cylinder engine block is shown in Fig.2.2.

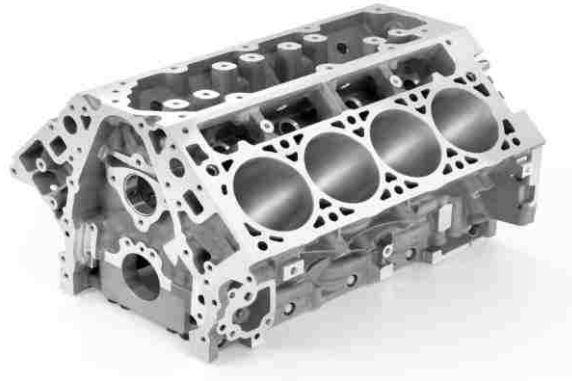


Fig.2.2 Aluminum cylinder block [15].

Because the engine block is a critical component of an engine, it must satisfy several functional requirements. These requirements include lasting the service life of the vehicle, housing internal moving parts and fluids, ease of service and maintenance, withstanding pressures created by the combustion process, withstanding the wear from the sliding move of piston rings, and having a low COF of the cylinder wall [14]. In order to meet the functional requirements listed above for an engine block, the engineering materials used to manufacture the engine block must have high strength, modulus of elasticity, abrasion resistance, and corrosion resistance [16]. Good machinability and castability of the metal alloy are also important factors in selecting the proper materials, since a harder material will cause a higher cost of the manufacturing [17].

Considering the material requirements of the engine block, cast iron and aluminum alloys are usually used as casting materials for engine blocks. Cast iron alloys are used because of the good mechanical properties, low cost, and availability [18]. Certain aluminum alloys combine the characteristics of iron alloys with low weight, thereby making the material appealing to automotive manufacturers. Compacted graphite cast iron is lighter and stronger than gray cast iron, making the alloy a more attractive alternative to the gray cast iron in the production of cylinder blocks [19]. The aluminum alloys can reduce the weight of the engine, but they cannot meet the tribological requirements for the surface of cylinder bore, such as wear resistance, corrosion resistance, and low COF. Thus, aluminum alloys cannot be used as cylinder material directly. Surface treatments or replacement by other material are necessary to improve the tribological properties of aluminum.

#### 4. Aluminum engine block with cast iron liners

In order to overcome the disadvantages of the low hardness and low wear resistance of the aluminum, the surface of the aluminum cylinder bore should be treated or replaced by other materials. Presently, cast iron liners are inserted in or cast in the aluminum engine block to increase the wear resistance. Cast iron liners have enough hardness to bear the wear from the motion of piston rings. The graphite cast inside the iron is also good for reducing the friction between piston rings and the wall surface of the cast liner [20]. Besides, crosshatches can be honed on the surface of cast iron liner, which is good for improving the oil retention.

Currently, most of the passenger cars use this kind of technology. However, the cast iron liners in aluminum engine blocks also suffer the inherent weight, thermal conductivity, and thermal expansion problems. The thermal conduction coefficients and thermal expansion of cast iron and aluminum alloys are different, and these will cause heat transfer and deformation problems [21]. The deformation of the liner gives rise to an increase of fuel consumption and emissions. Thus, this is not the best solution. An aluminum alloy engine block with cast iron liners is shown in Fig.2.3.



Fig.2.3 Aluminum cylinder engine block with inserted cast iron liners [22].

#### 5. Thermal spray coating treatment

One option to improve the wear resistance and tribological properties of the aluminum alloy cylinder bore is applying the thermal spray coatings on the soft

aluminum bore surface [23]. Thermal spray coatings are widely used in a variety of industrial applications, for example, they can protect products from wear, temperature extremes, and chemicals. Thermal spray coating processes are differentiated by heat source and base materials, including combustion flame spraying, high velocity oxy-fuel spraying (HVOF), two-wire electric arc spraying, plasma transferred wire arc (PTWA) spraying, and vacuum plasma spraying [24].

Now, the PTWA thermal spray coating is in commercial use on aluminum alloy engine blocks to protect the surface of the cylinder bores, for example, the Ford Mustang and the Nissan GTR. PTWA thermal spray coating is a nanoscale depositing coating, and the thickness of this coating can be varied easily by treatment time. It is also hard enough to bear the wear from the sliding piston rings. Due to the high density of the PTWA coating, the porosity of the coating is low (only 4%), so the oil retention is not good [25]. Crosshatches need to be honed on the surface of PTWA coating to increase the oil retention. Currently, Ford is trying to improve the PTWA process to increase the porosity up to 10% for a better oil retention [26]. The schematic view of PTWA spray process is shown in Fig.2.4.

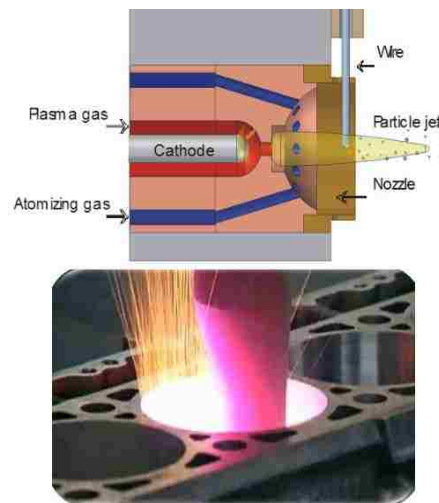


Fig.2.4 Schematic view of the PTWA spray process [27].

## 6. Plasma electrolyte oxidation coating treatment

Plasma Electrolytic Oxidation (PEO), also called Micro-arc oxidation (MAO), is a plasma-chemical and electrochemical process to generate an oxide coating on the lightweight metals. The process combines electrochemical oxidation with a high voltage spark treatment in the electrolytes, resulting in the formation of a physically protective oxide film on the metal surface to improve wear and corrosion resistance, as well as extending component's lifetime. It is similar to anodizing, but it employs higher potentials, and discharges occur to generate plasma modified structures of the oxide layer [28]. It is suitable for the surface oxidation and pigmentation of aluminum, titanium, niobium, zirconium, magnesium and their alloys. The PEO treated components are used in the building, mechanical, medical and energy sectors [29]. This technology is simple, low cost and can offer high quality coatings with high wear resistance and good tribological properties, as well as environmental friendliness. The PEO process is shown in Fig.2.5.

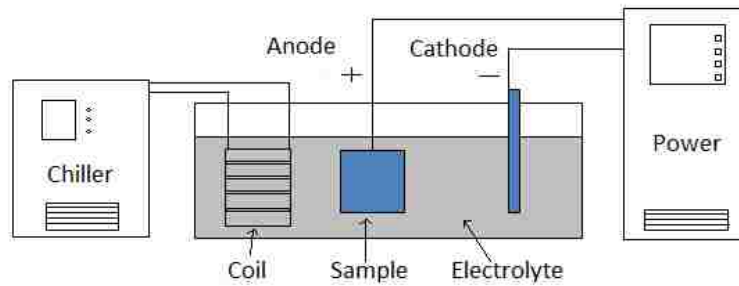


Fig.2.5 Schematic view of the PEO process.

This advanced anodizing process was developed by Russian scientists G.A. Markov and G.V. Markova in the mid-1970 [30]. In recent years, researchers in the United Kingdom, North America and China are also involved in this technology. This process can make dense, and very hard coatings on aluminum and aluminum alloy surfaces. An important characteristic of this coating is that the oxide layer grows both inwards and outwards from the aluminum substrate surface. Thus, the adhesion force of the coating is higher than those depositing coatings, such as PTWA coating. Because of those attractive

properties, recently the PEO coatings are investigated for automotive applications, particularly in powertrain parts.

Several studies have been done on the tribological properties of the PEO coatings. X. Nie [31] reported the effect of coating thickness on the tribological properties. The coatings with thickness from 100  $\mu\text{m}$  to 250  $\mu\text{m}$  were used to test the tribological properties using a ball-on-plate reciprocating-sliding tribometer with a load of 10N over 5000 cycles, at a frequency of 2 Hz. The COFs of the PEO coatings against bearing steel (BS) and tungsten carbide (WC) balls were measured and the results showed that those coatings all showed excellent wear resistance. PEO coating was applied on SAE 6061 aluminum alloy cylinder liners from a 4.6 L-V8 aluminum block engine. Frictional properties of the PEO coatings along with a cast-iron liner were evaluated in a cylinder bore/piston ring test. The results showed that the COF of PEO coating was significantly lower than that of cast iron [32].

Thus, PEO coating is a candidate to provide a wear resistant surface for the aluminum alloy cylinder bore. The PEO process is a cost effective, environmentally surface treatment for lightweight metals, especially for aluminum [33]. PEO coating can improve the lightweight metals' hardness, corrosion resistance (when sulphur-contained fuel is used), and thermal protection [34]. Compared with thermal spray coating, PEO coating has high adherent force to the substrate due to the coating grows both inwards and outwards from the surface of the substrate metal. The topography and thickness of the PEO coating can be changed by varying the current density and treatment time. The composition of the coating can also be changed by changing the chemicals in the electrolyte [35]. After the PEO treatment, a lot of crater-like holes are distributed on the surface of the coating, which is beneficial to improve the oil retention [36]. Sufficient oil retention is beneficial to reduce the wear and friction between piston rings and the coating surface. All these features demonstrate that the PEO coating can be qualified to provide a wear resistant and low COF surface for the aluminum cylinder bore.

## 7. Summary of literature review

Aluminum is a lightweight, corrosion resistant, and easily castable and machinable material, yet the wear resistance and the tribological properties inhibit its use. To reduce the fuel consumption and improve the fuel efficiency, automotive manufactures would like to use a high strength-to-weight ratio material to replace the heavy cast iron. The properties of aluminum have led to its common use in automotive industries. However, to be a viable casting material for an engine block, aluminum must overcome issues, such as low wear resistance and poor tribological properties. Cast iron liners are inserted or cast in the aluminum engine block to improve the hardness and tribological properties. Thermal spray coatings are also applied to protect the soft surfaces of aluminum cylinder, for example, PTWA coating is already successfully applied on the linerless aluminum engine block. The high wear resistance and excellent tribological properties of PEO coatings also allow them to be candidates to protect the soft surface of cylinder wall and reduce the frictional force.



## References:

- [1] C. Fabio, A. Akshay, W. Ian A, Y. H.L. Steve, R.H. Steven, (November 2013). Air pollution and early deaths in the United States. Part I: Quantifying the impact of major sectors in 2005. *Atmospheric Environment* (Elsevier) 79: 198–208. Bibcode: 2013AtmEn.79.198C. doi:10.1016/j.atmosenv.2013.05.081. Retrieved 25 October 2013.
- [2] Allen, Mike & Javer, Eamon, Obama announces new fuel standards, [www.politico.com](http://www.politico.com), accessed Oct 19, 2014.
- [3] Financial Trend Forecaster. Inflation Adjusted Average Annual Gasoline Prices 1918-2009, Copyright 2010. Chart prepared by Timothy McMahon, Updated 7/21//2010.
- [4] R. Naranjo, D. Huang, F. Her-Ping, Gwyn, Mike, Castings Drive Fuel Efficiency, *Modern Casting*; Sep 2004, 94, 9, ABI/INFORM Trade & Industry, pg. 20.
- [5] Mid-Atlantic Casting Services. A Guide to Aluminum Casting Alloys. [www.Mid-AtlanticCasting.com](http://www.Mid-AtlanticCasting.com).
- [6] Flory, J. Kelly, Jr. *American Cars 1946-1959* (Jefferson, NC: McFarland & Coy, 2008), p.1021.
- [7] [http://www.hemmings.com/hsx/stories/2011/04/01/hmn\\_feature22.html](http://www.hemmings.com/hsx/stories/2011/04/01/hmn_feature22.html).
- [8] Inventory of U.S. Greenhouse Gas Emissions and Sinks: 1990-2008. U.S. Environmental Protection Agency. April 15, 2010.
- [9] G. Valtierra, Salvador et al. Wear-Resistant Aluminum Alloy for Casting Engine Blocks with Linerless Cylinders. Patent Application – Publication Number: WO 2008/053363 A2. 8 May 2008.
- [10] I.J. Polmear, (1995). *Light Alloys: Metallurgy of the Light Metals* (3rd ed.). Butterworth-Heinemann. ISBN 978-0-340-63207-9.
- [11] J.F. Cochran, D.E. Mapother, Superconducting Transition in Aluminum, *Physical Review* 111 (1): 132–142. Bibcode: 1958 PhRv.111.132C. doi:10.1103/PhysRev.111.132.
- [12] Vargel, Christian (2004) [French edition published 1999]. *Corrosion of Aluminium*. Elsevier. ISBN 0 08 044495 4.
- [13] R.E. Sanders, Technology Innovation in aluminium Products, *The Journal of The Minerals*, 53(2):21–25, 2001.

- [14] E.P. Degarmo, J.T. Black, Kohser, A. Ronald (2003). *Materials and Processes in Manufacturing* (9th ed.). Wiley. p. 133. ISBN 0-471-65653-4.
- [15] Keay, Sue: Diet of Australian metal lightens cars and pollution, Media release, 14 October 2002.
- [16] Anonymous, Aluminum Cylinder Block for General Motors Truck/SUV engines, A Design Study in Aluminum Casings, pp. 1-31.
- [17] P.N. Anyalebechi, *Essentials of Materials Science & Engineering*, January 2005, p. 94.
- [18] K.G. Budinski, M.K. Budinski, *Engineering Materials: Properties and Selection*, Prentice Hall of India Ltd., 2006.
- [19] *Metals Handbook: Properties and selection of Non-ferrous alloys and pure metals*, American society of metals (ASM), USA, 1979.
- [20] E. Köhler, J. Niehues, K.U. Kainer, *Metal Matrix Composites: Custom-made Materials for Automotive and Aerospace Engineering*, Wiley-VCH, Weinheim, pp.95–108 (2006).
- [21] Grosselle, Fabio, G. Timelli, Bonollo, Franco, et al., Correlation between microstructure and mechanical properties of Al-Si die cast engine blocks. *Metallurgical Science and Technology*. Vol 27-2 – Ed 2009.
- [22] <http://www.knowyourparts.com/technical-articles/installing-cylinder-sleeves>.
- [23] R.K. Betts, *Motor Vehicle Applications of Thermally Sprayed Specialty Coatings*, Proceedings of the 1st International Surface Engineering Congress and the 13th, IFHTSE, Congress of the International Federation for Heat Treatment and Surface Engineering, 13, ISEC, International Surface Engineering Congress, 2003, Vol 1, p 716-721.
- [24] D.R. Marantz, K.A. Kowalsky, J.R. Baughman, and D.J. Cook, Plasma Transferred Wire Arc Thermal Spray Apparatus and Method, U.S. patent No. 799242, Sept. 15, 1998.
- [25] K. Bobzin, et al., Thermal Spraying of Cylinder Bores with the PTWA Internal Coating System, Conf. Proc., ASME Internal Combustion Engine, Charleston, SC, ICEF07-1745, Oct. 14-17, 2007.
- [26] Ford Motor press release, [http://media.ford.com/images/10031/2011\\_GT500\\_Engine.pdf](http://media.ford.com/images/10031/2011_GT500_Engine.pdf), Feb. 2010.
- [27] <http://www.iot.rwth-aachen.de/index.php?id=915>.

- [28] G.A. Markov and G.V. Mmarkova, USSR Patent 526961, Bulletin of Inventions, 32 1976.
- [29] A.V. Nikolaev, G.A. Markov, B.I. Peshchevitskij, Izv. SO AN SSSR. Ser. Khim. Nauk, 5 (12) (1977), 32.
- [30] G.A. Markov, V.V. Tatarchuk, M.K. Mironova, Izv. SO AN SSSR. Ser. Khim. Nauk, 3 (7) (1983), 34.
- [31] X. Nie, A. Leyland, H.W. Song, A.L. Yerokhin, S.J. Dowey, A. Matthews, Surface and Coatings Technology, 116-119 (1999), 1055-1060.
- [32] V.D.N Rao, H.A. Cikanek, B.A. Boyer, SAE paper, 970022, 1997.
- [33] X. Nie, X. Li, and D. O. Northwood, Mater. Sci. Forum. 546, 1093 (2007).
- [34] X. Nie, X. Li, L. Wang, and D. O. Northwood, Surf. Coat. Tech. 200, 1994 (2005).
- [36] A. L. Yerokhin, X. Nie, A. Leyland, A. Matthews, and S. J. Dowey, Surf. Coat. Tech. 122, 73 (1999).
- [36] P. Zhang, X. Nie, L. Han, and H. Hu, SAE Int. J. Mater. Manuf. 3, 55 (2010).

## Chapter 3

### EXPERIMENTAL PROCEDURES

#### 1. Low speed pin-on-disc tests

The tribological tests were carried on the low speed pin-on-disc tribometer, and the COF data were recorded by a data acquisition system. The experiments were carried out in an environment at room temperature (24°C) and ~50% humidity. SAE 5W-20 full synthetic motor oil was selected to do the low speed oil tests. The load was 10 N, and the steel balls (3mm in radius) were used as the counterface materials.

Small A356 Al alloy samples (discs of 1 inch in diameter) were treated by PEO process, and the coated samples were polished from  $R_a = 0.8 \mu\text{m}$  to  $R_a = 0.3 \mu\text{m}$  on the polishing machine using polishing cloth and powder. The stylus type surface profilometer was employed to measure the surface roughness.

The rotation speed was changed from 4 r/s to 6 r/s and then to 8 r/s stepwise. Accordingly, the sliding velocity was changed from 0.050 m/s to 0.075 m/s then to 0.100 m/s. The low speed pin-on-disc tests would run 50 m at each velocity, and 150 m for each roughness. During the test, the volume of the oil was kept at the same level. After the pin-on-disc test, the electron microscope was used to observe the wear track on the coating, and measure the ball wear. The low speed pin-on-disc test instruments are shown in Fig.3.1.

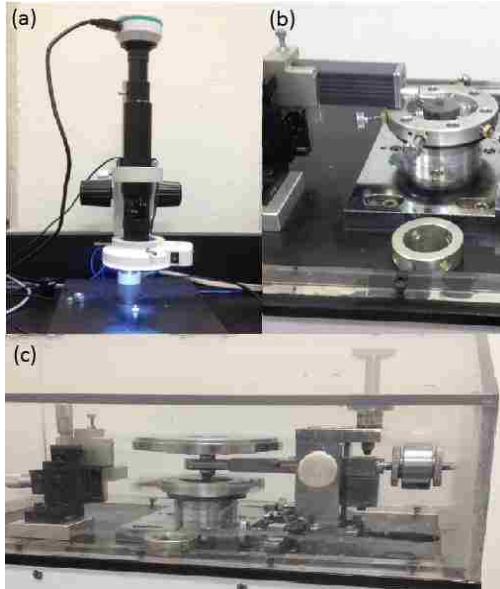


Fig.3.1 Experimental instruments of low speed pin-on-disc tests, (a) Optical microscope, (b) stylus type surface profilometer, (c) low speed pin-on-disc tribometer.

## 2. High speed pin-on-disc tests

In the high speed pin-on-disc tests, A6061 and A356 aluminum-silicon cast alloys were used as substrate materials. The alloys were machined to a ring shape with a dimension of 105 mm (outer diameter)  $\times$  78 mm (inner diameter)  $\times$  12 mm (thickness). The large diameter of the ring-shaped sample could generate high sliding velocities when the rotational speed was high.

The high speed pin-on-disc tribometer was used to generate different lubrications including boundary, mixed, and hydrodynamic lubricating conditions. The oil tribological tests were carried out at a room temperature of 24 °C and a humidity of around 50-60%. SAE 5W-20 full synthetic motor oil was selected to do the oil tests. An oil tube was installed in front of the pin and the oil flow rate was high enough (100 ml per-minute) to make sure that there was enough oil to form the mixed or hydrodynamic lubricating regimes at high sliding velocities. The load for the oil tribological tests was 10 N. AISI 52100 steel balls (3 mm in radius), as pins, were used as counterface material, and the rotation diameter of the wear track was 100 mm.

Two kinds of PEO coatings were produced on each material. The coatings' surfaces were polished to have different roughnesses. Surface roughness and sliding velocity

effects on the COF of the PEO coating in different lubricating regimes were particularly studied. Cast iron was used as reference material for comparison. The high speed pin-on-disc tribometer is shown in Fig.3.2.

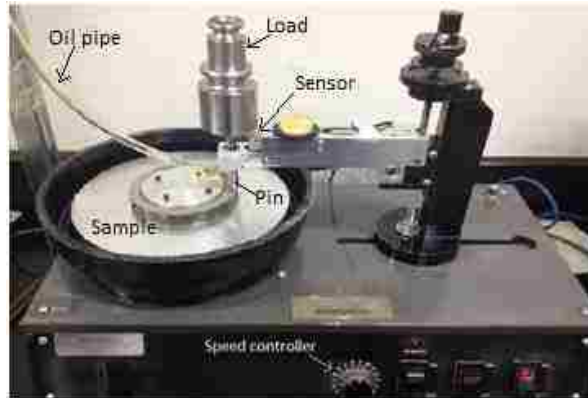


Fig.3.2 High speed pin-on-disc tribometer.

### 3. High speed piston ring on liner tests

In this test, A356 aluminum alloy liner was selected to do the test. The inside diameter of the liner was 87.5 mm, and the length of the liner was 130 mm. In the PEO process, a spray head was used to spray the electrolyte on the inside surface of the liner and produce a PEO coating on the liner. An 800 grit flex honing brush was used to polish the inside coating surface to have different roughnesses. A liner holder was designed to hold the liner and installed on the disc of the high speed pin- on-disc tribometer. Segments of piston ring were used as counterface material, and a special piston ring holder was designed to hold the segment of piston ring. 5W-20 synthetic oil was used as lubricant, and the load was 10 N. Surface roughness, sliding velocity, and the oil flow rate effects on the COF of the PEO coated liner in different lubricating regimes were particularly studied. The piston ring on liner tribometer is shown in Fig.3.3.

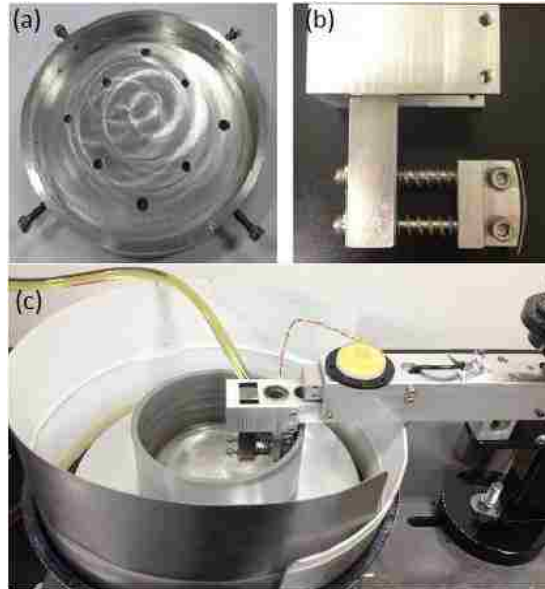


Fig.3.3 High speed piston ring on liner tribometer, (a) liner holder, (b) piston ring holder, (c) high speed piston ring on liner tribometer.

## CHAPTER 4

### Effect of Surface Roughness and Sliding Velocity on Tribological Properties of an Oxide-coated Aluminum Alloy

#### 1. INTRODUCTION

Aluminum alloys, known as weight-saving materials, have already been widely used in the area of automotive and aerospace. To be an engineering material, the hardness and strength are both taken in to account, so the aluminum-silicon alloys are the most popular materials in industry [1]. Aluminum engine has been successfully used to replace the heavy gray cast engine to lighten the car's weight and reduce the fuel consumption. Compared with aluminum alloys, the gray cast iron liners have high hardness and higher wear resistance [3, 4]. However, the aluminum alloys are not very wear-resisting. It is obvious that the good wear-resisting property is very important to the engine block life. Many engineers have done research to find a solution to reduce the wear between the cylinder and the sliding piston ring [2].

The PEO technique was successfully used to produce an oxide coating on the surface of aluminum alloy. This kind of coating can adhere on the aluminum alloy firmly and is not easily worn out. It is a good solution to enhance the wear resistance between the cylinder and the sliding piston ring. However, the surface roughness of the coating affects the friction between the cylinder and the piston a great deal [5]. The most simple friction model:  $COF = \tan \theta$ , where  $\theta$  meant the angle between the asperity and the surface, had already been proposed by Bowden and Amontons (1699) [6]. It was found that the smoother the surface, the lower the COF is. In 1975, Bayer and Sirico found that the wear was more sensitive to the low roughness [7]. However, roughness has different effects on different materials. For example, for SiC, the smoother the surface, the lower the COF is, for  $Al_2O_3$ , higher the roughness is, the lower the COF is [8]. So roughness effect on tribology properties is very complex.

In order to conserve more fuel, a stopping and restarting system was introduced to reduce the amount of time the engine spent idling [13]. This system would force the engine to shutdown and restart when the vehicle was forced to stop immediately for a



short time in the heavy traffic. It was known that when the engine was restarted, the reciprocating speed of piston was low and the resistance was high because of the inertia. So the friction between the piston and the cylinder would be high, and the wear of the PEO coating and the piston would be greater. This reduced the engine block life.

In this work, the tribology test will be done on different samples with different roughness and different sliding velocities to simulate this situation, and find a suitable combination of roughness and sliding velocity to reduce the wear and COF. The roughness will be changed a lot in a large scale. After the test, all the data will be compared together to get a whole picture of the relationship between the roughness and COF. At the same time, the velocity will be changed during the tribological test on different roughness.

The relationship between the different sliding velocities and the COF tested on the same roughness and different roughness will be studied in this work. After these two effects are studied separately, they will be combined together to get the lowest COF. So a proper combination of coating surface roughness and sliding velocity could provide a significant lower COF.

## 2. EXPERIMENT DETAILS

In this work the PEO technique was used to get the coating. After treatment different aluminum alloys would get different coating. In order to simulate the true engine block, A356 was chosen to do the experiment (circular coupons:  $3.14 \times 12.52 \times 4 \text{ mm}^3$ ). The composition of the A356 alloy (in wt.%) was 6.5~7.5%Si, 0.20~0.40%Mg,  $\leq 0.20\%$  Fe,  $\leq 0.20\%$  Cu,  $\leq 0.10\%$  Mn,  $\leq 0.10\%$  Zn,  $\leq 0.20\%$  Ti,  $\leq 0.05\%$  other elements (individual),  $\leq 0.15\%$  other elements (total), and the balance Al [10].

To compare different experimental conditions' effects on the coating and COF, three substrates were prepared for the PEO coating process. The samples were identified by S1, S3, and S7. The number 1, 3, 7 meant three different solution. The No.1 solution only contained 8% sodium silicate which helped the sample to discharge under the high voltage. The No.3 solution was added a kind of additive which was supposed to be

helpful to decrease the friction between the coating and the pin, the volume of this additive was medium. However, the No.7 solution was similar to No.3 solution, but the volume of the additive was four times more than No.3. After treated, three kinds of coating were ready for the tests. The original roughness and thickness of the coatings were recorded.

In order to get smooth coating surface, all the substrates were polished to  $R_a = 0.1 \mu\text{m}$  ( $R_a$  means roughness). After polished, all the samples were washed by distilled water and dried by air. Then the electrolytic plasma process (EPP) was carried out under the symmetrical AC power source (60 Hz).

In this work, the unipolar power was used, and the current density was  $0.06 \text{ A/cm}^2$ . The positive electrode was connected to the sample, and the negative electrode was connected to the solution container. The EPP treatment continued 15 minutes, and the temperature of the solution was controlled around  $45\text{-}50^\circ\text{C}$  by the tap water cooling system. After the EPP treatment, 3 different coatings with different colors and thickness were produced. The original parameters of the coatings were shown in the Table 4.1, and Fig.4.1.

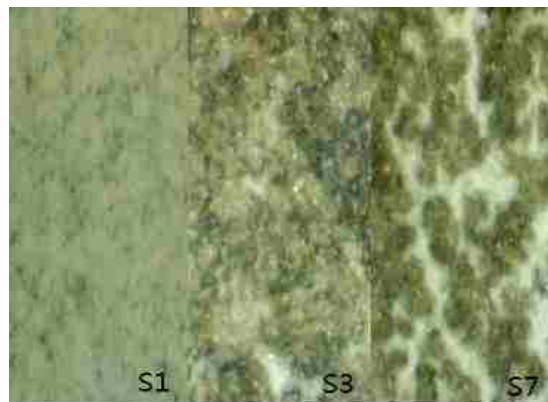


Fig.4.1 Coated samples before polishing

Table 4.1 Process parameters, thickness and roughness of coatings.

Samples(A356)	Treat time(min)	Roughness( $\mu\text{m}$ )	Thickness( $\mu\text{m}$ )
S1	15	2.23	18
S3	15	2.15	16
S7	15	3.32	16

Treated by different solution and current, the surface morphology and roughness would be different. As shown in Table.4. 1 and Fig.4.2, the samples which were treated by the No.3 solution had smaller roughness, and higher density. The color of the samples became darker and darker from S1 to S7, which meant the additive had already grown inside the coating.

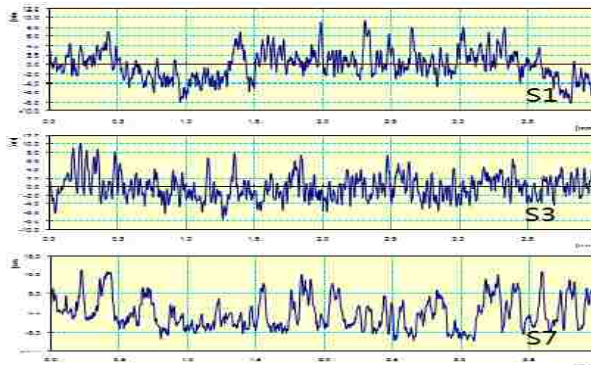


Fig.4.2 Surface topography of coated samples

The tribological tests were carried on the pin-on-disc tribometer, and all the data were recorded by software. The experimental environment was kept at a room temperature ( $24^{\circ}\text{C}$ ) and  $\sim 31\%$  humidity. The tribological tests were oil tests, and SAE 5W-20 full synthetic motor oil was selected to do the tests. Each tribological testing was carried out under the 10N normal load, the steel balls (3 mm in radius) were used as the counterface material, and the rotation diameter was 4 mm. All the coated samples were polished from  $R_a = 0.8 \mu\text{m}$  to  $R_a = 0.3 \mu\text{m}$  on the polishing machine using polishing cloth and powder, and the stylus type surface profilometer was employed to measure the surface roughness. The rotation speed was changed from 4 r/s to 6 r/s and then to 8 r/s stepwise. Accordingly, the sliding velocity was changed from 0.050 m/s to 0.075 m/s

then to 0.100 m/s. The pin-on-disc test would run 50 m at each velocity, and 150 m for each roughness. During the rotation test, the volume of the oil was kept at the same level. After the pin-on-disc test, the electron microscope was used to observe the wear track on the coating, and measure the ball wear.

### 3. RESULTS AND DISCUSSION

#### 3.1 The effect of roughness

In order to find the effect of surface roughness on the tribological properties on the coating, especially at the low sliding velocity range, all the samples were polished from  $R_a = 0.8 \mu\text{m}$  to  $R_a = 0.3 \mu\text{m}$ . Each sample was polished four times to get the four different degrees of roughness. After each polish, the roughness and the thickness of the coating were measured and recorded. All the roughness and thickness are listed in Table.4.2.

Table 4.2 Roughness and thickness of all samples after polish.

Polishing process	Sample A356	S1	S3	S7
After 1st step of polishing	Roughness( $\mu\text{m}$ )	0.78	0.8	0.75
	Thickness( $\mu\text{m}$ )	13	11	10.5
After 2nd step of polishing	Roughness( $\mu\text{m}$ )	0.68	0.69	0.63
	Thickness( $\mu\text{m}$ )	11	9.5	9
After 3rd step of polishing	Roughness( $\mu\text{m}$ )	0.5	0.51	0.51
	Thickness( $\mu\text{m}$ )	7	9	8.5
After 4th step of polishing	Roughness( $\mu\text{m}$ )	0.3	0.36	0.34
	Thickness( $\mu\text{m}$ )	4	8	8

In the process of polishing, the S1 sample was easy to polish, and the others were difficult to polish. The data from Table 4.2 show that the thickness of sample S1 decrease much faster than sample S3, and S7. It proves that the coatings treated by No.1 solution are softer than those treated by No.3 solution and No.7 solution. That means the additive in No.3 and No.7 solution can improve the coating's hardness.

The roughness and top morphology of the coatings were measured and recorded by the stylus type surface profilometer. Four surface profiles of S3 with different roughness were shown in Fig.4.3. The curve in the figure showed that the less the coating was polished, the thicker the coating was, and the holes on the coating were much deeper which was good for holding the oil. The oil was stored in the holes and an oil film was formed on the surface of coating. The oil film on the coating can reduce the friction and protect the coating [9]. However, the surface roughness of the cylinder could not be much high in the reality, otherwise, the wear of the cylinder and the piston would be so much that the engine could not serve for a long time. So a suitable roughness should be found to reduce the wear and friction when the vehicle was forced to stop and restart.

At the same time, the skewness  $R_{sk}$  of the samples was also measured by the profilometer. Skewness of the surface was found important to the tribological Properties. Skewness describes the asymmetry of the height distribution histogram. If  $R_{sk} = 0$ , height distributions on the surface is balanced. If  $R_{sk} < 0$ , it means surface is flat with holes, and if  $R_{sk} > 0$ , the surface is even with peaks. The skewness and kurtosis of different samples were show in Table 4.3. All  $R_{sk}$  numbers are negative, but there was no obvious pattern of COF vs skewness in this research where a boundary lubricating condition was applied.

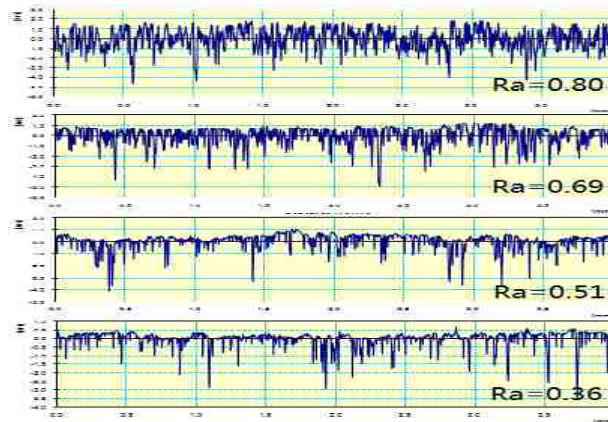


Fig.4.3 Surface morphology of S3 after polish

Table 4.3 Skewness and kurtosis of all samples after polish.

SampleA356	S1	S3	S7
Roughness( $\mu\text{m}$ )	0.78	0.8	0.75
Skewness( $\mu\text{m}$ )	-1.92	-0.62	-0.48
Roughness( $\mu\text{m}$ )	0.68	0.69	0.63
Skewness( $\mu\text{m}$ )	-1.61	-0.88	-2.13
Roughness( $\mu\text{m}$ )	0.5	0.51	0.51
Skewness( $\mu\text{m}$ )	-2.23	-0.76	-1.10
Roughness( $\mu\text{m}$ )	0.3	0.36	0.34
Skewness( $\mu\text{m}$ )	-1.38	-2.05	-2.03

The pin-on-disc tribometer was employed to analyze the tribological properties of the coating. In this test, the rotation speed was kept at 4 r/s. The load was 10 N, and the roughness of the coating was changed from 0.8  $\mu\text{m}$  to 0.3  $\mu\text{m}$ . The volume of the oil was also kept the same during this test. In this way, the influence of roughness could be studied. After the test, the COF was calculated and the ball wear was captured by electron microscope. The COF and ball wear were shown in Table 4.4 and Table 4.5. A group of COF drafts were chosen to shown in Fig.4.4 and the ball wears wear shown in Fig.4.5 to Fig.4.7.

Table 4.4 COF of each sample with different roughness.

Roughness( $\mu\text{m}$ )	$R_a=0.8$	$R_a=0.6$	$R_a=0.5$	$R_a=0.3$
S1(COF)	0.095	0.107	0.112	0.108
S3(COF)	0.091	0.105	0.107	0.106
S7(COF)	0.099	0.11	0.18	0.15

Table 4.5 Ball wears of each sample with different roughness-displayed in diameter ( $\mu\text{m}$ ).

Roughness( $\mu\text{m}$ )	$R_a=0.8$	$R_a=0.6$	$R_a=0.5$	$R_a=0.3$
S1-ball wear( $\mu\text{m}$ )	557.53	475.21	443.58	410.43
S3-ball wear( $\mu\text{m}$ )	475.02	465.18	410.76	392.71
S7-ball wear( $\mu\text{m}$ )	748.30	525.09	516.66	439.97

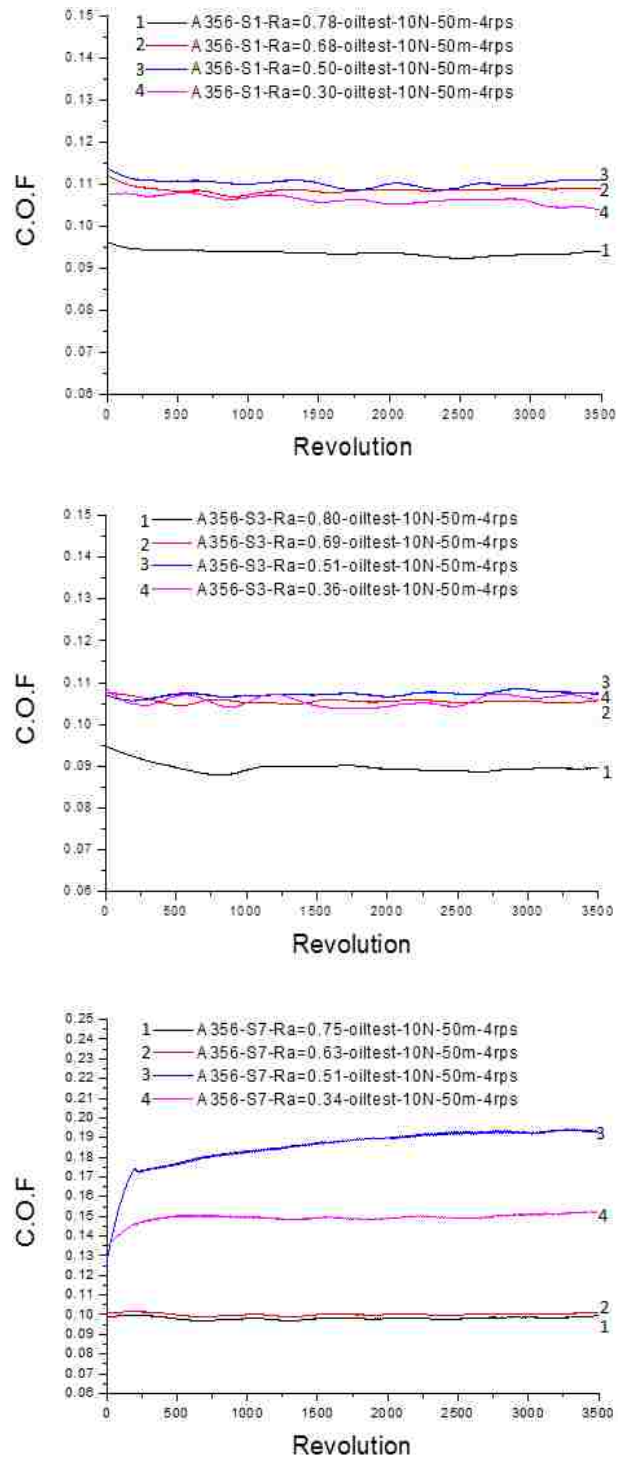


Fig.4.4 COF of A356 samples with different roughnesses.

Table 4.3 and Fig.4.4 present the relationship between COF and roughness of the coatings. It is obvious that with the roughness decreases from 0.8  $\mu\text{m}$  to 0.5  $\mu\text{m}$ , the COF

increases continuously. However, when the roughness reduces from  $0.5 \mu\text{m}$  to  $0.3 \mu\text{m}$ , the COF trend stops to go up and begins to drop down. As mentioned before, the more the coating was polished, the thinner the thickness was, and the shallower the holes on the coating were. As a result, the oil stored in the holes would become less and less [11]. According the data from Table 4.3, the roughness affects the COF a lot, and there is a turning point in the relationship between the roughness and COF. The turning point is the value of the roughness. Before this value, the roughness and the COF have inverse relationship, and the oil plays the leading role of reducing the friction. After this value, the roughness and the COF have the positive relationship. In this work, the turning point may be around  $R_a = 0.3 \mu\text{m}$  to  $R_a = 0.5 \mu\text{m}$ .

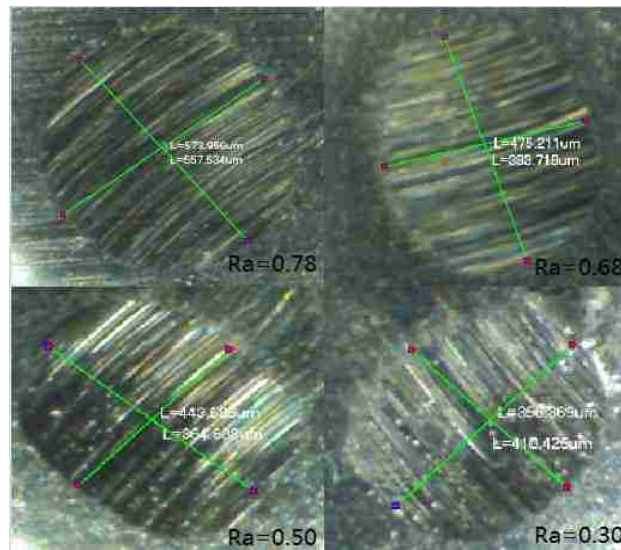


Fig.4.5 Ball wears after tested on sample S1.



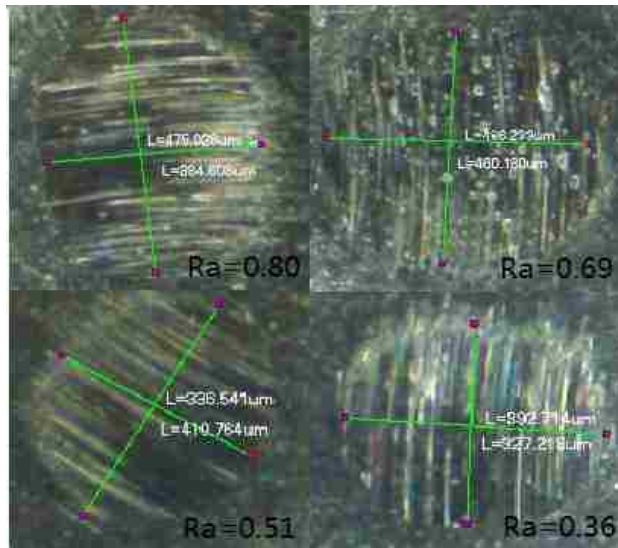


Fig.4.6 Ball wears after tested on sample S3.

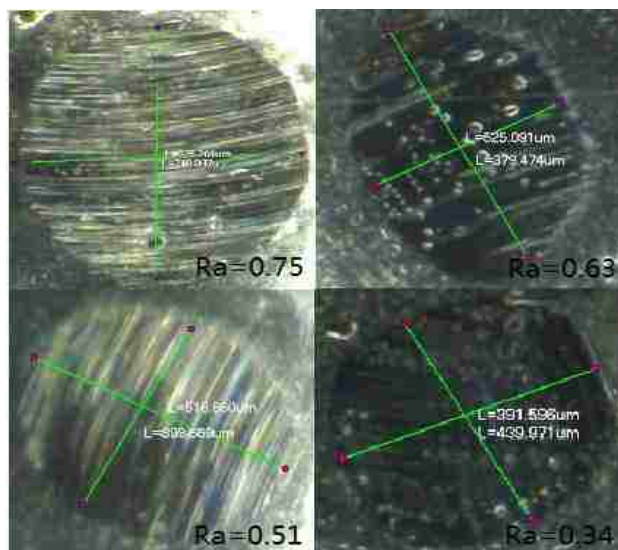


Fig.4.7 Ball wears after tested on sample S7.

Table 4.4 shows the relationship between roughness and ball wear. Obviously, they have the positive relationship. Low roughness leads to slight ball wear. Fig.4.5 to Fig.4.7 recorded the degrees of the ball wear. It was interesting that the ball wear tested on S3 was much smaller than others. That meant the additive in No.3 solution was helpful to reduce the wear. However, the amount of the additive in solution should be moderate, not the more the better. The amount of the additive in No.7 solution was twice of that in No.3 solution, but the degrees of ball wear tested on S7 were much higher. In order to reduce

the wear between the piston and the coating on the cylinder, the surface roughness of the coating should be lower, and a certain amount of the additive was necessary.

### 3.2 The effect of velocity

In this test, all the experiment conditions were stable, only the rotation speed was increased stepwise during the test. The pin-on-disc tribometer was employed to do the test and record the experiment data. The roughness of the sample is  $0.6 \mu\text{m}$ , and the rotation speed was changed from 4 r/s to 6 r/s and then to 8 r/s stepwise. After the test, the COF was calculated, and shown in Table 4.6.

Table 4.6 The COF of each sample tested at different velocity ( $R_a=0.6\mu\text{m}$ ).

Velocity	4r/s	6r/s	8r/s
S1(COF)	0.107	0.106	0.104
S3(COF)	0.105	0.102	0.10
S7(COF)	0.101	0.095	0.094

In order to see the relationship directly, a group of data was selected randomly to draw a curve. The relation was shown in Fig.4.8.

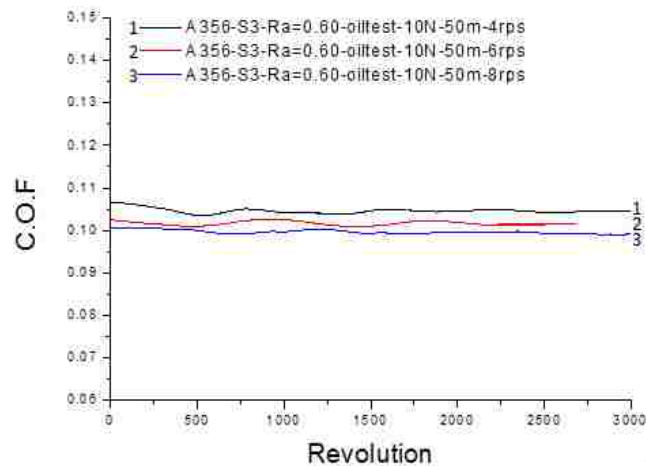


Fig.4.8 The relationship between COF and velocity.

Table 4.6 and Fig.4.8 show the relationship between the COF and the velocity. The COF and the velocity have the inverse relation, which means the COF will decrease when

the velocity rises. In this work, in order to simulate the stop-restart system, the velocity should be changed in a very small range. However, this conclusion is only valid in this low sliding velocity range.

### **3.3 The effect of oil thickness**

These oil tests were used to simulate the real situation of cylinder, so SAE 5W-20 full synthetic motor oil was used to do the tests. A few drops of oil were dropped on the surface of the sample to work as the lubricant. The volume of the oil was not too much, but the steel ball which was fixed on the pin could immerse in the oil. In order to investigate the formation of hydrodynamic friction conditions, the Stribeck-curve was generated by a specific tribo-system. Generally, this curve described all the characters of any lubricated system: boundary friction conditions, mixed friction behavior with lubrication effects and remaining contact of the surface peaks, and the hydrodynamic motion for high velocity. In this work, the sliding velocity was increased from 0.05 m/s to 0.075 m/s and to 0.1 m/s, which was a very low sliding velocity in the stribeck-cure. Although the speed was changed and some oil was swung out, the oil still adhered to the ball. So the influence of the oil thickness was very small. The purpose of this work was to study the tribological properties at the boundary friction conditions. The mixed friction behavior and the hydrodynamic motion for high velocity would be studied later.

### **3.4 Other influences on COF**

There are many other factors affect the COF, for example, the material of the substrate, the additive in the solution, and the different treatments to get the coating. According to the data shown ahead, sample S1 have higher COF compared with samples S3 and S7. This may be caused by the different surface morphology which was generated by the different solution during the PEO process [12]. That means the additive has the function of reducing the friction. Here, the effect of surface roughness and sliding velocity are mainly talked about. Suitable roughness combined with suitable sliding velocity will get the lower COF and less wear. In this work, if set the sliding velocity at 8 r/s and polished the coating to  $R_a = 0.8 \mu\text{m}$ , the COF would be the lowest, however, the ball wear would be the largest. If the COF and the wear were both valued, the

combination of  $R_a = 0.3 \mu\text{m}$  and  $V = 8 \text{ r/s}$  was the best one. If the friction between the piston and the coating on the cylinder was lower, the engine could be easily restarted, and more fuel would be conserved. Besides, if the wear of the coating and the piston was less, the engine would serve a long time. So in the reality, with the population of the stop-restart control system, the roughness and sliding velocity effects should be considered. According to this work, the rotational speed of the starting motor should be higher, and the roughness of the coating on the cylinder should be lower.

#### 4. CONCLUSION

The surface roughness of the coating and the coefficient of friction had a dynamic relation at the tested boundary lubricating conditions. There was a roughness acted as a demarcation point. If the roughness was higher than this point, the COF increased accompanied with the reduction of roughness. If the roughness was lower than this point, the COF decreased accompanied with the reduction of roughness. The sliding velocity and the COF had inverse relation. With the increase of sliding velocity, the COF decreased. Therefore, a proper combination of coating surface roughness and sliding velocity could provide a significant lower COF. More research is needed at high sliding velocities where a mixed or hydrodynamic lubricating condition can form.

Copyright © 2014 SAE International. This paper is included in this thesis with permission from SAE International. Further use, copying or distribution is not permitted without prior permission from SAE.

## References

- [1] X. Nie, L. Wang, E. Konca, A.T. Alpas, *Surface & Coatings Technology*, 188–189, 207–213, 2004.
- [2] J.F. Su, X. Nie, and H. Hu, J. Tjong, Friction and counterface wear influenced by surface profiles of plasma electrolytic oxidation coatings on an aluminum A356 alloy, *Vacuum Science and Technology A*, (30) 061302-11, 2012.
- [3] A.D. Sarkar, *Friction and Wear*, Academic, London, 1980, doi:10.1016/0043-1648(80)90120-9.
- [4] P. Zhang, X. Nie, H. Henry, and J. Zhang, *Surface & Coatings Technology*, 205, 1689, 2010, doi:10.1166/jnn.2010.1668
- [5] S.F. Tian, L.T. Jiang, Q. Guo, G.H. Wu, Effect of surface roughness on tribological properties of TiB<sub>2</sub>/Al composites, *Materials and Design* 53, 129–136, 2014, doi:10.1016/j.matdes.2013.02.074.
- [6] R. Bayer, J. Sirico, The influence of surface roughness on wear, *Wear* 35:251–60, 1975. doi:10.1016/0043-1648(75)90074-5.
- [7] A. Wang, H. Rack, Dry sliding wear in 2124 Al–SiCw/17-4 PH stainless steel systems, *Wear* 147:355–74, 1991.
- [8] S. Natarajan, R. Narayanasamy, SPK. Babu, G. Dinesh, et al, Sliding wear behaviour of Al6063/TiB<sub>2</sub> in situ composites at elevated temperatures, *Mater Des* 30:2521–31, 2009.
- [9] X. Nie, A. Wilson, A. Leyland, A. Matthews, *Surface & Coatings Technology*, (121) 506, 2000.
- [10] J. Martina, A. Melhema, I. Shchedrina, T. Duchanoya, et al, Effects of electrical parameters on plasma electrolytic oxidation of aluminium, *Surface & Coatings Technology* (221), 70–76, 2013. doi:10.1016/j.surfcoat.2013.01.029.
- [11] X. Nie, L. Wang, Z.C. Yao, L. Zhang, et al, Sliding wear behaviour of electrolytic plasma nitrided cast iron and steel, *Surface & Coatings Technology*, (200), 1745-1750, 2005. doi:10.1016/j.surfcoat.2005.08.046.
- [12] R.O. Hussein, P. Zhang, X. Nie, Y. Xia, et al, "The effect of current mode and discharge type on the corrosion resistance of plasma electrolytic oxidation (PEO) coated

magnesium alloy AJ62, " Surface & Coatings Technology, (206), 1990–1997, 2001.  
doi:10.1016/j.surfcoat.2011.08.060.

[13] B. Dunham (October 1974). Automatic on/off switch gives 10-percent gas saving.  
Popular Science. p. 170.

## CHAPTER 5

### Surface effect of a PEO coating on friction at different sliding velocities

#### 1. INTRODUCTION

It is well known that the energy and global warming problems have been of great concern. The governments pay more and more attentions to the environment protection and the energy conservation. The vehicles consume gasoline and exhaust carbon dioxide into the air. Research showed that the carbon dioxide (CO<sub>2</sub>) generated by the burning gasoline and diesel fuel in the automotive engines is contributing to global climate change [1]. The public's perception of the importance of automobile fuel efficiency becomes more and more popular. The united States also proposed a new fuel economy program which requires an increase of average fuel economy from 25 miles per gallon to 35.5 mile per gallon by 2016 [2]. This program would save 1.8 billion barrels of oil over the lifetime of the vehicles sold in the next five years. The increased miles per gallon should cut greenhouse emissions by more than 900 million tons [3]. The government has urged the automakers to design the vehicles with more fuel economy and less carbon dioxide emissions [4]. One of cost-effective ways for improving the powertrain efficiency is to reduce the frictional loss and the powertrain's weight.

At present, most of the heavy cast iron engine blocks for passage cars are replaced by aluminum engine blocks conjuncts with iron liners [5]. The commonly-used aluminum material surface doesn't have the good tribological properties, and not hard enough to resist the wear between components, so cast iron liners are inserted in the aluminum engine block. The cast iron liners can meet the required tribological characteristics, and the cast iron liners are cheap, durable, and recyclable. In this way, the weight of the vehicle can be reduced greatly and at the same time the required surface tribological characteristics can also be reserved. Historically, this solution worked for a long time. However, there are also some inherent defects for the combination of cast iron liners and aluminum engine blocks, such as weight, thermal conductivity, and thermal expansion mismatching problems [6]. The different thermal expansion coefficients will cause an

increased distortion of cylinder bores, which may lead to increase the friction between the piston and the cast iron liner, the consumption of oil and fuel, and the release of carbon dioxide emissions [7].

Aluminum engine block without liners is also proposed as a solution for further reducing the weight of engine block. Removing the cast iron liners in the aluminum engine block will lighten the weight of engine block more for gasoline engines [8]. However, the material of the cylinder has to be strong enough to bear the high temperature, high pressure and heavy load. Usually, the pressure generated by the combustion process in the cylinder can go up to 100 to 200 bar [9]. The surface of the cylinder bore has to be hard enough to against the wear from the piston and piston rings piston sliding on the surface. Requirements for the surface of the cylinder bore include good oil retention, high wear resistance, low coefficient of friction, and long serving life time. Good oil retention of the surface of cylinder bore is very important, because the bad oil lubricant will induce wear and scuffing on the surface of cylinder which is fatal damage to the engine. Besides, the coefficient of the friction of the cylinder material affects the fuel efficiency of the vehicle greatly. The frictional loss between piston rings and the surface of cylinder bore accounts for more than 20% of the total vehicle power loss [10]. Considering the requirements above, surface treatment on the surface of the cylinder is needed before the linerless aluminum cylinder bore can be applied.

Several surface treatment techniques have already been available in the market, for example, Alusil, Nikasil, Lokasil, plasma transferred wire arc (PTWA) thermal spray coating, and other plasma coatings. The thermal spray coatings (e.g., PTWA) are already applied on the aluminum engine block cylinders in the mass production. Ford mustang GT500 is a good example. In the PTWA process, a single conductive wire is used as feedstock material and it is melted by a supersonic plasma jet. The wire is melt and atomized, then the molten particles are transferred to the cylinder wall by forced gas. After the particles are cooling down, they deposit and form a flat coating on the surface of cylinder wall [11, 12]. PTWA thermal spray coating provides a chance for automakers to remove the cast iron liners out of the aluminum engine block. However, there is a



room for improvement in reducing cost, for instance. Research and exploration for a better solution have never been stagnant.

Plasma electrolytic oxidation (PEO) coating is also a kind of surface treatment technique that automakers are interested in. PEO treatment can be applied on different metals, such as aluminum, magnesium, and titanium. The PEO coating on the surface of the aluminum engine cylinder can protect the surface of cylinder. PEO process is a low cost and environment friendly treatment which is an electrochemical surface treatment for generating an oxide coating on metals. It is similar to the hard anodizing, but it applies a much higher potential to induce the discharge and plasma on the surface of substrate, then the oxide coating is generated. It converts the substrate metal to its oxide, and the oxide coating grows both inward and outward from the original substrate surface. The hard PEO coating grows from the substrate other than deposit on the top of surface of substrate metal, so the adhesion strength of the PEO coating will be very strong. The surface morphology, roughness, and thickness of the PEO coating can be easily varied by changing the current density, solution composite, and the treat time [13]. A large number of pores are formed during the discharging, which is good for oil retention. Tribological tests at low sliding speeds have been done, and the results show that the tribological performance of PEO coating could be better than that of cast iron. If the PEO coating can be successfully applied to protect the surface of aluminum cylinder bore, it will be a transformative change in the automobile industry.

Reducing the weight of the vehicle is a good approach to improve the fuel efficiency and reduce the emissions. The engine fuel efficiency would be also improved, if the frictional loss can be reduced [14]. Normally, the frictional force is thought to be constant when the material roughness and pressure are fixed. Actually, the frictional force can be affected by a lot of factors in the tribological tests, such as environment temperature, lubricant, and sliding velocity. The COF of PEO coating is also affected by those factors. Tribological tests have been performed on a traditional (low speed) pin-on-disc tribometer (the sliding speed is less than 1 m/s) to study the roughness and sliding velocity effect on PEO coating [15]. The results show that the COF reduces with the decreases of the roughness from  $R_a = 0.80 \mu\text{m}$  to  $R_a = 0.30 \mu\text{m}$ , and the COF goes up

with the decrease of roughness from  $R_a = 0.30 \mu\text{m}$  to  $R_a = 0.1 \mu\text{m}$ . At boundary lubricant condition, the COF decreases slightly when the sliding velocity increases [15]. Actually, the contact between the piston rings and the surface of cylinder bore is dynamic, and the oil lubricating conditions will be changed when the sliding speed of piston changes. It is very important to study the roughness and sliding velocity effect on the COF of PEO coating, especially when the sliding velocity is very high, because the reciprocating speed of piston can be very high when the engine runs.

While, a traditional pin-on-disc tribometer can only test at low sliding speeds (less than 1m/s), the authors have developed a high speed pin-on-disc tribometer which can be used to generate a Stribeck curve [16] covering a whole spectrum of boundary, mixed and hydrodynamic lubricating conditions. In this study, the tribological performance of PEO coating was studied at mixed and hydrodynamic oil lubricants. Large ring-shaped disc samples (diameter was 110 mm) were coated by PEO process for the tribological tests in engine oil. The high speed (up to 6 m/s) pin-on-disc tribometer was employed to do the oil tribological tests, and the boundary, mixed and hydrodynamic oil lubrications can be formed with the increase of sliding speed. Roughness and sliding velocity effect on the COF was studied at mixed and hydrodynamic lubricant conditions.

## 2. EXPERIMENT DETAILS

In this work, Al 6061 was conveniently selected as the substrate material. After plasma electrolytic oxidation (PEO) treatment [6], the oxide coating on Al 6061 was smoother and denser compared with a similar coating on Al-Si alloys. The porosity of the coating on Al 6061 was also lower. Tribological performance of the PEO coating on Al 6061 was studied in this paper. The experience accumulated here would benefit for future investigation into coated Al-Si engine alloys.

High speed pin-on-disc tribological tests were carried out on the PEO coatings which were deposited on large ring-shaped disc samples in order to have a high sliding velocity ( $V = 2\pi Rn$ , where  $R$  is radius of wear track, and  $n$  is rotation speed in per second (rps)). The aluminum rings had a dimension of 110 mm (external diameter)  $\times$  78 mm (internal diameter)  $\times$  12 mm (height). In order to avoid the substrate's surface roughness

influence on the coating's topography, the top surface of each aluminum ring was polished to mirror-like finish, and the roughness went down to 0.1  $\mu\text{m}$ . The shape of the aluminum ring is shown in Fig.5.1.



Fig.5.1 The ring-shaped aluminum 6061 sample.

Two different concentrations of electrolyte were used to treat the Al rings. Since the growth rate of PEO coating in a diluted electrolytic solution (S-3) was half, the treatment time was double, compared to the case in a concentrated solution (S-2), in order to have a similar initial coating thickness. The samples treated in solutions S-2 and S-3 were correspondingly named as S-2 and S-3. The power supplied for the PEO process was a pulsed DC power (2000 Hz). A tap water cooling system was used to cool down the solution. After the electrolytic plasma oxidation process, colors of the coatings were different. Coating S-2 was yellow, while, coating S-3 was black. The original roughness and thickness of the coatings were measured. The coated samples are shown in Fig.5.2, and the original roughness and thickness of the coatings are shown in Table 5.1.



Fig.5.2. PEO coated samples S-2 and S-3.

Table 5.1 The original roughness and thickness of two PEO coatings.

Samples	Roughness( $\mu\text{m}$ )	Thickness( $\mu\text{m}$ )
S-2	0.34	21
S-3	2.12	20

As shown in Table 5.1, original roughness of coating S-2 was significantly lower than that of coating S-3. Besides, the thickness of coating S-2 was slightly higher than coating S-3 even though the PEO treatment time of S-2 was shorter. The surface profiles of the PEO coatings were measured by Mitutoyo surface profiler SJ201P and presented in Fig.5.3.

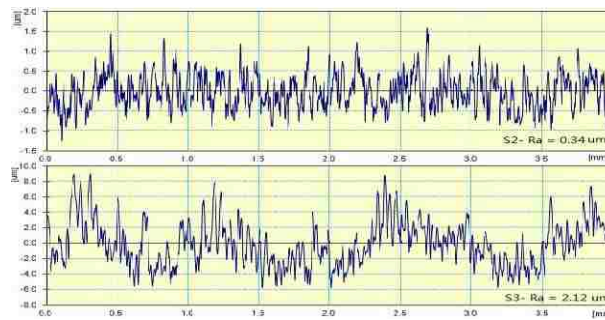


Fig.5.3. The original profile of two PEO coatings.

Fig.5.3 showed that the coating S-2 was flat with small valleys (due to the holes) distributed uniformly. Coating S-3 was different; it had a waved topography with a lot of small holes on it. This kind of topography might be good for oil retention and reducing the COF at the mixed and hydrodynamic oil lubricating conditions.

A high speed pin-on-disc tribometer was used to do the oil tribological tests on the PEO coatings. The speed of the tribometer can be changed from low to high. The highest sliding velocity can go up to 6.0 m/s where mixed or hydrodynamic oil lubrication can be formed. In this way, the tribological performance of PEO coating especially the COF of PEO coating in mixed and hydrodynamic lubricating regimes can be studied. SAE 5W-20 full synthetic motor oil was used as oil lubricant. AISI 52100 Steel balls (3 mm in radius)

were used as counterface materials. The load applied on the counterface was 10 N. The PEO coatings were polished to different roughness and then used to do oil tests to see the roughness effects on COF at different modes of lubrications. In order to distinguish the sliding velocity effect on COF, the rotation speed of the high speed pin-on-disc tribometer was increased step by step up to 1200 rpm (20 rps). When the sliding velocity was high enough, the mixed and hydrodynamic lubricating could be formed. After each tribological test, the wear scar of the steel ball was measured using an optical microscope.

### 3. RESULTS AND DISCUSSION

#### 3.1 Roughness effect on the COF of PEO coating

Both PEO coatings were polished several times to get different surface roughness. The original roughness of coating S-2 was pretty low, and the surface of the coating could be polished easily to mirror-like finish. The surface roughness of S-2 was polished to various levels from  $R_a = 0.30 \mu\text{m}$  to  $R_a = 0.05 \mu\text{m}$ , and S3 was polished from  $R_a = 0.80 \mu\text{m}$  down to  $R_a = 0.20 \mu\text{m}$ . When the surface roughness of the coating decreased, the thickness of the coating reduced either. The roughness and thickness changes were recorded and shown in Table 5.2.

Table 5.2 Changes of roughness and thickness after polish.

PEO coating S-2		PEO coating S-3	
Roughness ( $\mu\text{m}$ )	Thickness ( $\mu\text{m}$ )	Roughness ( $\mu\text{m}$ )	Thickness ( $\mu\text{m}$ )
0.30	20	0.80	15
0.20	18	0.60	12
0.10	16.5	0.40	10
0.05	15	0.30	9
N/A	N/A	0.20	8

The coating thickness in Table 5.2 showed that coating S-2 could be polished very smooth and the thickness of the coating could be reserved more. While coating S-3 was

different, the thickness of the coating reduced greatly when the surface roughness was polished to  $R_a = 0.20 \mu\text{m}$ . The topography of the coatings changed with the surface roughness. The surface profiles of the coatings were recorded and shown in Fig.5.4 and Fig.5.5.

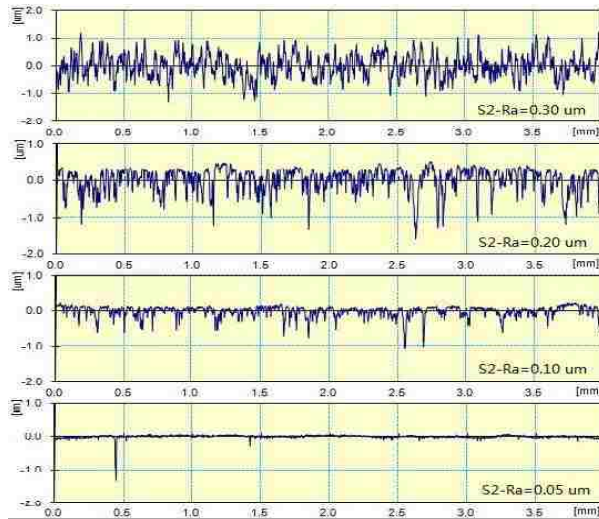


Fig.5.4. Surface profile of polished coating S-2.

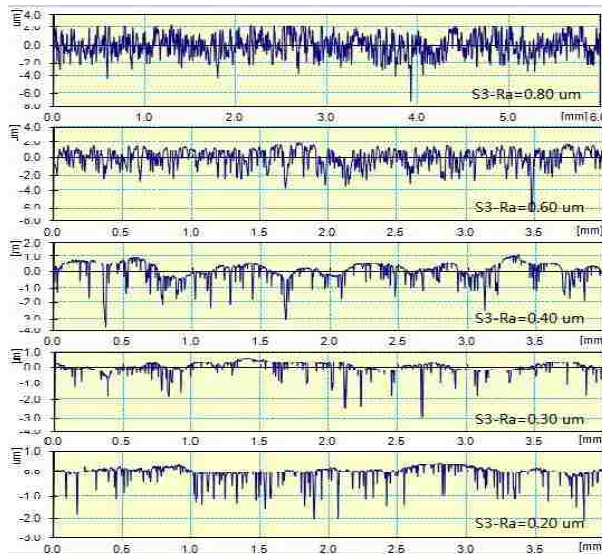


Fig.5.5. Surface profile of polished coating S-3.

The profiles in Fig.5.4 and Fig.5.5 showed that the thickness of the coating reduced with the decrease of the surface roughness. The depth of the holes on the coating also

became shallow when the roughness decreased. Compared with the flat profile of coating S-2, coating S-3 had a wavy surface profile, and the holes on coating S-3 were deeper than that on coating S-2. When the two samples were coated in the PEO process, high voltage was applied to induce the plasma discharge on the samples. The discharge process generated a large number of holes on the coating. However, the strength of the discharge was different because of the different solutions. The discharge strength of coating S-3 was much stronger than that of coating S-2. That was the reason why the holes on coating S-3 were more and deeper than that of coating S-2. Suppose these holes were beneficial for oil retention and the formation of oil film at mixed or hydrodynamic oil lubricating conditions.

The roughness effect on the COF of PEO coating at boundary lubrication has already been studied [5], where the sliding velocity was slow (0.050 m/s to 0.075 m/s) and the contact between the steel ball and the coating was solid point contact. The results showed that the COF would increase with the decrease of the roughness from  $R_a = 0.80 \mu\text{m}$  to  $R_a = 0.30 \mu\text{m}$ , and the COF would then decrease with the decrease of roughness from  $R_a = 0.30 \mu\text{m}$  to  $R_a = 0.10 \mu\text{m}$  [15]. When the sliding velocity is high enough, the mixed and hydrodynamic lubrications would be formed. The contact between the steel ball and the coating would not be solid contact, there was an oil film between the steel ball and the coating, and the frictional force should be from shearing force of the oil film. So the roughness effect on the COF of PEO coating at mixed and hydrodynamic lubrications would be different from the effect at boundary lubricating.

The tribological tests in this work were carried out on the high speed pin-on-disc tribometer. The sliding velocity was increased step by step, the highest speed could go up to 6 m/s, according to the circular motion formula:  $V = 2\pi Rn$  ( $R = 0.05 \text{ m}$ ,  $n = 20 \text{ rps}$ ). The raw data of each test was recorded and transferred in to COF of the coatings. The relationships between the roughness and the COF of two kinds of coatings are shown in Fig.5.6 and Fig.5.7.

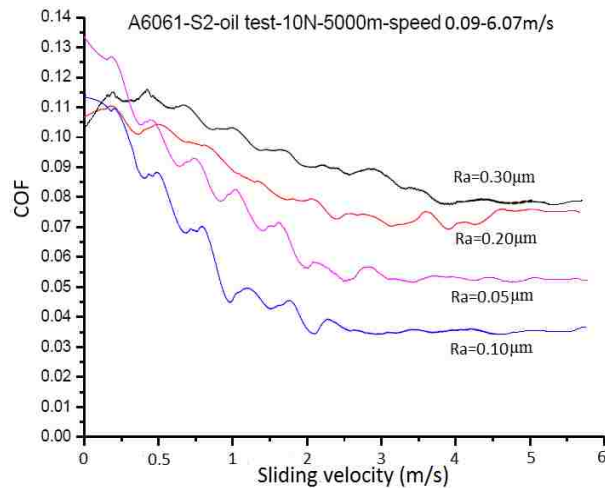


Fig.5.6. Roughness effect on the COF of PEO coating S-2.

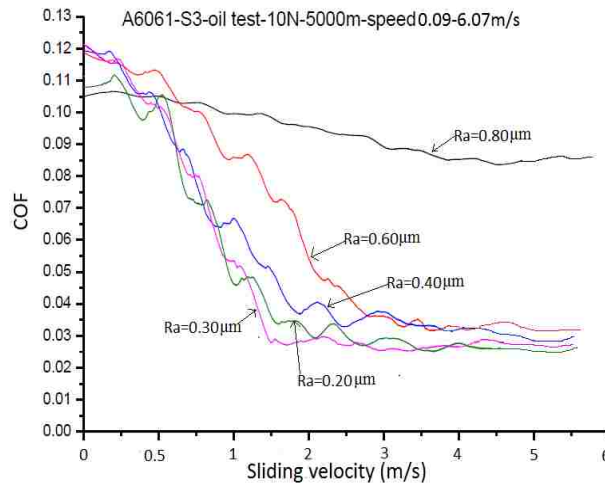


Fig.5.7. Roughness effect on the COF of PEO coating S-3.

The results showed that the roughness affected the COF values of PEO coating significantly. Actually, the roughness also affected the descent rate of the COFs. For all the cases, the COF decreased when the sliding speed was increased. However, the descent rate of the COF was different because of the different surface roughness. Fig.5.6 and Fig.5.7 showed that the descent rate of the COF was low when the roughness was high. On the contrary, the descent rate of the COF was high when the roughness was low. Furthermore, the results also showed that the smoothest surface did not have the lowest COF. The COF of the PEO coating was reversed to increase when the surface roughness was low to certain degree (in this case, S-2:  $R_a < 0.1\mu\text{m}$ , S-3:  $R_a < 0.3\mu\text{m}$ ). For example,



the COF of coating S-2 was the lowest (0.035) when  $R_a = 0.10 \mu\text{m}$ . However, the COF went up to 0.055 when  $R_a = 0.05 \mu\text{m}$ . For coating S-3, the lowest COF was 0.025 when  $R_a = 0.30 \mu\text{m}$ . However, the COF rose to 0.03 when  $R_a = 0.20 \mu\text{m}$ . Surface profile in Fig.5.4 and Fig.5.5 showed that the depth of valleys (holes on the coating) became shallow when the roughness decreased, and then the oil retention of the coating became degraded. During the measurement of the coating roughness, DIN (German roughness measurement standard) standard was also applied to measure the facts of  $R_{pk}$ ,  $R_{vk}$ ,  $R_k$ ,  $Mr_1$ , and  $Mr_2$ , which were used to calculate the oil retention volume. The oil retention volume was calculated by the formula:  $V_o = R_{vk} (100 - Mr_2) / 200$  in  $\mu\text{m}^3/\mu\text{m}^2$ . Those data were shown in Table 5.3.

The data in Table 5.3 showed that the oil retention volume changed with different surface roughness. Usually, high roughness possessed deep holes on the surface, but the oil retention might not be good. Fig.5.5 shows the profile of coating S-3, indicating that a large number of deep holes existed on the surface when the roughness was  $0.80 \mu\text{m}$ . However, the oil retention volume was low. On the other hand, the oil retention capability was also inadequate when the polished coating surface was too smooth. Smooth surface was strong to bear the load, but the valleys on the surface were not deep enough to possess good oil retention.

Table 5.3 DIN factors and volumes of holes on PEO coating.

Factors	S-2				S-3				
	0.30	0.20	0.10	0.05	0.80	0.60	0.40	0.30	0.20
$R_a(\mu\text{m})$	0.30	0.20	0.10	0.05	0.80	0.60	0.40	0.30	0.20
$R_{pk}(\mu\text{m})$	0.27	0.10	0.10	0.09	0.42	0.22	0.31	0.09	0.17
$R_{vk}(\mu\text{m})$	1.64	1.32	1.28	1.07	2.01	1.90	1.25	1.19	1.09
$R_v(\mu\text{m})$	0.94	0.75	0.70	0.63	2.40	2.09	1.10	0.66	0.64
$Mr_1$	7%	2%	6%	4%	7%	4%	5%	2%	12%
$Mr_2$	92%	89%	87%	86%	92%	89%	82%	80%	79%
$V_o(\mu\text{m}^3/\mu\text{m}^2)$	0.066	0.072	0.08	0.074	0.08	0.104	0.112	0.119	0.114

Data from Table 5.3 showed the oil retention volume of coating S-3 increased from the case of  $R_a = 0.80 \mu\text{m}$  to  $R_a = 30 \mu\text{m}$ , but it decreased from the case of  $R_a = 0.30 \mu\text{m}$  to  $R_a = 0.20 \mu\text{m}$ . Table 5.3 and Fig.5.6 and Fig.5.7 showed that an inferior oil retention surface would induce a high COF. Therefore, in order to obtain a low COF, the coating surface needs to be polished to have an optimized surface profile.

### **3.2 Sliding velocity effect on the COF of PEO coating**

In order to study the sliding velocity effect on the COF of the PEO coating, the rotating speed of the pin-on-disc tribometer was changed during the test. The results in Fig.5.6 and Fig.5.7 also showed effect of sliding velocity on the COF. When the sliding velocity increased, the COF of coating decreased, like a typical Stribeck curve showed. The Stribeck Curve is a plot of the friction as it relates to viscosity, speed and load. The vertical axis is COF, while the horizontal axis is combination of  $\text{mN/p}$  (m: oil viscosity, N: speed, p: load) [16]. Here, the oil viscosity and load were constant, only the speed was increased continuously. The mixed and hydrodynamic lubrications are formed when the surface topography, oil viscosity, and surface motion speed combine to increase the oil pressure enough to support the load. When the pressure is high enough, the surfaces are forced to separate apart, and an oil film is formed between the pin and the coating surface. The friction force will decrease greatly when oil film is formed between the separated surfaces at mixed and hydrodynamic oil lubricating conditions [16]. Test on coating S-3 ( $R_a = 0.30 \mu\text{m}$ ) was chosen as example to study the sliding velocity effect. The sliding velocity effect was shown in Fig.5.8.

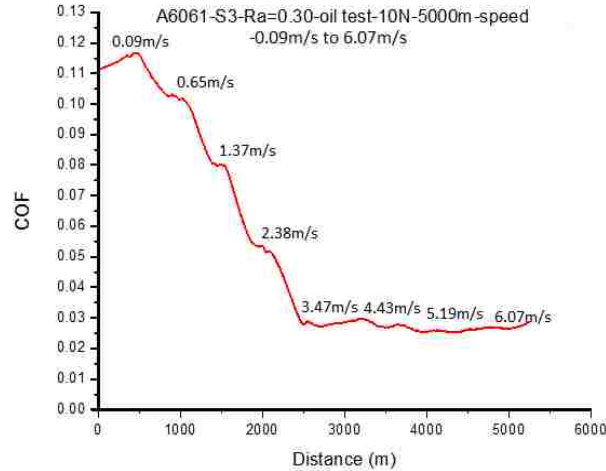


Fig.5.8. Sliding velocity effect on COF of PEO coating S-3.

The result in Fig.5.8 showed that the COF dropped quickly when the sliding velocity increased. The mixed oil lubricant was formed between speed of 0.09 m/s and 3.47 m/s. The COF decreased sharply at the mixed oil lubrication. From 3.47 m/s to 6.07 m/s, the hydrodynamic oil lubrication was formed. After this hydrodynamic oil lubricating started to take place, the COF stopped decreasing but increasing slightly as the contrary. At the mixed and hydrodynamic oil lubrications, the contact between the steel ball and the surface of the coating was not a solid contact. Because of the high sliding velocity, the steel ball pin floated on the oil film and the friction force between the steel pin and coating became viscous shear force. Compared with the real contact-induced friction force, the viscous shear force was much lower, and the COF was much lower correspondingly. That seems one of the reasons why the vehicle's fuel economy is better at high express way.

Compared the results in Fig.5.6 and Fig.5.7, the sliding velocity effect on the COF of the PEO coating S-3 was more distinct. The descent rate of COF on coating S-3 was higher than that on coating S-2, which meant the COF of coating S-3 was more sensitive on sliding velocity. However, the sliding velocity effect was also different on the same roughness of coating S-2 and S-3. The COF of coating S-2 dropped from 0.115 to 0.08 when the sliding velocity increased from 0.09 m/s to 6 m/s (for a case of  $R_a = 0.30 \mu\text{m}$ ), while, the COF of coating S-3 reduced from 0.108 to 0.025 when sliding velocity

increased to 6 m/s (for a case of  $R_a = 0.30 \mu\text{m}$ ). The profiles in Fig.5.4 and Fig.5.5 show that the topography of coating S-2 and S-3 were different even the roughness were same. Table 5.3 also shows that coating S-3 had a better oil retention than coating S-2 ( $R_a = 0.30 \mu\text{m}$ ). So coating S-3 had a better tribological performance when the sliding velocity increased. Besides, the sliding velocity could be increased to around 4.5 m/s to obtain the lowest COF (0.035) on coating S-2 of  $R_a = 0.10 \mu\text{m}$ , while, it was around 3.5 m/s to obtain the lowest COF (0.025) on coating S-3 ( $R_a = 0.30 \mu\text{m}$ ). Thus, an even lower COF could be obtained at a lower sliding velocity on coating S-3 compared with coating S-2, and the sliding velocity effect on coating S-3 was more distinct.

### 3.3 Steel ball wear against the PEO coatings

After each test on the PEO coating, both of the steel pin ball and the coating were observed using an optical microscope. Under the microscope, the wear track on the coating could not be seen which meant the hardness of the coating was high enough to resist the wear. However, the wear on the steel ball could be observed. All the ball wear were measured and shown in Table 5.4.

Table 5.4 Ball wears vs different coating roughness - showed in diameter.

PEO coating S-3		PEO coating S-2	
Roughness( $\mu\text{m}$ )	Ball wear( $\mu\text{m}$ )	Roughness ( $\mu\text{m}$ )	Ball wear( $\mu\text{m}$ )
0.80	553	0.30	350
0.60	522	0.20	291
0.40	461	0.10	262
0.30	412	0.05	254
0.20	388	N/A	N/A

The measured results showed that the ball wear on coating S-2 was smaller than the wear on coating S-3. The different topography of the two coatings resulted in the different wear. The surface of coating S-2 was much smoother than coating S-3, and the holes on coating S-2 were less and shallower. Although there was difficulty to precisely

measure coating hardness, the hardness of coating S-2 was believed to be lower than that of coating S-3. As a result from those facts, the ball wear on coating S-2 was smaller.

Compared these two coatings, each had its own advantages and disadvantages. For example, the COF of coating S-2 was not that low, but the ball wear caused by coating S-2 was less and the thickness of the coating could be reserved more after polish. For coating S-3, the COF was low, but the ball wear was relatively high. For the application on engine cylinder, both of these two coatings can be polished to a specific roughness to get a low COF and minor wear.

#### 4. CONCLUSIONS

The effect of surface roughness and sliding velocity on the COF of PEO coating at mixed and hydrodynamic oil lubrication is significant. When the sliding velocity is high enough, the mixed and hydrodynamic oil film lubricating can be formed. The surface roughness affects the descent rate of the COF of the PEO coating. When the surface roughness is high, the descending rate of the COF is low, and the COF doesn't decrease much when the sliding velocity increases. A smooth surface exhibits a low COF in general. However, an over-polished surface shows a reversed trend.

The sliding velocity also affects the COF of PEO coating. When the sliding velocity increases, the COF decreases. At the mixed oil lubricant stage, the COF decreases significantly with the increasing of sliding speed. At the hydrodynamic oil lubrication, the COF value is the lowest for each case and it begins to increase slightly with further increases of sliding speed.

Compared coating S-2 with coating S-3, coating S-3 has a lower COF but a higher ball wear. Coating S-2 has a higher COF but a smoother surface and minor ball wear. Both of the two coating can be polished to have a lower COF and minor wear. More research is needed to compare the COF and wear between a PEO coating, PTWA coating and the cast iron in the future.

## **ACKNOWLEDGEMENT**

The project was supported by Natural Science and Engineering Research Council (NSERC) of Canada.

Copyright © 2015 SAE International. This paper is included in this thesis with permission from SAE International. Further use, copying or distribution is not permitted without prior permission from SAE.

## References

- [1] Inventory of U.S. Greenhouse Gas Emissions and Sinks: 1990-2008. U.S. Environmental Protection Agency. April 15, 2010.
- [2] Allen, Mike & Javer, Eamon, Obama announces new fuel standards, [www.politico.com](http://www.politico.com), accessed Oct 19, 2014.
- [3] Financial Trend Forecaster, Inflation Adjusted Average Annual Gasoline Prices 1918-2009, Copyright 2010. Chart prepared by Timothy McMahon, Updated 7/21//2010.
- [4] D. Naranjo, Robert, F. Huang, Her-Ping, Gwyn, Mike, Castings Drive Fuel Efficiency, *Modern Casting*; Sep 2004; 94, 9; ABI/INFORM Trade & Industry, pg. 20.
- [5] Mid-Atlantic Casting Services. A Guide to Aluminum Casting Alloys, [www.Mid-AtlanticCasting.com](http://www.Mid-AtlanticCasting.com), accessed Oct 2014.
- [6] J.F. Su, X.Y. Nie, H. Hu, and J. Tjong, Friction and counterface wear influenced by surface profiles of plasma electrolytic oxidation coatings on an aluminum A356 alloy, *Journal of Vacuum Science & Technology A*, (30) 061302-11, 2012, doi: 10.1116/1.4750474.
- [7] T. Tian, Modeling the Performance of the Piston Ring Pack in Internal Combustion Engines, PhD Thesis, Department of Mechanical Engineering, Massachusetts Institute of Technology, June 1997.
- [8] Grosselle, Fabio, T. Giulio, Bonollo, Franco, et al., Correlation between microstructure and mechanical properties of Al-Si diecast engine blocks, *Metallurgical Science and Technology*. Vol 27-2 – Ed 2009.
- [9] V. Gallardo, Salvador, et al., Wear-Resistant Aluminum Alloy for Casting Engine Blocks with Linerless Cylinders, Patent Application – Publication Number: WO 2008/053363 A2. 8 May 2008.
- [10] T. Tian, V.W. Wong, and J.B. Heywood, A Piston Ring Pack Film Thickness and Friction Model for Multigrade Oils and Rough Surfaces, SAE Paper 962032, 1996; Also in *SAE Trans., J. Fuels Lubricants*, 1996, 105(4), pg. 1783-1795, doi:10.4271/962032.
- [11] K. Bobzin, F. Ernst, K. Richardt, T. Schlaefel, C. Verpoort, and G. Flores, *Surf. Coat. Tech.* 202, 4438 (2008), doi:10.1016/j.surfcoat.2008.04.023
- [12] K. Bobzin, et al., *Therm. Spray. Tech.* 17, 344 (2009), doi:10.1007/s11666-009

9409-z.

[13] P. Zhang, X.Y. Nie, H. Hu, and J. Zhang, *Surf. Coat. Tech.* 205, 1689 (2010), doi:10.1166/jnn.2010.1668.

[14] D.A. Parker, and D.R. Adams, *Tribology—Key to the Efficient Engine* (Inst. Mech. Eng. Conf. Pub., London, England, 1982), pp. 31–39.

[15] G. Wang, and X. Nie, Effect of Surface Roughness and Sliding Velocity on Tribological Properties of an Oxide-Coated Aluminum Alloy, SAE Technical Paper 2014-01-0957, 2014, doi:10.4271/2014-01-0957.

[16] B.J. Hamrock, S.R. Schmid, and B.O. Jacobson, *Fundamentals of fluid film lubrication*. (CRC press, Boca Raton, 2004), Vol. 169.



## CHAPTER 6

### **Friction influenced by surface roughness and sliding speeds at oil lubricating conditions**

#### 1. INTRODUCTION

Vehicles bring a lot of benefits to humanity. However, they also brought a lot of problems because of the huge amount of fuel consumption and the emission of carbon dioxide. The government has required automakers to increase their vehicle fleets' miles per gallon. This demand will challenge the automobile manufacturers to reduce the weight of their vehicles and frictional loss between components, along with other strategies to improve the vehicles' fuel economy [1].

A good method of reducing the vehicles' weights is to use a lighter engine block to replace the typical cast iron engine block [2, 3]. Most of the automakers prefer to use aluminum to make an engine block where cast iron liners are inserted or casted in the aluminum engine block [4]. However, the cast iron liner is heavy and leads to a few disadvantages due to its difference in thermal conductivity and coefficient of expansion. Also, cast iron is not the best material to have a low coefficient of friction (COF) [5].

Aluminum engine blocks without liners could have been a good method to reduce weight, if the hardness of the cylinder surface made of commonly-used Al-Si cast alloys was high enough to bear the wear between the piston rings and the surface of the cylinder bore. Some additional treatments would be needed before the liners can be removed [6].

Recently, it has become practical for a thermal spray coating, for instance, plasma transferred wire arc (PTWA), to be applied to protect cylinder surfaces and improve wear resistance [7]. PTWA is a thermal spraying process that deposits a coating on the surface of an aluminum cylinder. A single wire is used as feedstock in this system. A supersonic plasma jet melts the wire, atomizes it and propels the atoms onto the substrate [8]. The PTWA process can provide a coating with high wear resistance, lower cost, and lower friction potential. Currently, PTWA is used on aluminum engine blocks by Ford and Nissan.

Plasma electrolytic oxidation (PEO) coating is also a promising candidate to protect the surface of aluminum cylinder. PEO is an electrochemical surface treatment to get an oxide coating on light metals. The process employs high potentials to activate the discharges and generate the plasma to modify the structure of the oxide layers [9, 10]. This kind of coating grows both inwards and outwards from the substrate surface. PEO coating can offer protection against wear, corrosion, and heat.

Compared with other coatings such as, PTWA, anodizing, or physical vapor deposition, PEO coating has a lot of advantages. For example, it has high adherent strength to substrate, high hardness and thickness, high corrosion resistance, high wear resistance, low environment pollution, relatively low cost, and outstanding tribological performance because of its exceptional oil retention ability [11, 12]. Additionally, the roughness and the surface topography of the PEO coating can be easily changed by changing the electrolyte composition, current, and treatment time. All of these factors can provide PEO coating with an ability to reduce the friction in tribology [13]. Therefore, it is necessary to study the tribological properties of the PEO coatings.

To reduce the fuel consumption and the emission of carbon dioxide, the automakers have to reduce both the weight of vehicle and the frictional loss between components. It is widely recognized that the energy generated by the combustion of fuel doesn't transfer to the wheels completely. Much of the energy is lost in the way of thermal loss and frictional loss. Among them, the frictional loss between the piston rings and the surface of cylinder bore accounts for more than 15% - 20% of the total vehicle power [14, 15]. Therefore, the tribological performance of PEO coating, specially the COF of PEO coating on aluminum, must be well studied before it can be applied.

The tribological properties can be affected by a number of factors, for example, the viscosity of the oil, the roughness of the counterface, the load, the sliding velocity, the temperature and the humidity [16]. In this project, two critical factors are focused for study: surface roughness and sliding velocity. Roughness can considerably affect friction force and wear. Since an as-prepared PEO coating usually has a rough surface, the coating should be polished to some degree. High speed pin-on-disc tribological tests can be carried out on the coating with different surface roughness finish. In this way, the

relationship between roughness and COF can be studied. When the PEO coating is applied on a linerless aluminum engine block, it can be polished to a suitable roughness to get a low friction and wear.

The sliding velocity is another object of study in this work. The vehicle always runs at different speeds on the road, so the sliding velocity of the piston also always changes. At different sliding velocities, the piston rings and the cylinder bore will work under different lubricant conditions. At top dead center (TDC) and bottom dead center (BDC) where the sliding velocity is extremely low and the load is high, the piston rings and cylinder bore work under boundary lubrication. At the middle of the cylinder bore where the sliding velocity of the piston is very high, the piston rings and the cylinder bore will work under mixed or hydrodynamic lubrication [17]. The Stribeck curve was first used to illustrate a relationship between COF and sliding velocity under different lubrication conditions as shown in Fig.6.1. In the boundary lubrication, the counterface contact is solid contact. In the hydrodynamic lubricating condition, the contact is viscous shear, and the contact is combination of these two in the mixed lubrication [18, 19]. However, little is known about the tribological performance of a PEO coating in the mixed or hydrodynamic lubrication regime.

Usually, the tribological tests are carried out on a low speed pin-on-disc tribometer (sliding velocity less than 1 m/s), and the whole picture of the Stribeck curve cannot be gained. The limited (low) sliding velocity can only generate a boundary oil lubricating. However, the tribological performance of PEO coating at mixed and hydrodynamic oil lubricating conditions is hardly known. Therefore, it is necessary to find the relationship between COF and the sliding velocity for the PEO coating at various lubricating conditions. Although, a high speed reciprocating sliding test is always desired to simulate the real piston motion in an engine combustion chamber, vibration may be a problem to affect the accuracy of the test when the reciprocating speed is high. Furthermore, affordable data acquisition system requiring very high sampling rates may also be of challenge to collect the COF data of each cycle at different speeds. Thus, in this work, a variable high speed pin-on-disc tribometer (sliding velocity goes up to 6.07 m/s) was designed to generate a boundary, mixed or hydrodynamic oil lubricating regime. The

radius of the wear track can be adjusted from 0 mm to 100 mm, and the rotation sliding speed can also be changed from 0 m/s to 6.07 m/s (when the radius of wear track on sample is 50 mm). The connection between the motor and the sample holding disc is a rubber corn, and vibration is limited to an unnoticed level. A high-precision load cell is applied to collect data during the tests, and load calibration is carried out before use. The rotation speed of the driving motor is adjustable from 0 to 1200 rpm. By change of the rotation speed, tribological performance of the PEO coating at all lubricating regimes can be studied. The high speed pin-on-disc tribometer is shown in Fig.6.2.

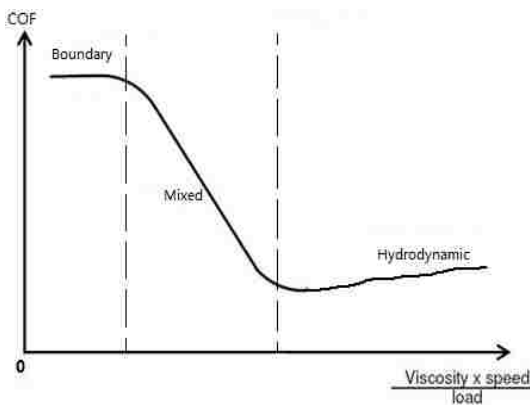


Fig.6.1. A typical Stribeck curve [18].

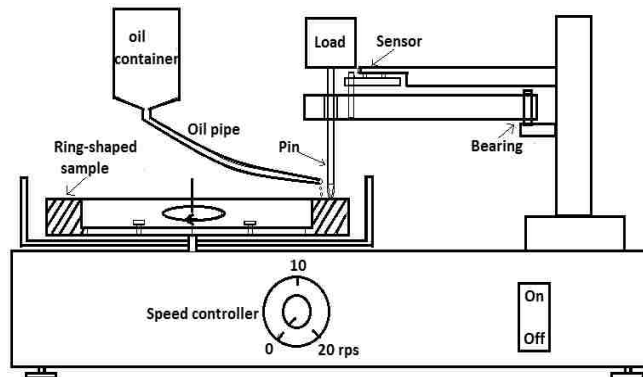


Fig.6.2. Schematic view of high speed pin-on-disc tribometer.

Previous studies show that the roughness and sliding velocity indeed influence the COF at the boundary lubricating condition but not that significant [20]. At a low sliding speed and thus a boundary lubrication, the COF increases, instead of decreases, when the PEO coating surface is polished from surface roughness of  $R_a = 0.8 \mu\text{m}$  to  $R_a = 0.5\mu\text{m}$ .

Then, the COF decreases with the decrease of coating surface roughness from  $R_a = 0.5 \mu\text{m}$  to  $R_a = 0.3 \mu\text{m}$ . Unlike the roughness effects, the COF always decreases when the sliding velocity increases even in the low speed region (sliding velocity less than 0.1 m/s) [20].

In this paper, the PEO process was applied to produce two coatings on an aluminum-silicon A356 alloy. The high speed pin-on-disc tribometer was used to generate the mixed or hydrodynamic oil lubricating conditions. The effects of surface roughness and sliding velocity on tribological properties at mixed or hydrodynamic lubricant conditions were particularly studied based on these two coatings. A cast iron material was also employed to do the same tests as a reference for comparison.

## 2. EXPERIMENT DETAILS

In this work, A356 aluminum-silicon cast alloy was used as substrate material. The alloy was machined to have a shape of a ring with a dimension of 105 mm (outer diameter)  $\times$  78 mm (inner diameter)  $\times$  12 mm (thickness). This large diameter of the ring-shaped sample can generate high sliding velocities when the high speed pin-on-disc tribometer works at fast rotation. The top surface of the disc rings was polished to roughness equal to  $R_a = 0.1 \mu\text{m}$  before a PEO coating was applied.

After the substrates were prepared, the PEO technology was used to produce two different coatings. A similar coating process has been reported in a previous publication [20]. The samples were identified by S3 and S12. The two coatings have different surface profiles because of the different discharge strength in the different electrolytic solutions. A cast iron ring was also prepared to do the tribological tests as reference.

For the PEO process, the A356 aluminum alloy ring (anode) and a stainless steel (cathode) were dipped into electrolytic solutions [20]. The anode and the cathode were connected to a pulsed DC power supplier which worked at a frequency of 2 kHz and a duration time of 80% duty cycle. The current density was controlled at  $0.1 \text{ A/cm}^2$ , and the treatment time was maintained in 20 minutes. The voltage was increased gradually with time because of the increasing thickness of the coating. The temperature of the solution

was maintained around 300K by a tap water cooling system, as the temperature would influence the quality of the coating.

After the coatings were produced, a Mitutoyo surface profiler SJ201P was employed to measure the surface roughness and record the coating surface profiles. The coating thickness was measured using PosiTector 2000 thickness meter. The PEO coating thickness and surface roughness are listed in Table 6.1.

Table 6.1 The original PEO coating thickness and surface roughness of samples.

Samples	PEO S3	PEO S12	Cast iron
Thickness ( $\mu\text{m}$ )	23	21	N/A
Roughness ( $\mu\text{m}$ )	2.58	1.89	0.28

The original roughness and topography of the two coatings were significantly different. The surface roughness of coating S3 was much higher than coating S12. The peaks were much higher and valleys much deeper on coating S3, which was supposed to be good for holding the lubricating oil on coating surface for tribological applications. During the PEO process, the degree of discharge on coating S3 was stronger than that on coating S12, which led to the rougher surface of coating S3. Cross hatches were produced on the cast iron ring disc surface to simulate a honed cylinder bore surface. The coatings were then polished to different roughness to do oil tests using the high speed pin-on-disc tribometer to find the roughness effect on friction at oil lubricating conditions. The original profile of the PEO coatings and cast iron were presented in Fig.6.3.

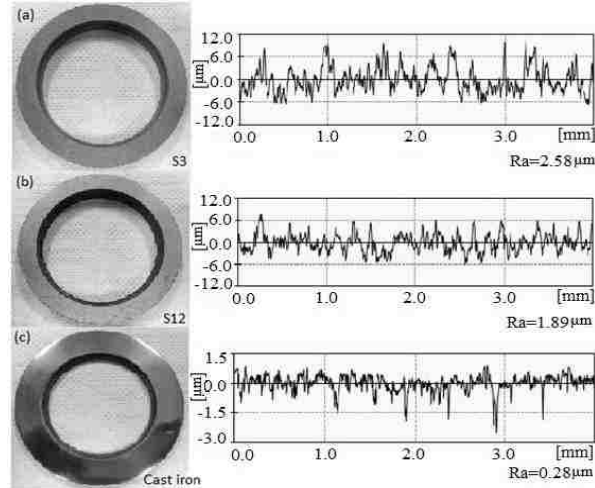


Fig.6.3. Original surface roughness and profiles of the PEO coatings and cast iron, (a) S3, and (b) S12, and (c) cast iron.

During the tribological tests carried on the high speed pin-on-disc tribometer, the highest rotating speed could go up to 20 rps (revolutions per second). The oil tribological tests were carried out at a room temperature of 24 °C and a humidity of around 50-60%. SAE 5W-20 full synthetic motor oil was selected to do the oil tests. An oil tube was installed in front of the pin and the oil flow rate was high enough (100 ml per-minute) to make sure that there was enough oil to form the mixed or hydrodynamic lubricating regimes at high sliding velocities. The load for the oil tribological tests was 10 N. AISI 52100 steel balls (3 mm in radius) as pins were used as counterface material, and the rotation diameter of the wear track was 100 mm.

All the coatings and cast iron were polished to different roughness before the oil tests were carried out. The lowest roughness was around 0.2 μm after the polishing. The rotation speed of the tribometer was increased from 0.3 rps (0.09 m/s) to 20 rps (6.07 m/s) step by step, and the highest sliding velocity would be 6.07 m/s, according to the circular motion formula:  $V = 2\pi Rn$ , where R is radius of wear track, and n is rotation speed (rps). After each increase of speed, the testing speed would be sustained for a few seconds to obtain a stabilized COF at each speed. In this test, 1000 data were collected at each speed. Thus, the COF decreased in the shape of a stair when the sliding velocity was increased.

COF data were recorded by software, and the relationships between COF and roughness or sliding velocity were studied and reported in the following section.

### 3. RESULTS AND DISCUSSION

#### 3.1 The effect of roughness

The coatings can have a smoother surface after a polishing process that also brought down the coating thickness. After the polishing, the topography and thickness of the coating were significantly changed, as shown in Fig.6.4.

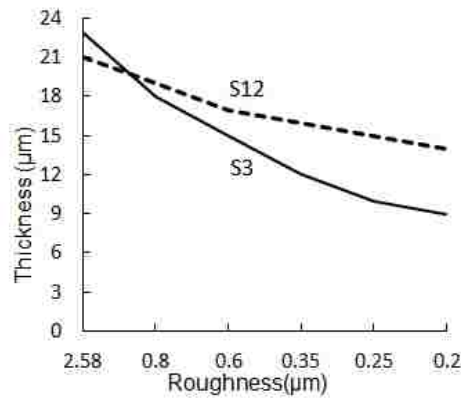


Fig.6.4. The relationship between roughness and thickness of coating S3 and S12.

Coating S12 was easily polished to  $R_a = 0.2 \mu\text{m}$  because the loose layer of the coating was relatively thin. Compared with coating S12, coating S3 was difficult to polish because of the deep valleys and pores on the coating. As shown in the Fig.6.4, the thickness would decrease with the reduction of roughness on both coatings. However, the slope was different. At the same surface roughness, the thickness of coating S3 was reduced at a larger degree than that of coating S12, which indicated that the coating S12 might be denser than coating S3. Seen from the Fig.6.6 and Fig.6.8, numerous pits were distributed on the surface of coating. After polished, the surface became even with pits on it which could be good for holding oil on the coating surface. That might be the reason why PEO coating can have good oil retention. Besides, the depth of the pits would decrease with the reduction of surface roughness. The skewness ( $R_{sk}$ ) of the coating was also measured by the profilometer. Skewness describes the asymmetry of the height



distribution histogram. If  $R_{sk} = 0$ , height distributions on the surface is balanced. If  $R_{sk} < 0$ , it means the surface is flat with holes, If  $R_{sk} > 0$ , the surface is even with peaks [12]. All the  $R_{sk}$  data exported from the profilometer and shown in Table II were negative. That meant the coating surface was even with pits, which was also observed from Fig.6.5 and Fig.6.6. The profiles showed that the topographies of the two coatings were actually quite different. There were a lot of big waves with pits on the coating S12, while coating S3 was even with pits. The kurtosis ( $R_{ku}$ ) data was obtained from coatings S3 and S12 as well. If  $R_{ku} > 3$ , the coating had a leptokurtic surface. If  $R_{ku} < 3$ , the coating had a platykurtic surface [13]. This feature might affect the tribological properties to some extent. Surface with low kurtosis is likely to flat with blunt tops other than sharp peaks. For the lubricating contact, surfaces with more negative skewness and higher kurtosis will benefit to reduce the frictional force, on account of a feature of flat surface with many deep valleys. Sedlacek et al. found that the more negative  $R_{sk}$  was, the lower the friction was in the boundary lubricating condition, even the surface roughness was high [21]. The  $R_a$ ,  $R_{sk}$  and  $R_{ku}$  of the PEO coatings affected the oil retention and contact area (thus oil film thickness) in hydrodynamic lubricating conditions. The optimum roughness, skewness, and kurtosis of PEO coatings for achieving low COFs seem be around  $0.4 \mu\text{m}$ ,  $-1.8$  and  $10$ , higher or lower than these values would induce a higher COF [13].

Table 6.2  $R_{sk}$  and  $R_{ku}$  data of PEO coating S3 and S12 after polished to different surface roughness.

PEO S3 $R_a$ ( $\mu\text{m}$ )	0.80	0.70	0.50	0.35	0.25
$R_{sk}$	-0.42	-0.59	-0.61	-1.29	-0.66
$R_{ku}$	-0.13	0.01	0.12	4.36	0.03
PEO S12 $R_a$ ( $\mu\text{m}$ )	0.80	0.60	0.35	0.25	0.20
$R_{sk}$	-0.94	-2.24	-2.64	-2.21	-2.62
$R_{ku}$	3.66	7.26	11.04	7.71	7.32

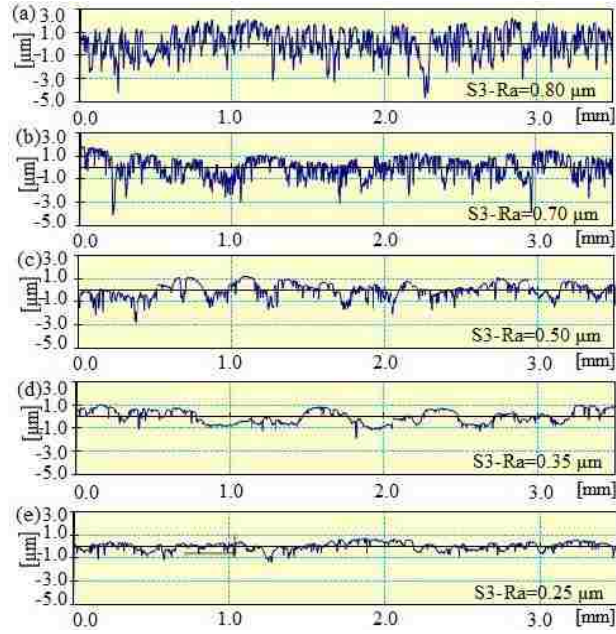


Fig.6.5. Surface profile of coating S3 after being polished to different roughness,  $R_a$ : (a)  $0.80\mu\text{m}$ , (b)  $0.70\mu\text{m}$ , (c)  $0.50\mu\text{m}$ , (d)  $0.35\mu\text{m}$ , and (e)  $0.25\mu\text{m}$ .

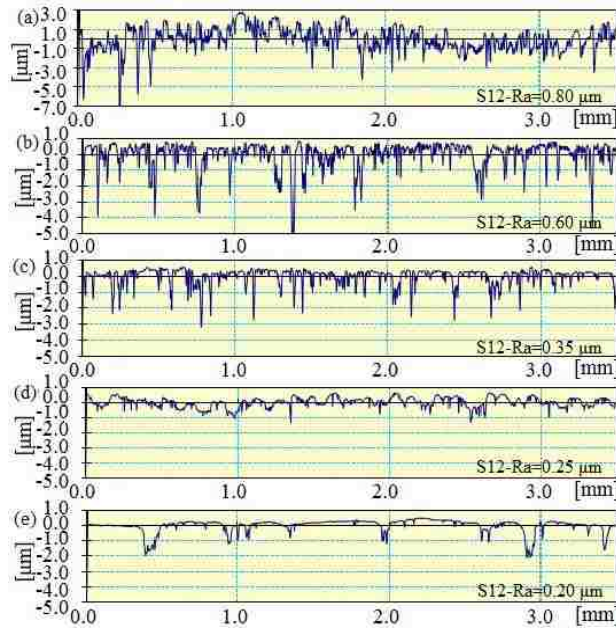


Fig.6.6. Surface profile of coating S12 after being polished to different roughness,  $R_a$ : (a)  $0.80\mu\text{m}$ , (b)  $0.60\mu\text{m}$ , (c)  $0.35\mu\text{m}$ , (d)  $0.25\mu\text{m}$ , and (e)  $0.20\mu\text{m}$ .

During each tribological test on a sample with a given surface roughness, the rotating speed was increased from 0.3 rps (0.09 m/s) to 20 rps (6.07 m/s) step by step.

The roughness of the coating was polished to have 5 values from  $R_a = 0.8 \mu\text{m}$  to  $R_a = 0.2 \mu\text{m}$ . The tribological tests would run about 4200 meters for each roughness. The oil flow was kept at the same level for each case during the test. When the speed went up, the mixed oil lubricant could be formed. If the sliding velocity was high enough, the hydrodynamic oil lubricant could also be formed. Cast iron was the reference material, and the same tribotests were carried out on its surfaces with three different surface finish conditions. After the tests, the COF was obtained, and the roughness and sliding velocity effects were shown in Fig.6.7 to Fig.6.9.

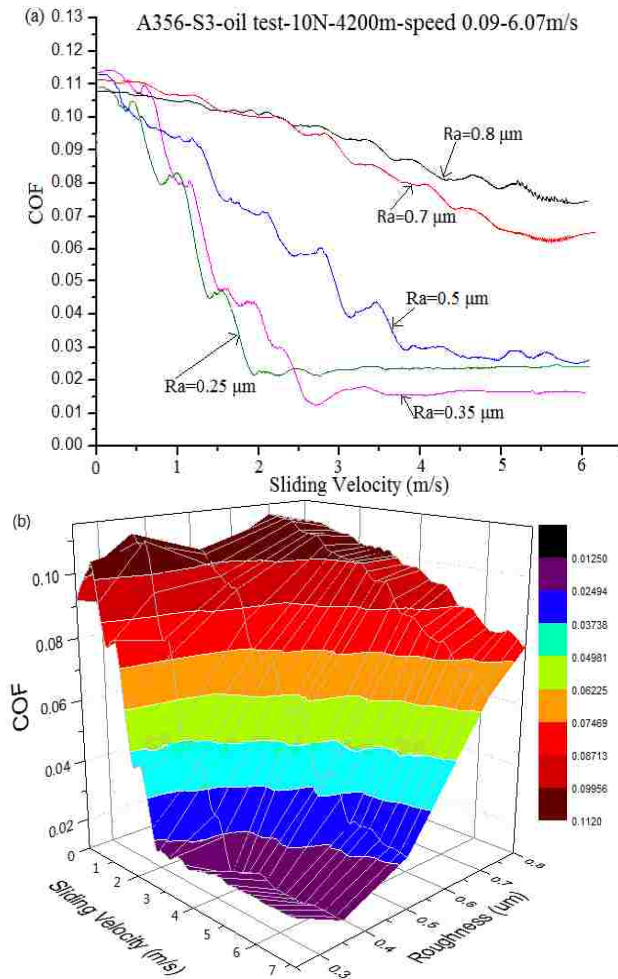


Fig.6.7. Roughness effect on COFs of coating S3, (a) 2D plot, (b) 3D plot.

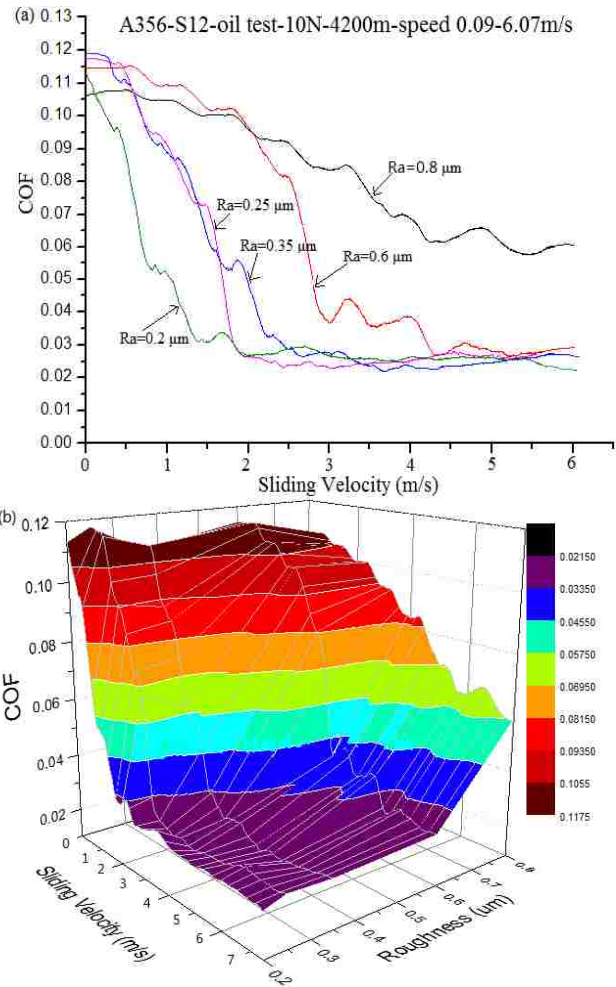


Fig.6.8. Roughness effect on COFs of coating S12, (a) 2D plot, (b) 3D plot.

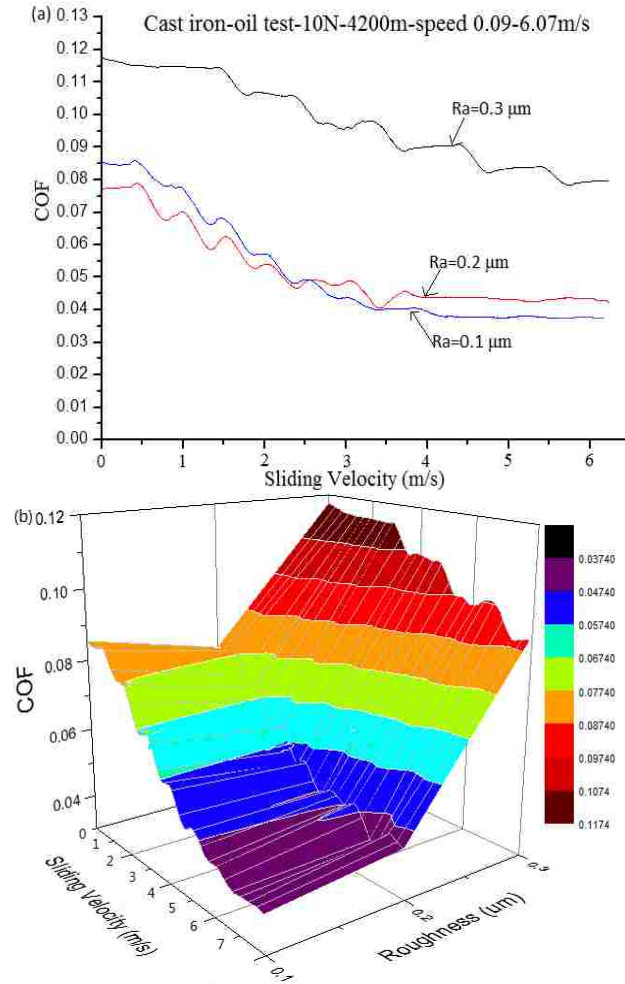


Fig.6.9. Roughness effect on COFs of cast iron, (a) 2D plot, (b) 3D plot.

As shown in Fig.6.7 to Fig.6.9, the roughness indeed affected the COF greatly in the high speed pin-on-disc tribological tests. All the tests started from low sliding velocities, so the COF in boundary oil lubricant could also be studied. As mentioned before, the COF have two different trends with the different surface roughness in boundary oil lubricating condition. The first tendency is that the COF would increase with the decrease of the roughness from  $R_a = 0.8 \mu\text{m}$  to  $R_a = 0.5 \mu\text{m}$ , and the second is that the COF would decrease with the decrease of roughness from  $R_a = 0.5 \mu\text{m}$  to  $R_a = 0.3 \mu\text{m}$  [20]. Here, the correlation of COF and roughness at low speed boundary conditions was observed again. When the roughness was high, the COF decreased slowly with the increase of sliding velocity. The mixed oil lubricating regime could not be formed. However, when the sample had a low roughness, the COF decreased very quickly with the increase of sliding

velocity. It also showed that the smoother the surface was, the higher the rate of descent was. When the roughness was low enough ( $R_a < 0.5 \mu\text{m}$ ), the mixed and hydrodynamic lubricant films could be formed and the Stribeck curve could be obtained at high sliding speeds. Compared with cast iron, the roughness effect on coatings was much more prominent. It also showed that the PEO coatings could have a much lower COF than cast iron. The lowest COF gained from PEO coating was 0.013 (coating S3), while the lowest COF obtained from cast iron was 0.037 under the same testing condition. The results also showed that PEO coating S12 was more sensitive to roughness than coating S3. As shown in Fig.6.7 and Fig.6.8, the COF of coating S12 dropped much faster than coating S3 with the increase of sliding velocity. However, coating S3 could have a lower COF than coating S12. The 3D plots in Fig.6.7 to Fig.6.9 also show the roughness effect on COF at any given sliding velocity. At a certain sliding velocity, the COF decreased together with the reduction of roughness. Compared with the roughness effect on the COF of PEO coating and cast iron, the PEO coating had a lower COF and a more sensitive reaction to roughness.

For the case of this work, the lowest hydrodynamic COFs of PEO coatings were obtained from  $R_a = 0.35 \mu\text{m}$ ,  $R_{sk} = -1.29$ ,  $R_{ku} = 4.36$  (for coating S3) and  $R_a = 0.35 \mu\text{m}$ ,  $R_{sk} = -2.64$ ,  $R_{ku} = 11.04$  (for coating S12), as presented in Table 6.2 and Fig.6.7 and Fig.6.8. These combinations of  $R_a$ ,  $R_{sk}$ , and  $R_{ku}$  might achieve the optimal oil retention and contact area to reduce the COF, and either higher or lower values would induce a higher COF. Compared between these two kinds of coatings, they had different skewness and kurtosis for each roughness, but roughness effect on each coating had the same trend, and the lowest COF was obtained at the highest kurtosis and the lowest skewness for each coating itself.

In order to understand the roughness effect on the COF of PEO coating better, the oil retention volume of the PEO coatings was calculated for each roughness. DIN (Germany roughness measurement standard) standard was also used to measure the facts of  $R_{pk}$ ,  $R_{vk}$ ,  $R_k$ ,  $M_{r1}$ , and  $M_{r2}$ . The oil retention volume was determined by the formula:  $V_o = R_{vk} (100 - M_{r2}) / 200$  in  $\mu\text{m}^3/\mu\text{m}^2$ . The DIN surface parameters and the oil retention volume were shown in Table 6.3.

Table 6.3 DIN surface parameters and oil retentions of PEO coatings and cast iron.

Samples	S3					S12					Cast iron		
$R_a(\mu\text{m})$	0.80	0.70	0.50	0.35	0.25	0.80	0.60	0.35	0.25	0.20	0.30	0.20	0.10
$R_{pk}(\mu\text{m})$	0.45	0.37	0.21	0.16	0.14	0.91	0.42	0.24	0.21	0.17	0.11	0.10	0.09
$R_{vk}(\mu\text{m})$	1.81	1.38	1.32	1.29	1.21	1.79	1.63	1.55	1.21	1.18	0.92	0.91	0.83
$R_v(\mu\text{m})$	0.92	0.79	0.71	0.61	1.32	1.81	2.50	1.15	0.65	0.74	0.85	0.70	0.23
$M_{r1}$	7%	2%	6%	4%	7%	6%	9%	7%	6%	10%	2%	6%	4%
$M_{r2}$	92%	89%	87%	84%	86%	91%	90%	87%	85%	85%	84%	83%	81%
$V_o(\mu\text{m}^3/\mu\text{m}^2)$	0.072	0.076	0.085	0.103	0.084	0.080	0.082	0.097	0.093	0.088	0.074	0.078	0.079

The data in Table 6.3 showed that different surface roughness had different oil retention volumes, and it also showed that the oil retention volumes were not high for either very rough or very smooth surfaces. Taking coating S3 for example, the surface roughness was polished from  $R_a = 0.80 \mu\text{m}$  to  $R_a = 0.25 \mu\text{m}$ , but the oil retention volume  $V_o$  kept increasing from  $0.072 \mu\text{m}^3/\mu\text{m}^2$  to  $0.103 \mu\text{m}^3/\mu\text{m}^2$  when the roughness decreased from  $0.80 \mu\text{m}$  to  $0.35 \mu\text{m}$ , and then  $V_o$  decreased to  $0.084 \mu\text{m}^3/\mu\text{m}^2$  when  $R_a = 0.25 \mu\text{m}$ . For this case, the best oil retention was obtained from coating S3 with a roughness  $R_a$  equaled to  $0.35 \mu\text{m}$ . A schematic was drawn to help in understanding of the relationship between roughness, skewness, kurtosis and oil retention as shown in Fig.6.10.

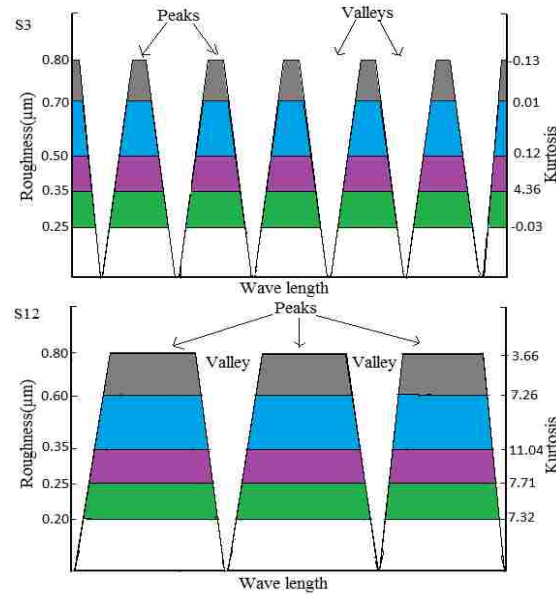


Fig.6.10 Schematic illustration of the topographic changes with different roughness.

As shown in Fig.6.10, the valleys on a rough surface (high  $R_a$  values) were deep and the peaks on the surface were sharp and narrow, which were not strong enough to withstand a load applied. The peaks would deform when the load was applied through the counterpart pin. The actual oil retention was degraded. However, when the polished surface was too smooth, the oil retention was not good either. The nicely finished surface might be strong to support the load, but the valleys were too shallow to have good oil retentions as shown in Fig.6.10 for the smoothest surfaces. The wavelength of coating surface profile seems larger for S12 than for S3 (Figs. 6.6, 6.7 and 6.10). The oil retention could significantly affect the tribological performance of PEO coating, and good oil retention would lead to a low COF. According to the Stribeck curve, the COF decreases greatly at mixed and hydrodynamic oil lubricating conditions, where the friction force changes from solid contact friction force to viscous shear force. The oil film between the contact surfaces results in the transformation of friction force. To form such an oil film, high sliding velocity is necessary, and good oil retention is also preferred. High sliding velocity is critical to build up the hydrodynamic pressure in the lubricant. Enough oil is desired to stay between the counterpart surfaces and separate them from direct contact when the lubricant pressure is built up. Thus, it was necessary to measure the oil retention volume of the surfaces with different roughness, and study the relationship between oil



retention and surface roughness. The results from Fig.6.7 to Fig.6.9 and Table 6.3 also indicated that different surface roughness possessed different oil retention volumes, and a better oil retention was beneficial in reducing the COF to a higher extent.

After tribological tests, the wear tracks on the coating surface were observed using an optical microscope. Images of the samples after the tests were presented in Fig.6.11, where so different surface morphology of each sample is illustrated. It should be noted that the samples in Fig.6.11 were the smoothest surface finished samples of coatings S3 ( $R_a$ : 0.25  $\mu\text{m}$ ) and S12 ( $R_a$ : 0.2  $\mu\text{m}$ ) and cast iron ( $R_a$ : 0.1  $\mu\text{m}$ ).

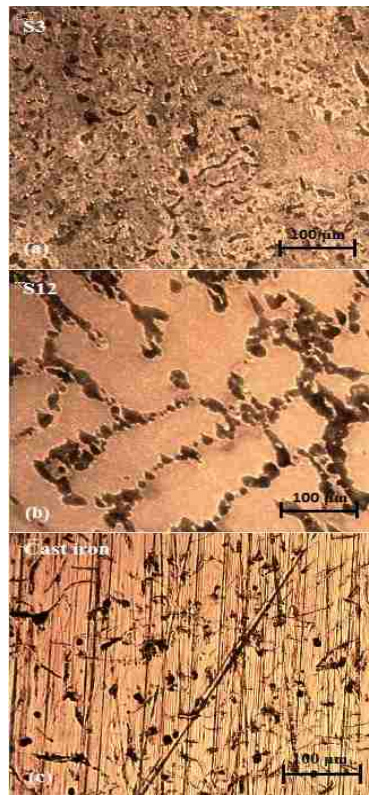


Fig.6.11 Wear tracks on the finally polished surfaces ( $\times 200$ ) on, (a) coating S3, (b) coating S12, and (C) cast iron.

As shown in Fig.6.11, the anti-wear performance of PEO coating was very good and no wear scar could be distinguished using the optical microscope. The surface profile of the wear track was also measured by the profile meter, but no dents or wear tracks could be measured. There were some tiny scratches that could be observed on the cast iron sample, but still no dents could be measured. Fig.6.11 clearly presents that the three

different materials possessed different morphologies. PEO coating S3 owned more pores than PEO coating S12, and the distance between pores on coating S3 was much smaller than that on coating S12. This feature has been measured in Fig.6.5 and Fig.6.6, where coating S12 showed a longer wave-length of surface profile than coating S3. From Fig.6.11c The cross hatches and graphites (dark colored) could be seen on the cast iron sample.

For both PEO coatings, the lowest COF was obtained from a surface with roughness equaled to  $0.35\ \mu\text{m}$ , where the largest kurtosis and highest oil retention volume were obtained from each coating. However, the COF obtained from coating S3 was lower than that from coating S12. PEO coating S3 possessed more dimples than PEO coating S12, and a higher oil retention volume. As shown in Fig.6.10 and Fig.6.11, the wave length of surface profile on coating S3 was much smaller, which meant the real contact area between the counterfaces for coating S3 was smaller. All these factors resulted in a lower COF on coating S3 than on coating S12 when both coatings had the same roughness  $R_a = 0.35\ \mu\text{m}$ . For the comparison of COFs with cast iron, the COFs obtained from PEO coatings were much lower, especially in the mixed and hydrodynamic lubrication regimes. Probably, the cross hatches on the cast iron were not deep enough to have an efficient oil retention which caused a higher COF in this case.

Roughness effects among the three different materials were not easy to compare, because the roughness, skewness, kurtosis, topographies, and oil retention volumes all play a role. However, the roughness effects within each material case were quite similar. In the boundary lubrication regime, the COF would increase with the decrease of the roughness from  $R_a = 0.80\ \mu\text{m}$  to  $R_a = 0.35\ \mu\text{m}$ , and the COF would decrease with the decrease of roughness from  $R_a = 0.35\ \mu\text{m}$  to  $R_a = 0.20\ \mu\text{m}$ . In the mixed lubrication regime, the descent rate of the COF increased with the decrease of roughness. In the hydrodynamic lubrication regime, the COF decreased with the decrease of roughness from  $R_a = 0.80\ \mu\text{m}$  to  $R_a = 0.35\ \mu\text{m}$ , and then the COF increased with the roughness decreased from  $R_a = 0.35\ \mu\text{m}$  to  $R_a = 0.20\ \mu\text{m}$ .

If the PEO coating was applied successfully on the engine cylinder bore, the surface should be honed or polished, and  $R_a = 0.20\text{-}0.35\ \mu\text{m}$  seems an appropriate number for its

surface finish. In this way, when the vehicle engine was sped up, the COF could drop very quickly and to a very low value. On the other hand, the surface roughness can be relatively high at TDC and BDC areas where the boundary lubricant exists, based on the results shown in Fig.6.7 and ref. [20]. A right design of cylinder bore surface finish would benefit in friction reduction and fuel economy. Certainly, more research can be done in this regard.

### 3.2 The effect of sliding velocity

While the effect of sliding velocity was already shown in Fig.6.7 to Fig.6.9, such an effect was particularly studied by investigating into Fig.6.12.

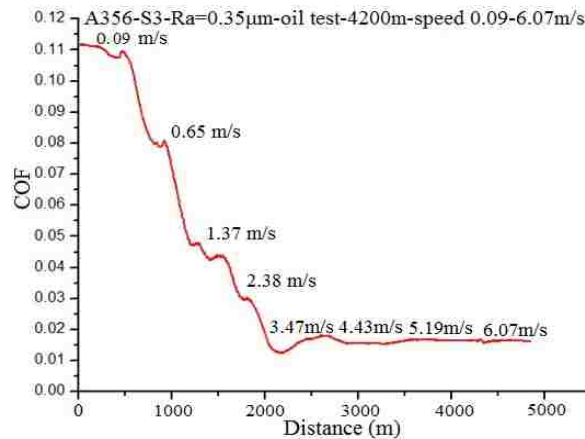


Fig.6.12. Sliding velocity effect on COF of PEO coating S3 ( $R_a = 0.35 \mu\text{m}$ ).

As shown in Fig.6.12, the sliding velocity effect on COF was very remarkable. When the sliding velocity increased, the COF of the PEO coating dropped quickly. When the sliding velocity was high enough, the COF stopped decreasing, but it slightly increased, like a case in a typical Stribeck curve. The Stribeck Curve shows the relationship between the COF and viscosity, speed and load. The vertical axis is COF, while the horizontal axis is expression of  $m \text{ N/p}$  (m: oil viscosity, N: speed, p: load) [18]. In this work, the oil viscosity and the load were invariant, only the speed was increase continuously. When the speed is high enough, an oil pressure is generated by the combination of surface topography, oil viscosity and the surface moving speed, to support the load applied through on the counterface pin. The oil pressure increases with the increase of sliding velocity, and when it is high enough, the contact surfaces will be

forced to separate. There will be an oil film between the two related contact surfaces, and the mixed and hydrodynamic oil lubricating conditions are formed as a result. Meanwhile, the solid contact friction force at boundary oil lubrication will transfer to viscous shear force at mixed and hydrodynamic oil lubrications. Hence, the COF decreases greatly at high sliding speeds.

For the case of Fig.6.12, the COF dropped from 0.112 to 0.013 when the sliding velocity increased from 0.09 m/s to 3.47 m/s. After the sliding velocity increased from 3.47 m/s to 6.07 m/s, the COF increased slightly to 0.017, which is similar to the Stribeck curve. The mixed lubricant was formed when sliding velocity increased from 0.09 m/s to 3.47 m/s in this case, and the COF considerably decreased at the formation of the mixed lubrication. The hydrodynamic friction could also form when the sliding velocity increased from 3.47 m/s to 6.07 m/s, where the COF increased to some degree. In this curve, the relationship between COF and sliding velocity could be easily understood. It should be mentioned again that the step-wards of COF curve at mixed regime was due to the way of the speed increasing (i.e., in a step-by-step way).

Compared with the results shown in Fig.6.7 to Fig.6.9, the sliding velocity effect on the COF of PEO coating was more distinct than that of cast iron. The PEO coating reduced its COF more quickly than cast iron, when the sliding velocity increased, because of a better oil retention (according to Fig.6.7 to Fig.6.9 and Table 6.3). The lowest COF value obtained from PEO coating was also significantly smaller than that obtained from cast iron. As for the sliding velocity effect on the COFs of PEO coatings S3 and S12, the difference in COF was less significant, but it seems that coating S3 slightly outperformed over coating S12 because of their different surface topographies, and oil retentions. However, the descent rate of COF on coating S12 was higher than that on coating S3 (even though the lowest COF was obtained from coating S3), which meant the COF reaction on sliding velocity was more sensitive for coating S12. Thus, the COF of coating S12 could quickly decrease to a very low value at low sliding velocities, which benefits to save fuels at a low driving speed if this kind of coating can be applied on cylinder bores.

A similar relationship between piston rings and the PEO coated cylinder bore might be expected. The friction between piston rings and cylinder bore would decrease when the vehicle speeds up. A low COF at the hydrodynamic lubricating condition of an engine is important, since the hydrodynamic regime exists between TDC and BDC and most of the time an engine runs at high revolutions. Therefore, the frictional loss would decrease and the efficiency would increase for the engines that exhibit low friction particularly at high speeds.

#### 4. CONCLUSIONS

The effect of surface roughness on COF of PEO coating and cast iron is significant. The surface roughness can decide how low the COF can be when the sliding velocity increases. When the surface roughness is high, the sliding velocity effect on COF is not very dramatic, which means that the COF cannot decrease to a great extent. However, when the surface roughness is low enough (lower than 0.5-0.6  $\mu\text{m}$  in this work), the sliding velocity effect on the COF is distinct, and the COF can drop tremendously when the sliding velocity increases. Furthermore, the surface roughness also affects the rate of descent of the COF. The smoother the surface is, the earlier and faster the COF decreases when the sliding velocity increases. Beyond a certain sliding velocity, the mixed and hydrodynamic lubrications can be formed. The COF decreases greatly at a mixed lubricating condition, and the COF keeps at a very low level with a slight increase in hydrodynamic lubrication regime. For each sample studied, the lowest COF is observed when the sample surface has the lowest skewness, the highest kurtosis and oil retention volume. Compared with cast iron, the PEO coatings can have much lower COFs. The results indicate that the PEO coating on aluminum engine blocks may be a very good solution to replace the cast iron liners for both weight and friction reduction.

#### **ACKNOWLEDGEMENTS**

The research was supported by Natural Sciences and Engineering Research Council of Canada (NSERC), and Ontario Centre of Excellence (OCE).

## References

- [1] KS-Aluminium-Technologie, Aluminum Cylinder Blocks—Designs, Materials, Casting Methods and Cylinder Bore Surface Technologies for Lightweight Passenger-Car Engines (Verlag Moderne Industrie 2005).
- [2] J.J. Lenny, Replacing the Cast Iron Liners for Aluminum Engine Cylinder Blocks: A Comparative Assessment of Potential Candidates, an Engineering Project Submitted to the Graduate Faculty of Rensselaer Polytechnic Institute (2011).
- [3] G. Barbezat, Advanced thermal spray technology and coating for lightweight engine blocks for the automotive industry, *Surf. Coat. Tech*, 200, 1990–1993 (2005).
- [4] J.G. Kaufman, (John Gilbert). Aluminum alloy castings properties, processes and applications. ISBN 0-87170-803-5 (1931).
- [5] D.A. Parker and D.R. Adams, Tribology—Key to the Efficient Engine (Inst. Mech. Eng. Conf. Pub., London, England, 1982), pp. 31–39.
- [6] E. Köhler, J. Niehues, K.U. Kainer, Metal Matrix Composites: Custom-made Materials for Automotive and Aerospace Engineering, Wiley-VCH, Weinheim, pp.95–108 (2006).
- [7] K. Bobzin, F. Ernst, K. Richardt, T. Schlaefer, C. Verpoort, and G. Flores, *Surf. Coat. Tech.* 202, 4438 (2008).
- [8] K. Bobzin, K. Maes, A. Abdel-Samad, E. Lugscheider, *J. Therm. Spray Tech.* 17, 344 (2008).
- [9] C.S. Dunleavy, I.O. Golosnoy, J.A. Curran, T.W. Clyne, Characterisation of discharge events during plasma electrolytic oxidation. *Surf. Coat. Tech.* 203 (22): 3410. doi:10.1016/j.surfcoat (2009).
- [10] A.L. Yerokhin, X. Nie, A. Leyland, A. Matthews, S.J. Dowey, *Surf. Coat. Tech.* 122, 73–93 (1999).
- [11] X. Nie, X. Li, L. Wang, D. O. Northwood, *Surf. Coat. Tech.* 200, 1994 (2005).
- [12] Y.X Tang, P.X Wee, Y.K Lai, X.P Wang, D.G Gong, P.D. Kanhere, T.T Lim, Z.L Dong, and Z. Chen, Hierarchical TiO<sub>2</sub> Nanoflakes and Nanoparticles Hybrid Structure for Improved Photocatalytic Activity, *J. Phys. Chem. C*, 116, 2772–2780 (2012).

- [13] J.F Su, X. Nie, H. Hu, J. Tjong, Friction and counterface wear influenced by surface profiles of plasma electrolytic oxidation coatings on an aluminum A356 alloy, AVS Journals & Magazines, 30, 061402 - 061402-11 (2012).
- [14] B. Andersson, Tribol. Ser. 18, 503 (1991).
- [15] K. Funatani and K. Kurosawa, Adv. Mater. Process. 146.6, 27 (1994).
- [16] B. Andersson, Tribol. Ser. 18, 503 (1991).
- [17] B. Armstrong, C.C. de Wit, Friction Modeling and Compensation, The Control Handbook, (CRC Press, Boca Raton, 1995).
- [18] B.J. Hamrock, S.R. Schmid, and B.O. Jacobson, Fundamentals of fluid film lubrication. (CRC press, Boca Raton, 2004), Vol. 169.
- [19] D. Zhu, On some aspects of numerical solutions of thin-film and mixed elastohydrodynamic lubrication. Proceedings of the Institution of Mechanical Engineers, Part J: Journal of Engineering Tribology, 221, 561-579 (2007).
- [20] G. Wang, X. Nie, J. Tjong, Effect of Surface Roughness and Sliding Velocity on Tribological Properties of an Oxide-coated Aluminum Alloy, SAE-2014-01-0957 (2014).
- [21] M. Sedlacek, B. Podgornik, and J. Vizintin, Tribo. Intel. 48, 102 (2012).

## Chapter 7

# High speed tribotests on a PEO coated aluminum liner after flexible honing

### 1. INTRODUCTION

Recently, in order to reduce weight and improve efficiency of an engine, light metal alloy was used to replace cast iron and steel for many engine components. Among them, AlSi-alloys are the most popular materials used to replace the cast iron because of their lighter weight and better heat transfer. The weight of the engine block made of AlSi-alloys is about 50% of those made of gray cast iron [1]. However, the mechanical properties of the aluminum alloys are not as good as gray cast iron, such as Young's modulus, tensile strength, and hardness. Besides, the aluminum surface of the cylinder bore cannot meet the tribological requirements against piston rings, such as oil retention, wear resistance, and coefficient of friction (COF) [2]. Thus, the AlSi-alloy materials cannot be used directly as the surface of the cylinder bore wall.

To overcome the disadvantage of the low hardness and low wear resistance of the aluminum, the aluminum bore surface should be treated or replaced by other materials. Presently, cast iron liners are inserted in or casted in the aluminum engine block to increase the wear resistance. Cast iron liners have enough hardness to bear the wear from the motion of piston rings. The graphite precipitates inside the cast iron are also good for reducing the friction between piston rings and the liner wall [3]. Besides, crosshatches can be engraved on the surface of cast iron liner, which is good for improving the oil retention. Most of the passenger cars use this kind of technology now. However, the cast iron liners in aluminum engine blocks also have drawbacks, such as inherent heavy weight, low thermal conductivity, and thermal expansion mismatching problems [4].

High-silicon aluminum alloy is used to cast the engine block without liners to get a better weight to power ratio. The high amount of separated silicon in the aluminum alloy can provide good tribological properties. However, the high-silicon aluminum alloy engine block is difficult to machine and the aluminum cylinders may suffer from corrosion problems when a biofuel or sulphur-contained fuel is used [5].



One option to improve the wear resistance and tribological properties of the aluminum alloy cylinder bore is applying a thermal spray coating [6]. Thermal spray coatings are widely used in a variety of industrial applications, for example, they can protect products from wear, temperature extremes, and chemicals. Thermal spray coating processes are differentiated by varying heat sources and base materials. Processes include combustion flame spraying, high velocity oxy-fuel spraying (HVOF), two-wire electric arc spraying, plasma transferred wire arc (PTWA) spraying, and vacuum plasma spraying [7]. The thickness of a PTWA coating can be varied easily by treating time, and it is also hard enough to bear the wear from the sliding piston rings [8]. The porosity of the coating is low (only 4%), and cross hatches are engraved on the surface to increase the oil retention. Development of a higher porosity (up to 10%) is underway for the PTWA process [9].

Plasma electrolyte oxidation (PEO) coatings can also provide a wear resistant surface for the aluminum alloy cylinder bore. Due to the high hardness, chemical stability including corrosion/oxidation resistance, wear resistance and low coefficient of friction, PEO coatings have been proposed to be used in automotive industry [11, 12]. Successful applications are in corrosion prevention of magnesium components. The PEO process is considered as a cost effective, environmental friendly surface treatment for lightweight metals. Compared with thermal spray coating, PEO coatings have high adherent strength to the substrate because the coating grows both inwards and outwards from the surface of the substrate metal [13]. The composition, thickness, and topography of a PEO coating can be tailored for different applications. During the PEO process, a large number of crater-like holes are generated on the surface of the coating, which is beneficial to obtain good oil retention [14]. Various tribological tests on PEO coatings have been done to study the wear resistance and tribological properties of PEO coatings.

Usually, small PEO coated samples are used to do pin-on-disc tribological tests. Due to the small radius of a wear track on the sample, the sliding velocity is quite low (around 0.1 m/s). Thus, all the low speed pin-on-disc tests are carried out in the boundary lubricating regime [15]. The COF of PEO coatings decrease slightly when the sliding velocity increases in the low speed range [16]. The tribological properties of PEO

coatings in the mixed and hydrodynamic lubricating regimes cannot be studied using the low speed pin-on-disc tests.

In order to simulate the piston motion in an engine combustion chamber, a reciprocating sliding test is always desired. The counterface materials are usually steel balls or segments of piston rings. However, the reciprocating sliding tests can only be carried out in the boundary lubricating regime. Severe vibration may influence the accuracy of the testing results when a high reciprocating sliding speed is applied. A data acquisition system with very high sampling rates would need to collect the COF data at different speeds of each reciprocating cycle [17].

A high speed pin-on-disc tribometer with various speeds is used to generate the mixed and hydrodynamic lubricating regimes. A ring-shaped sample with a large diameter provides the test with a high sliding velocity in order to show possible mixed and hydrodynamic friction behaviors. The rotational speed of the high speed pin-on-disc tribometer can be changed from low to high, thus the boundary, mixed, and hydrodynamic lubricating regimes can be formed. A typical Stribeck curve can be obtained. In the boundary lubricating regime, the COF of PEO coating stays at a high level. In the mixed lubricating regime, the COF decreases quickly to a low level. The COF of PEO coating remains at a low level in the hydrodynamic lubricating regime [18]. The results show that a good surface polishing (roughness is around 0.35  $\mu\text{m}$ ) and high sliding velocity can reduce the COF of the PEO coating to a level lower than the cast iron [19]. However, little is known about the tribological performance between the piston ring and the PEO coated aluminum liner.

In this work, an aluminum 356 alloy liner was coated by the PEO process, and a special piston ring holder was designed to hold a segment of piston ring and apply the load. The PEO coated liner was installed on a high speed tribometer, and the piston ring holder was connected on the arm of the tribometer where a load cell was located to record the frictional force. Prior to the friction tests, the PEO coated liner was polished to have different roughness. The sliding velocity was also changed during each test, so the roughness and sliding velocity effect on the COF of the PEO coated liner could be

studied. Furthermore, effect of oil flow rate on the COF of the PEO coated liner was also studied.

## 2. EXPERIMENTAL DETAILS

An A356 aluminum alloy liner was used for this study. The inner diameter and length of the liner was 87.5 mm and 130 mm respectively. The inner wall surface was polished to  $R_a = 0.1 \mu\text{m}$  before the PEO treatment. A flex honing brush was used for the polishing.

The electrolyte used in the PEO coating process was 8 g/L sodium silicate, 1 g/L potassium hydroxide, and some additives. In the PEO process, a spray head was used to supply the electrolyte to the liner inner surface without a need to dip the whole liner in the electrolyte. The liner, as the anode and the spray head, as the cathode, were connected to a pulsed DC power supplier which worked at a frequency of 2 kHz and a duration time of 80% duty cycle. The current density was  $0.1 \text{ A/cm}^2$ . During the PEO process, the spray head was rotated and the electrolyte was sprayed on the inner surface of the liner. The gap between the spray head and the liner was filled with the electrolyte which functioned as an electrical conductor between the anode and the cathode. A PEO coating was generated on the liner bore surface uniformly, based on the PEO coating growth mechanism [13]. A chiller was used to cool down the electrolyte and keep the temperature around 300K. After the coating process, a PosiTector 2000 coating thickness probe was used to measure the coating thickness. The coating thickness was found to be  $23 \mu\text{m}$ . A Mitutoyo surface profiler SJ201P was employed to measure the surface roughness. The surface roughness of the as-prepared coating was  $1.42 \mu\text{m}$ . The coated liner and the coated inner surface profile are shown in Fig.7.1.

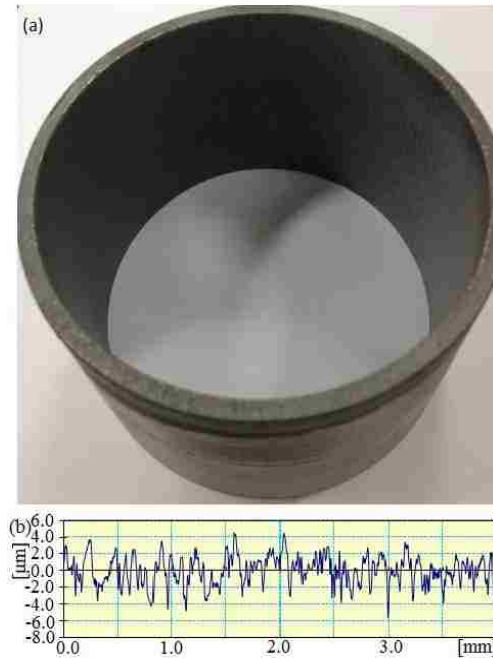


Fig.7.1. PEO coated liner and the original coating surface profile: (a) PEO coated liner, (b) original coating profile.

To study surface roughness effect on COF of the PEO coating, the inner surface of the PEO coated liner was polished to have different roughnesses. An 800 grit flexible honing brush (as shown in Fig.7.2) was used to polish the inner surface. The diameter of the brush was 89 mm, which was 1.5 mm larger than the inner diameter of the liner. SAE 5W-30 synthetic oil was used as a honing fluid in the honing process. The honing brush was locked onto a hand drill and moved backwards and forwards when the hand drill rotated in the liner. The coating roughness and thickness decreased with the increase of the honing time. The surface was polished to have four different roughnesses including  $R_a = 0.80 \mu\text{m}$ ,  $0.60 \mu\text{m}$ ,  $0.45 \mu\text{m}$  and  $0.35 \mu\text{m}$ . The number of honing strokes and changes of surface finish and coating thickness were recorded and shown in Table 7.1.



Fig.7.2. Honing brush and the honing process.

Table 7.1 Record of thickness and diameter changes in the honing process.

Strokes	0	30	50	80	110
Roughness( $\mu\text{m}$ )	1.42	0.8	0.6	0.45	0.35
Thickness( $\mu\text{m}$ )	23	18	15	14	11
Gage number	25.2	25.03	24.93	24.9	24.8
Diameter(cm)	87.454	87.464	87.47	87.472	87.478

Table 7.1 shows that the roughness and thickness of the coating were reduced at a quicker rate in the first 30 strokes than in the next 80 strokes. To obtain a smooth surface ( $R_a = 0.35 \mu\text{m}$ ), almost half of the coating thickness had to be polished away. The coating thinning rate was  $0.12 \mu\text{m}$  every 10 strokes on average in this case.

During the polishing process, the diameter changes of the liner were measured and recorded. A dial bore gage was used to measure the diameter changes. The method of measurement was shown in Fig.7.3 and the diameter changes of the liner are presented in Table 7.1.



Fig.7.3 Diameter measurement using a dial bore gage.

In the measurement, a higher gage number corresponded to a smaller diameter. After the final polishing, the diameter decreased 0.022 mm and the gage number increased 0.40. The diameter increased about 0.024 mm every 10 strokes in this case.

At the end of the last stroke, the roughness was close to 0.35  $\mu\text{m}$ . In order to preserve more coating, 1200 grit sandpaper was used to do the final polishing. Two different surface measurement standards were used to measure the roughness and oil retention volume including the International ISO standard and the German DIN (German roughness measurement standard) standard. The surface profiles of the PEO coating were measured after each of the polishing steps and are shown in Fig.7.4.

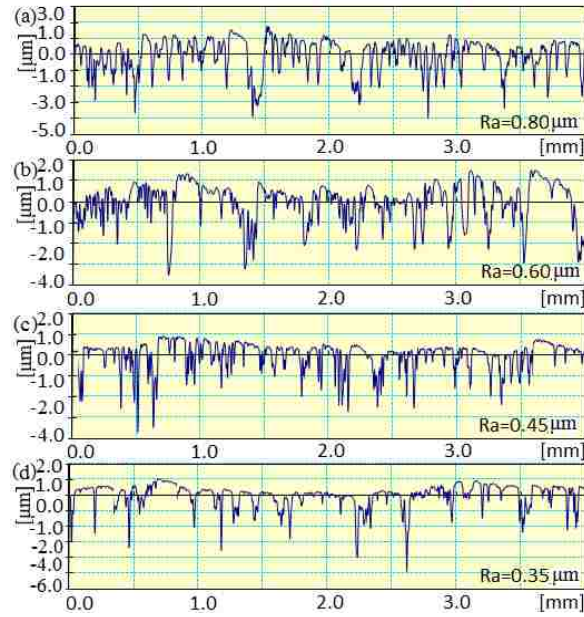


Fig.7.4. PEO coating surface profiles after honing: (a)  $R_a = 0.80 \mu\text{m}$ , (b)  $R_a = 0.60 \mu\text{m}$ ,  
(c)  $R_a = 0.45 \mu\text{m}$ , (d)  $R_a = 0.35 \mu\text{m}$ .

For each of the polishing surface conditions, a high speed piston ring-on-liner test was carried out. A liner holder was designed to align the center of the liner to the rotating axis of the disc stage of the tribometer. Thus, the disc would rotate together with the liner. A special piston ring holder was designed to hold a segment of a piston ring (Cr-plated steel) and apply a contacting load between the piston ring and the liner. The liner holder, piston ring holder and a schematic view of the high speed tribometer are presented in Fig.7.5.

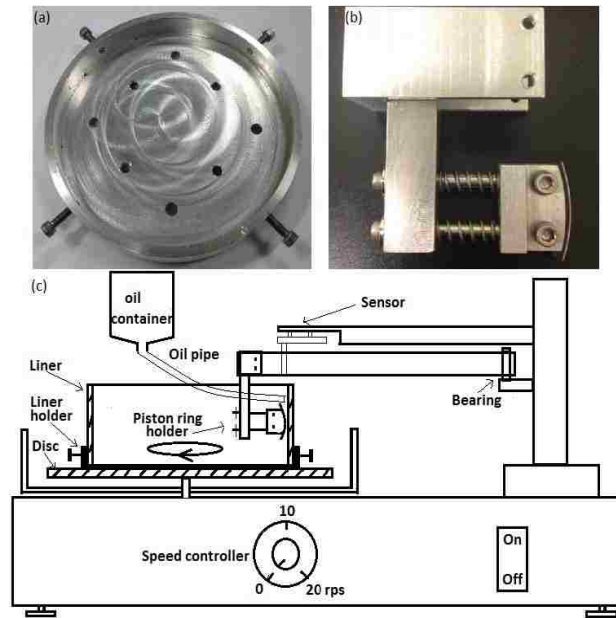


Fig.7.5. High speed piston ring on liner tribometer: (a) liner holder, (b) piston ring holder, (c) schematic view of the tribometer.

The oil tribological tests were carried out at a room temperature of 24 °C and a humidity of around 50-60%. SAE 5W-20 full synthetic motor oil was used as lubricant. A piston compression ring was used as a counterface material. The springs on the piston ring holder were calibrated before the tests. A 10N's weight was put on the springs and the length of the compressed springs was measured by a caliper. This calibration process was repeated 10 times, and the average length of compressed springs was used as a standard load for 10N. The springs on the piston ring holder were compressed to the same length in each test, so the load on the piston ring could be precisely applied. In this work, the load was 10N. The load cell in the arm section was also calibrated to make sure the load cell was accurate and sensitive enough to measure the frictional force between the piston ring and the coated liner bore. The results of the calibration are presented in Fig.7.6. The calibration results of the load cell showed that the lowest force that could be measured was 0.01N, and the linear trend line in Fig.7.6 shows that the load cell could have a linear behavior down to 0.025N. In other words, a COF higher than 0.0025 at the 10N's loading condition could be reliably measured.



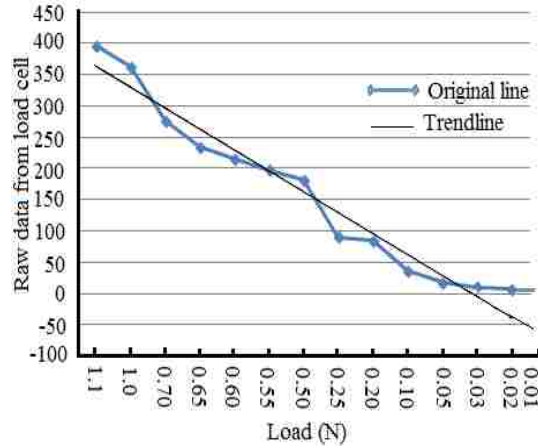


Fig.7.6. Calibration results of the load cell.

An oil tube was installed and located just before the piston ring which contacted the inner wall of the liner, thus the oil could be retained on the wall of liner and provide lubricant for the piston ring. Two different sizes of oil tubes were used to have the oil flow rates of 100 ml per-minute and 200 ml per-minute. The effect of oil flow rates on the COF was observed. A new segment of the piston ring was used in each test.

In order to study the sliding velocity effect on the COF of the PEO coated liner, the rotational speed of the tribometer was increased step by step from 0.3 rps (revolution per second) to 20 rps. The highest sliding velocity would be 5.5 m/s, according to the circular motion formula:  $V = 2\pi Rn$ , where R is radius of liner, and n is rotation speed (rps). For each increment of speed, the test would be continued for a while to obtain a stabilized COF at each speed. In this test, 1000 data were collected at each speed. Thus, the COF showed a stepwise decrease when the sliding velocity was increased. The COF data was recorded using a data acquisition system. The effects of roughness and sliding velocity on the COF were therefore investigated.

### 3. RESULTS AND DISCUSSION

#### 3.1 Effects of roughness on COF

As shown in Table 7.1, the surface roughness and coating thickness were decreased as the number of strokes of the honing increased. Surface profiles of the PEO coating are

shown in Fig.7.3. The asperity of coating surface was flattened when the coating surface became smoother due to the polishing. The polished PEO coating surface was plateau-like with pits when the roughness was reduced to  $R_a = 0.35 \mu\text{m}$ . This kind of surface morphology would be beneficial in reduction of frictional force.

The tribological tests, for each roughness, were carried out on the high speed tribometer. With a 10N load applied on the piston ring, each tribotest was run for about 4200m sliding distance. During the test period, the rotation speed of the tribometer was increased step by step, which generated various sliding velocities (from 0.08 m/s to 5.5 m/s). The COFs influenced by surface roughness and sliding velocity are shown in Fig.7.7.

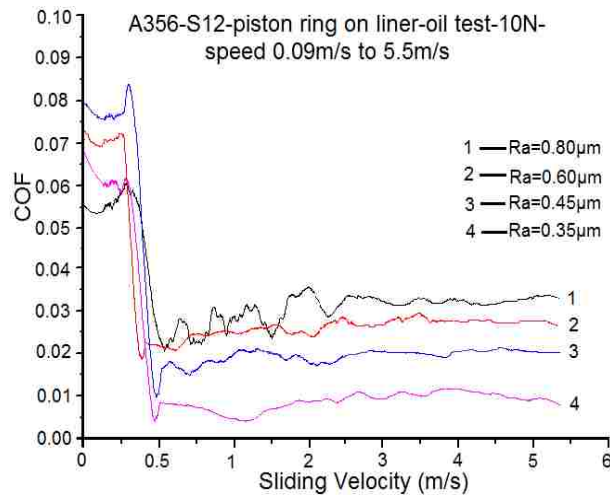


Fig.7.7. Roughness and sliding velocity effects on the COF of PEO coated liner at a high oil flow rate (100 ml/min).

The effect of coating surface roughness on the COF was significant. Since the tribological tests were carried out from a low sliding velocity to a high sliding velocity, the roughness effects on COFs in all the lubricating regimes (including boundary, mixed, and hydrodynamic lubricating regimes) could be studied [20]. The COFs in Fig.7.7 also show that the mixed lubricating regime was very narrow, and it could quickly transfer to a hydrodynamic lubricating regime when the sliding velocity increased to 0.5 m/s. The hydrodynamic lubricating regime formation at a relatively low speed can be beneficial to fuel economy for a combustion engine.

The effect of roughness on COFs was different for different lubricating regimes. In the boundary lubricating regime, the lowest COF was obtained from a higher surface roughness ( $R_a = 0.80 \mu\text{m}$ ). Two different trends of roughness effects were found in the boundary lubricating condition. The COF increased from 0.057 to 0.078 when the surface roughness decreased from  $R_a = 0.80 \mu\text{m}$  to  $R_a = 0.45 \mu\text{m}$ . The COF then reduced to 0.06 when the roughness decreased from  $R_a = 0.45 \mu\text{m}$  to  $R_a = 0.35 \mu\text{m}$ . These roughness effects on COF in boundary lubricant were also observed in low speed pin-on-disc tribological tests [18]. In the mixed lubricating regime, the COF was reduced so quickly that there were no obvious differences between tests. In the hydrodynamic lubricating friction regime, the COF decreased from 0.033 to 0.01 when the roughness was reduced from  $R_a = 0.80 \mu\text{m}$  to  $R_a = 0.35 \mu\text{m}$ . For those tests at high speeds, a smoother surface exhibited a lower COF.

Surface parameters, including  $R_{pk}$ ,  $R_{vk}$ ,  $R_k$ ,  $M_{r1}$ , and  $M_{r2}$ , were also measured. Some of those parameters were used to calculate the oil retention volume for the polished PEO coating according to the formula:  $V_o = R_{vk} (100 - M_{r2}) / 200$  in  $\mu\text{m}^3/\mu\text{m}^2$ . The DIN standardized surface parameters and the oil retention volume were presented in Table 7.2.

Table 7.2 DIN surface parameters and oil retention volume of the polished PEO coated liner.

$R_a(\mu\text{m})$	$R_{pk}(\mu\text{m})$	$R_{vk}(\mu\text{m})$	$R_v(\mu\text{m})$	$M_{r1}$	$M_{r2}$	$V_o(\mu\text{m}^3/\mu\text{m}^2)$
0.80	0.75	1.03	2.46	8%	83%	0.087
0.60	0.59	1.15	2.00	6%	84%	0.092
0.45	0.44	1.19	1.67	3%	83%	0.101
0.35	0.10	1.52	1.20	1%	85%	0.114

The data in Table 7.2 shows that different roughnesses had different DIN surface parameters and oil retention volumes. The oil retention volume increased from 0.087  $\mu\text{m}^3/\mu\text{m}^2$  to 0.114  $\mu\text{m}^3/\mu\text{m}^2$  as the roughness was decreased from  $R_a = 0.80 \mu\text{m}$  to  $R_a = 0.35 \mu\text{m}$ .

In the boundary lubricating regime, the sliding velocity was quite slow, and no continuous oil film was formed between the counterfaces. Thus, the contact area would affect the frictional force significantly. The surface profile in Fig.7.4 showed that a rougher surface had a large number of narrow and sharp peaks, and a smoother surface had wide and flat peaks. The contact area between the narrow peaks and the piston ring was smaller than that between the wide peaks and piston ring. A larger contact area would induce a higher COF in the boundary lubricating regime. That seems to be the reason why a low COF can be obtained from a rough surface of  $R_a = 0.8 \mu\text{m}$ .

In the hydrodynamic lubricating regime, the sliding velocity was very high and the hydrodynamic oil film was quickly formed between counterfaces. The frictional force was from viscous shear force rather than from solid contact friction. In this regime, oil retention affected the COF greatly. Good oil retention could form an oil film easily and was beneficial to reduce the COF. The COFs in Fig.7.7 showed that the COF decreased with the reduction of surface roughness. The oil retention volume of the polished coating surface increased gradually from  $0.0873 \mu\text{m}^3/\mu\text{m}^2$  to  $0.1139 \mu\text{m}^3/\mu\text{m}^2$  when the roughness decreased from  $R_a = 0.80 \mu\text{m}$  to  $R_a = 0.35 \mu\text{m}$ . Thus, a larger oil retention volume could lead to a lower COF.

For the mixed lubricating regime, the frictional force between the counterfaces was a combination of solid contact friction and viscous shear force. As shown in Fig.7.7, the COFs decreased quickly and greatly in the mixed lubricating regime. At the same sliding velocity, a higher surface roughness resulted in a higher COF. Thus, the roughness effects on COF were different in different lubricating regimes. If the PEO coating was applied successfully on the engine cylinder bore, the surface should be honed or polished to have a roughness around  $0.35 \mu\text{m}$  to obtain a lower COF. In this way, when the vehicle engine was sped up, the COF could drop very quickly to a low level. On the other hand, the surface roughness can be relatively high at top dead center (TDC) and bottom dead center (BDC) areas where the boundary lubricant exists, based on the results shown in Fig.7.7 and ref. [18]. A well designed cylinder bore surface finish would be beneficial to friction reduction and fuel economy. However, engine dynamometer tests would be needed to verify this analysis.

### 3.2 Effect of oil flow rate on COF

Effect of oil quantity on COF was also studied by using two different oil flow rates: 100 ml per-minute and 200 ml per-minute. The oil tube was extended to the front of the piston ring, so that the oil could stay on the inner wall of the coated liner and lubricate the piston ring. Due to the rotation of the PEO coated liner, the centrifugal force caused the oil to stay on the wall of liner and spread uniformly. It could be observed that an oil film was formed on the inner wall of the liner, and the thickness of the oil film was higher when the high oil flow rate was applied. The tribotests were carried out at the high oil flow rate (i.e., 200 ml/min). The COF results are shown in Fig.7.8.

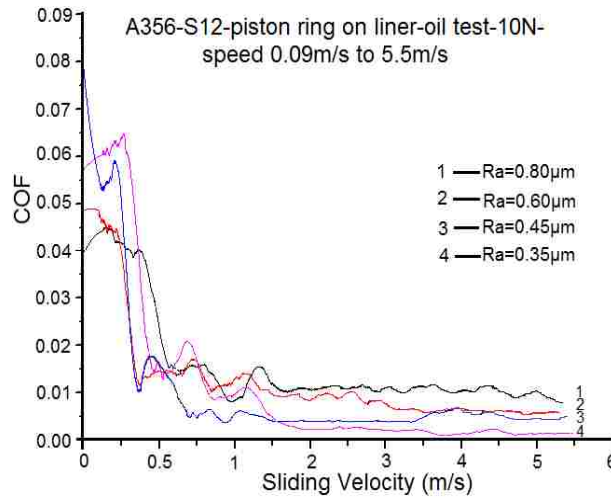


Fig.7.8 Roughness and sliding velocity effects on the COF of PEO coated liner at a high oil flow rate (200 ml/min).

The results in Fig.7.8 showed that the roughness effects on the COF of the PEO coated liner were similar to the low oil flow rate tests (100 ml/min in Fig.7.7). The lowest COF was obtained from the coating surface with  $R_a = 0.8 \mu\text{m}$  in the boundary lubricating regime. In the mixed lubricating regime, the COFs also decreased greatly and quickly. The COF decreased gradually with the reduction of roughness in the hydrodynamic lubricating regime. The COFs at the high flow rate were lower than the corresponding COFs obtained from the low oil flow rate tests for all lubricating regimes. The lowest COFs obtained in boundary and hydrodynamic lubricating regimes was 0.04 and 0.002

respectively, which is significantly smaller than the lowest COFs obtained in the low oil flow rate tests.

Thus, a higher oil flow rate was beneficial to reduce the COFs in this work. It was important for the wall of cylinder to possess higher oil retention volumes to reduce the frictional force between piston ring and the cylinder wall. However, too much oil retention was not desired, since the extra amount of oil would be burnt in the chamber of cylinder and caused more emissions. More research should be done to determine the proper oil retention volume to produce a low COF and less emission. Dyno tests are also needed in this regard in the future.

Compared with a high speed pin-on-disc test [19] where the counterpart was a steel ball of 5.5 mm in diameter, the COF obtained from the piston ring on the PEO coated liner was much lower, and the hydrodynamic oil film was formed much earlier and quicker. The mixed lubricating regime existed in a very limited speed range with a sharp drop of COF value, as shown in Fig.7.8. Contrary to the small spherical contact in the pin-on-disc test, the larger contact area between the piston ring and the bore of the PEO coated liner was beneficial for the piston ring floating on the oil film when the sliding speed increased. As a result, the sharp decrease of COF in mixed lubricating regime and the early formation of hydrodynamic oil film were presented.

As with the COFs of the PEO coated liner obtained from the two different oil flow rates, the effects of sliding velocity had a similar trend. However, a lower COF could be obtained from the high oil flow rate test for each surface finish condition. At a given sliding velocity, an even better lubrication (due to a larger amount of lubricate at the high oil flow) could further reduce the COF to a lower level.

There was no wear scar that could be observed on the PEO-coated liner after the tribotests. The low COF shows a promising tribological property of the coated liner. The high speed pin-on-disc tests have been conducted on the PEO coated Al disc and a grey cast iron disc, indicating the PEO coating can have a lower COF than cast iron. A comparison study on friction of a cast iron liner is still underway. Effects of different honing processes on COFs will be also studied and reported in the future.

## 4. CONCLUSIONS

In these high speed tribotests of a piston ring on PEO coated liner, surface roughness effects on the COFs of the coated liner are significant. The roughness effects on COFs are different in different lubricating regimes. In the boundary lubricating regime, the lowest COF is obtained from a surface with high surface roughness. The COF increases when surface roughness decreases from  $R_a = 0.80 \mu\text{m}$  to  $R_a = 0.45 \mu\text{m}$ . The COF then decreases at the case of  $R_a = 0.35 \mu\text{m}$ . In the mixed lubricating regime, the COFs drop quickly to a low level, and the hydrodynamic oil film forms quickly. In the hydrodynamic lubricating regime, the COFs decrease with the reduction of surface roughness. A larger quantity of oil retained can offer a lower COF at a given surface finish condition. The effects of sliding velocity on the COF of PEO coated liner are also remarkable. The COF of the PEO coated liner starts at a high level at the low sliding velocity, and then drops to a very low level with the increase of sliding velocity. The hydrodynamic oil film can be formed quickly at around 0.5 m/s sliding velocities. The COFs maintain a low level but with a slight increase at high sliding velocities. The test results indicate that the PEO coating may be a candidate as a coating that can be applied onto aluminum linerless engine blocks to replace cast iron liners for the reduction of weight and friction.

## ACKNOWLEDGEMENTS

The research was supported by Natural Sciences and Engineering Research Council of Canada (NSERC), and Ontario Centre of Excellence (OCE).

## References

- [1] J.F Su, X. Nie, H. Hu, J. Tjong, Friction and counterface wear influenced by surface profiles of plasma electrolytic oxidation coatings on an aluminum A356 alloy, *AVS Journals & Magazines*, 30, 061402 - 061402-11 (2012).
- [2] KS-Aluminium-Technologie, Aluminum Cylinder Blocks—Designs, Materials, Casting Methods and Cylinder Bore Surface Technologies for Lightweight Passenger-Car Engines (Verlag Moderne Industries, 2005).
- [3] Naranjo, D. Robert, F. Huang, Her-Ping, Gwyn, Mike, Castings Drive Fuel Efficiency. *Modern Casting*, Sep 2004, 94, 9; *ABI/INFORM Trade & Industry* pg. 20.
- [4] Grosselle, Fabio, G. Timelli, Bonollo, Franco, et al., Correlation between microstructure and mechanical properties of Al-Si die cast engine blocks. *Metallurgical Science and Technology*. Vol 27-2 – Ed 2009.
- [5] Valtierra-Gallardo, Salvador et al., Wear-Resistant Aluminum Alloy for Casting Engine Blocks with Linerless Cylinders. Patent Application – Publication Number: WO 2008/053363 A2. 8 May 2008.
- [6] R.K. Betts, Motor Vehicle Applications of Thermally Sprayed Specialty Coatings, *Proceedings of the 1st International Surface Engineering Congress and the 13th, IFHTSE, Congress of the International Federation for Heat Treatment and Surface Engineering*, 13, ISEC, International Surface Engineering Congress, 2003, Vol 1, p 716-721 .
- [7] D.R. Marantz, K.A. Kowalsky, J.R. Baughman, and D.J. Cook, Plasma Transferred Wire Arc Thermal Spray Apparatus and Method, U.S. patent No. 799242, Sept. 15, 1998.
- [8] K. Bobzin, et al., Thermal Spraying of Cylinder Bores with the PTWA Internal Coating System, *Conf. Proc., ASME Internal Combustion Engine*, Charleston, SC, ICEF07-1745, Oct. 14-17, 2007.
- [9] Ford Motor press release,  
[http://media.ford.com/images/10031/2011\\_GT500\\_Engine.pdf](http://media.ford.com/images/10031/2011_GT500_Engine.pdf), Feb. 2010.
- [10] G. Barbezat, Thermal Spray Coatings for Tribological Applications in the Automotive Industry, *Proceedings of the 2006 International Thermal Spray Conference*, B.R. Marple, M.M. Hyland, Y.-C. Lau, R.S. Lima, and J. Voyer, Eds., May 15-18, 2006 (Seattle), ASM International, 2006.



- [11] X. Nie, X. Li, and D. O. Northwood, *Mater. Sci. Forum.* 546, 1093 (2007).
- [12] X. Nie, X. Li, L. Wang, and D. O. Northwood, *Surf. Coat. Tech.* 200, 1994 (2005).
- [13] A. L. Yerokhin, X. Nie, A. Leyland, A. Matthews, and S. J. Dowey, *Surf. Coat. Tech.* 122, 73 (1999).
- [14] P. Zhang, X. Nie, L. Han, and H. Hu, *SAE Int. J. Mater. Manuf.* 3, 55 (2010).
- [15] B. Andersson, *Tribol. Ser.* 18, 503 (1991).
- [16] G. Wang, X. Nie, J. Tjong, Effect of Surface Roughness and Sliding Velocity on Tribological Properties of an Oxide-coated Aluminum Alloy, SAE-2014-01-0957 (2014).
- [17] K. Murat , D. Mesut , F. Ferit, Friction and wear studies between cylinder liner and piston ring pair using Taguchi design method, *Advances in Engineering Software*, August 2011, Vol.42(8), pp.595-603.
- [18] D. A. Parker and D. R. Adams, *Tribology—Key to the Efficient Engine* (Inst. Mech. Eng. Conf. Pub., London, England, 1982), pp. 31–39.
- [19] G. Wang, X. Nie, J. Tjong, Surface effect of a PEO coating on friction at different sliding velocities, SAE-2015-01-0687(2015).
- [20] D. Zhu, On some aspects of numerical solutions of thin-film and mixed elastohydrodynamic lubrication. *Proceedings of the Institution of Mechanical Engineers, Part J: Journal of Engineering Tribology*, 221, 561-579 (2007).

## Chapter 8

### Summary and future work

#### 1. Summary

Various advanced technologies are used to protect the cylinder bore surfaces of a linerless aluminum engine block, and improve their tribological properties. In this thesis, PEO coating technology was used to produce a hard, corrosion resistant, and excellent tribological performance coating to protect the soft surfaces of the aluminum cylinder. The tribological properties of the PEO coatings were investigated under different oil lubricating conditions including boundary, mixed, and hydrodynamic lubricating conditions. Surface roughness and sliding velocity effects on the COF of PEO coatings were particularly studied. Cast iron was used for comparison study. The tribological tests (including low speed pin-on-disc tests, high speed pin-on-disc tests, and high speed piston ring on liner tests) on PEO coatings showed that PEO coatings had high wear resistance and excellent tribological performances. The results and analysis are concluded with the organization of chapters as the following:

#### I. Effect of surface roughness and sliding velocity on tribological properties of an oxide-coated aluminum alloy.

Small round A356 aluminum alloy samples were coated by PEO process using different electrolytes. Low speed pin-on-disc tribometer was used to carry out the oil tests. Surface roughness and sliding velocity effects on the COF of the PEO coatings were investigated in the boundary lubricating regime. Results showed that a rougher surface had lower COF in boundary lubricating condition, and an increasing sliding velocity would reduce the COF in the boundary lubrication to some degree. Compared the COFs and wear tracks obtained from different PEO coatings, the PEO coating prepared in a medium concentrated electrolyte had the best tribological performance and wear resistance. In this work, the tribological properties of PEO coatings in boundary lubricating regime were understood.

#### II. Surface effect of a PEO coating on friction at different sliding velocities.

In order to understand the tribological properties of PEO coatings in mixed and hydrodynamic lubricating conditions, a high speed pin-on-disc tribometer was designed. The rotational speed could go up to 6.07 m/s in this case. A6061 aluminum alloy was used as substrate material and machined to ring-shaped with a diameter of 110 mm. two PEO coatings (S2, S3) were produced on the ring-shaped substrate. Surface roughness and sliding velocity effects on COF of PEO coating in different lubricating frictional regions were studied.

The results showed that the roughness and sliding velocity effects on the COF of PEO coatings in boundary lubricant were very similar to that obtained from low speed pin-on-disc tests. In the mixed lubricating regime, the COF decreased greatly to a pretty low level, and a lower surface roughness had a higher COF descent rate. In the hydrodynamic lubricating regime, the COF maintained at the low level but increased a little bit as the sliding velocity kept increasing, and a smoother surface had a lower COF. When the sliding speed increased, a typical Stribeck curve could be formed. Compared the results obtained from the two PEO coatings, the PEO coating prepared in the diluted electrolyte had better tribological properties, yet the PEO coating prepared in the undiluted electrolyte could reserve more coating during the polishing process and the wear was minor. Thus, two coatings had their own advantages and disadvantages which were beneficial for different applications.

### III. Friction influenced by surface roughness and sliding speeds at oil lubricating conditions.

In this work, A356 engineering aluminum alloy was used as substrate material to be machined to ring-shape. A new PEO coating (S12) which was expected to have a better combination of tribological properties and coating reserving ability was produced to compare with one of the best coatings prepared previously, which had a higher number of pores. (S3) High speed pin-on-disc tribological tests were carried out to study the surface roughness and sliding velocity effects on COF of PEO coatings. The results showed that the roughness and sliding effects on COF of PEO coatings were similar to results obtained from prior high speed pin-on-disc tests, but the COFs were much lower and descent rates of COFs were higher.

Compared the results obtained from the EPO coatings having more flat plateau (the new coating S12) vs. more pores (the previous coating S3), the new coating S12 had a higher COF descent rate (faster hydrodynamic oil film formation) and a higher coating reserve ability during polishing, even the lowest COF was obtained from coating S3. Cast iron was used to do the same tests for reference. The COFs obtained from PEO coatings were significantly lower than that from cast iron.

#### IV. High speed tribotests on a PEO coated aluminum liner after flex honing.

In the high speed tribotests of a piston ring on PEO coated liner, surface roughness and sliding velocity effects on the COFs of the coated liner are significant. These effects were similar to those in the high speed pin-on-disc tests. In the mixed lubricating regime, the COFs drop quickly to a low level in a cliffy way, and the hydrodynamic oil film forms faster than high speed pin-on-disc tests due to a larger counterface area (at around 0.5 m/s sliding velocities). In the hydrodynamic lubricating regime, the COFs decrease to pretty low levels with the reduction of surface roughness. The COF of the PEO coated liner starts at a high level at the low sliding velocity, and then drop to a very low level whilst the increase of sliding velocities. The COFs maintain at a low level but with a slight increase at high sliding velocities. In this test, a higher oil flow rate was beneficial to reduce the COF. The test results indicate that the PEO coating may be a candidate as a coating that can be applied onto aluminum linerless engine blocks to replace cast iron liners for reduction of weight and friction.

#### 2. Future work

The characteristics of the PEO coatings can be affected greatly by different experimental processing parameters (including current density, electrolyte, treatment time, etc.), future research should be directed to find an excellent coating with higher thickness, higher wear resistance, and lower COF.

More effects on the COF of PEO coatings should be studied in the future, such as temperature effects, lubricants effects (such as viscous, additive, etc.), humidity effects, and others.

More severe wear tests on PEO coatings should be carried out to study the wear resistance, which is vital for an engine block's serve life.

Study of honing effects on coated bore surface finish and morphology and thus COF would be an important step before the coating technology can be used for engine applications.

Reciprocating sliding tests on PEO coated liners are still desired to simulate the real movement of the pistons in the cylinder bores.

## Appendix

### 1. COPYRIGHT RELEASES FROM PUBLICATIONS

#### Chapter 4 and 5

**Terri Kelly** <terri@sae.org>

Fri, May 8, 2015 at 1:47 AM

To: "wang1161@uwindsor.ca" <wang1161@uwindsor.ca>

Dear Guang Wang,

Thank you for your email requesting permission to reprint SAE papers 2014-01-0957 and 2015-01-0687 – which you co-authored – in your thesis for the University of Windsor.

Permission is hereby granted, and subject to the following conditions:

Permission will be granted for non-exclusive world English language rights, for this one-time single use.

Permission is required for new requests, for reprints or excerpts, or further use of the material.

If you are including the paper in the final format as published by SAE International, the following copyright statement must appear on the papers “Copyright © XXXX\* SAE International. This paper is included in this thesis with permission from SAE International. Further use, copying or distribution is not permitted without prior permission from SAE.”

\*please insert the copyright year.

If you are not using the papers in the SAE technical paper format, the following statement must appear on the paper: “Reprinted with permission from SAE paper XXXXX\*\*Copyright © XXXX\* SAE International. Further use, copying or distribution is not permitted without prior permission from SAE. The official published version can be obtained from SAE at [www.sae.org](http://www.sae.org)”.

This permission does not cover any third party copyrighted work which may appear in the material requested. If any of the material you are reprinting originated from a source before the SAE paper, you need to obtain permission from this original source.

Reply to this email is required to validate the terms and conditions of this permission/license.

Licensor's use of this material, in whole or in part, is entirely its responsibility, and SAE International does not warrant or is not responsible for any use of the material.

Best regards,

**Terri Kelly**

Intellectual Property Rights Administrator

**SAE INTERNATIONAL**

400 Commonwealth Drive

Warrendale, PA 15096

**o** [+1.724.772.4095](tel:+17247724095)

**f** [+1.724-776-9765](tel:+17247769765)

**e** [terri@sae.org](mailto:terri@sae.org)

[www.sae.org](http://www.sae.org)

**From:** Guang Wang [<mailto:wang1161@uwindsor.ca>]

**Sent:** Wednesday, May 06, 2015 5:04 PM

**To:** SAE Customer Service

**Subject:** Asking for Permission to Use SAE Copyrighted Material

## 2. PUBLICATION LIST

### PUBLICATIONS:

1. G. Wang, X. Nie, J. Tjong, Effect of Surface Roughness and Sliding Velocity on Tribological Properties of an Oxide-coated Aluminum Alloy, SAE-2014-01-0957 (2014).
2. G. Wang, X. Nie, J. Tjong, Surface effect of a PEO coating on friction at different sliding velocities, SAE-2015-01-0687(2015).

3. Fuyan Sun, Guang Wang, Xueyuan Nie, Titanium-Aluminum Oxide Coating on Aluminized Steel, World Academy of Science, Engineering and Technology International Journal of Chemical, Nuclear, Materials and Metallurgical Engineering Vol:8, No:3, 2014. (Co-author)
4. G. Wang, X. Nie, J. Tjong, Friction influenced by surface roughness and sliding speeds at oil lubricating conditions, ICMCTF 2015. (Submitted)
5. G. Wang, X. Nie, J. Tjong, High speed tribotests on a PEO coated aluminum liner after flexible honing. (Proceed)

#### PRESENTATIONS:

6. G. Wang, X. Nie, J. Tjong, Effect of Surface Roughness and Sliding Velocity on Tribological Properties of an Oxide-coated Aluminum Alloy, SAE International Conference, Detroit, USA, 2014.
7. G. Wang, X. Nie, J. Tjong, Friction influenced by surface roughness and sliding speeds at oil lubricating conditions, AVS 61st International Symposium & Exhibition, Baltimore, USA, 2014.
8. G. Wang, X. Nie, J. Tjong, Surface effect of a PEO coating on friction at different sliding velocities, SAE International Conference, Detroit, USA, 2015.
9. G. Wang, X. Nie, J. Tjong, Friction influenced by surface roughness and sliding speeds at oil lubricating conditions, 42nd ICMCTF International Conference, San Diego, USA, 2015.



## VITA AUCTORIS

NAME: Guang Wang  
PLACE OF BIRTH: Hebei, China  
YEAR OF BIRTH: 1985  
EDUCATION: Hebei Normal University of Science and Technology,  
China, 2005-2009, B.Eng.  
University of Windsor, Canada, 2012-2015, M.A.Sc.